Statistical Methods for Biomarker Informed Personalized Medicine: Discovery and Translation

Xinyuan Dong

A dissertation
submitted in partial fulfillment of the
requirements for the degree of

Doctor of Philosophy

University of Washington

2021

Reading Committee:

Li Hsu, Chair

Yingqi Zhao, Chair

Yingye Zheng

Program Authorized to Offer Degree:
Biostatistics - Public Health

University of Washington

Abstract

Statistical Methods for Biomarker Informed Personalized Medicine: Discovery and Translation

Xinyuan Dong

Co-Chairs of the Supervisory Committee:
Affiliate Professor Li Hsu
Department of Biostatistics

Affiliate Associate Professor Yingqi Zhao
Department of Biostatistics

Identifying biomarkers is key to the success of personalized medicine. The recent progress in high throughput genotyping and genomics technologies has enabled rapid discovery of biomarkers that could potentially be used for informing clinical decision making. Towards this direction, we developed summary statistics-based mixed effects score test statistics (`sMiST`) for testing the association of multiple genetically predicted mediators simultaneously and direct association of individual variants independent of mediators by using a random effects model. Extensive simulation and real data analyses demonstrate that sMiST recovers the results of MiST that is based on individual level data, but is computationally much faster. We applied our approach to a genome-wide association study of colorectal cancer and gene expression and identified several novel and secondary genetic loci.

Medical decision making is often complex in that a treatment that improves clinical efficacy may also incur more medical costs, compared to standard care. In cost effectiveness analysis, incremental cost effectiveness ratio (ICER) is an important metric that measures the trade-off between the costs and health benefits of two medical programs. Individualized treatment regimes (ITRs) take into account patient heterogeneity and thus different ITRs may exhibit different health benefits and costs. Identifying a promising ITR that takes into account both efficacy and cost would be of great interest in practice. We construct ITRs that optimize the ICER, where we adopt Dinkelbach's algorithm to translate a fractional program into an equivalent parametric program that is easy to handle. We conduct extensive simulation studies to show satisfactory performances of our methods,

compared to ITRs that only optimizes one single outcome (benefits or costs). Lastly, we apply our method to Multicenter Automatic Defibrillator Implantation Trial with Cardiac Resynchronization Therapy (MADIT-CRT) study, a randomized trial.

Dynamic surveillance rules (DSRs) are sequential surveillance decision rules informing the monitoring schedules in clinical practice, which can adapt overtime according to a patient's evolving characteristics. In many clinical applications, it is desirable to identify and implement optimal stabilized DSRs, where the parameters indexing the decision rules are shared across different decision points and estimated simultaneously. We propose a new criterion for DSRs that account for benefit-cost tradeoff. We develop two methods to estimate the stabilized DSRs optimizing the proposed criterion, which are easy to implement using slightly modified standard statistical software. We establish the asymptotic properties of the estimated coefficient parameters of biomarkers indexing the decision rules. Extensive simulation studies are conducted to demonstrate the superior performance of the proposed methods. The methods are further applied to the Canary Prostate Active Surveillance Study(PASS) study.

TABLE OF CONTENTS

LIST OF FIGURES

ACKNOWLEDGMENTS

I wish to express sincere appreciation to my advisors Yingqi Zhao and Li Hsu for their tremendous support throughout my PhD study. I would also like to thank the co-authors including Yingye Zheng and Yu-Ru Su for important contributions to many parts of my dissertation.

Chapter 1

INTRODUCTION

In this chapter, we give an overview of the background and motivation of the three problems studied in the dissertation: summary statistics-based mixed effects score test, individualized treatment regimes for optimizing incremental cost effectiveness ratio, and stabilized dynamic surveillance rules.

1.1 Summary Statistics-based Mixed Effects Score Test

Genome-wide association studies (GWAS) have successfully identified tens of thousands of genetic variants associated with various phenotypes, but together they explain only a fraction of heritability, suggesting many variants have yet to be discovered. Recently it has been recognized that incorporating functional information of genetic variants can improve power for identifying novel loci. For example, PrediXcan[22, 5] and TWAS [27] tested the association between genetically predicted gene expression levels and phenotypes and identified..... some novel associations with certain diseases that were otherwise not detected in small individual samples? These approaches could be considered as a type of set-based association test, in which the predictor is the weighted sum of a set of genetic variants with weights being the effect sizes on gene expression. However, these methods do not take into account the potential effects of genetic variants beyond their effects on expression of a specific gene. Complex trait loci typically map to regions of the genome clustered with regulatory elements, which in turn have combinatorial effects on the expression of several target genes [17, 23]. Variants may have functional effects on more than one gene through their disruption of multiple regulatory elements [17]. Consequently, these approaches likely only capture part of the total effect of expression quantitative trait loci (eQTL).

We recently proposed a Mixed effects Score Test (MiST), which formulates the association of mediators (fixed effects), while allowing for effects of individual variants on disease risk directly adjusting for mediators (random effects) [80, 79]. Thus, MiST can increase power if some variants

individually influence disease risk through other functional mechanisms besides mediators (e.g., gene expression). Another advantage of MiST is that the test statistics for the mediation and direct effects are independent, providing a flexible framework for optimally combining the two components to achieve the maximal power. However, the test statistics of MiST were derived from individual-level data, which cannot be applied if there is difficulty in accessing individual-level data. To maximize power for detecting novel genetic association, it is desired to conduct association analysis using GWAS summary statistics, facilitating pooling data across studies and consortia.

In the first problem, we propose a summary statistics-based mixed effects score test (`sMiST`) that tests for the total effect of both the effect of the mediator by imputing genetically predicted gene expression, and the direct effects of individual variants. There are several novel contributions: 1) simultaneous testing of multiple mediators (e.g., gene expression and methylation); 2) testing of the variance component of the direct effects of genetic variants independent of the mediation effects; 3) combining the test statistics of both mediation and direct effects to form a single overall test that can capture information from both mediation and direct effects; 4) conditional testing of mediation and direct effects, adjusting for multiple other genetics variants. For example, one may perform conditional testing to examine whether a finding is novel conditional on known loci. When there is only one mediator, the test statistic for testing the association of the mediator under the assumption of no direct effects has the same form as PredXcan and TWAS [5, 27] and the Mendelian randomization two-stage estimator [10, 6]. Our method also avoids the direct inversion of the covariance matrix of genotypes as in the Mendelian randomization approach for dealing with correlated variants [6], therefore, it can work on genes with varying degrees of correlation structures, without any variant pruning. Extensive simulation and real data analyses demonstrate that `sMiST` yields p-values that agree well with those obtained from individual level data but with substantively improved computational speed. Importantly, a broad application of `sMiST` to GWAS is possible, as only summary statistics of genetic variant associations are required. We apply `sMiST` to a large-scale GWAS of colorectal cancer using summary statistics from $\sim 120,000$ study participants and gene expression data from the Genotype-Tissue Expression (GTEx) project. We identify several novel and secondary independent genetic loci.

1.2 Individualized Treatment Regimes for Optimizing Incremental Cost Effectiveness Ratio

In personalized medicine, there has been increasing interest in constructing individualized treatment rules (ITRs), which recommend treatments according to patients' characteristics. Typically, ITRs are constructed to optimize one single clinical outcome. Popular methods for this purpose include regression-based Q-learning [67] and classification-based outcome weighted learning [99]. The regression-based method models the conditional mean of the outcome given a set of covariates and treatment using parametric models with interaction?,I think in the literature it's common to use this notation $E(Y|X, A)$, the conditional mean of Y given covariates and treatment maybe since when you are given covariates and treatment, you also have their interactions, but yes the parametric models should be fitted on X, A, X*A to be more specific. and select the treatment with the larger conditional mean. Classification-based method estimates the optimal rule from a weighted classification perspective, with the objective to optimize the expected benefit under the ITRs. However, the goal of these methods is typically to maximize the expected benefit of a single clinical outcome if followed by the whole population.

While maximizing treatment efficacy is the primary goal, evaluation of costs and/or risks associated with the treatments is also important. There have been developments on constructing ITRs, taking into account both efficacy and risk outcomes. An existing body of literature focuses on constructing a utility function that jointly models efficacy and toxicity, and estimate an optimal ITR to maximize the utility function. These approaches construct an objective function, defined as the utility of benefits and toxicity, and estimate an optimal strategy to maximize the posterior expected mean of the objective function [30, 32, 47, 55, 83]. There are also methods focusing on estimating the optimal ITR to maximize the clinical benefit while directly imposing a constraint on the risk [92, 95]. Lizotte et al. [53] proposed to construct a linear combination of the competing outcomes as a composite primary outcome, and Laber et al. [43] proposed to construct set-valued treatment regimes that avoids eliciting trade-offs between outcomes, and can output multiple candidate treatments when there does not exist a treatment that is uniformly the best across all outcomes. However, all of these approaches either require joint modeling of the efficacy and safety outcomes, or require a pre-specification of threshold value on the risk constraint.

To account for the benefit-cost tradeoff, incremental cost-effectiveness ratio (ICER) is commonly used in health economics to assess the economic value of an intervention, compared with the alternative [61, 88, 60]. Existing statistical literature mainly focused on estimation and confidence interval (CI) construction for the ICER in order to compare the cost effectiveness of different arms [13, 35, 61, 64]. In the second problem, we generalize the notion of ICER as the criterion to evaluate the quality of the ITRs. Having a single criterion to optimize avoids partial orderings and the subsequent non-uniqueness associated with set-valued and other multi-objective regimes. However, to our knowledge, such a metric has not been proposed for a specified ITR, which is more complex than comparing two pre-specified interventions.

Figure 1.1. Cost-effectiveness plane

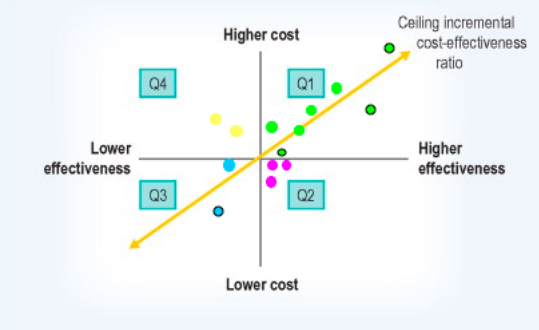

- Q1 quadrant: ITRs achieve higher benefits at higher costs.
- Q2 quadrant: ITRs achieve higher benefits at lower costs.
- Q3 quadrant: ITRs achieve lower benefits at lower costs.
- Q4 quadrant: ITRs achieve lower benefits at higher costs.

To define the ICER of an ITR, we first set the reference treatment regime, and derive the ratio of the change in the expected efficacy over the change in the expected cost over the whole population, when switching the reference to the ITR of interest. Therefore, different ITRs will exhibit varying ICERs, and our goal is to identify the one leading to the most desirable ICER. However, because

the ICER characterizes the incremental costs and benefits, it is not trivial to identify an ITR that optimizes this criterion. As shown in Figure 1.1, there are potentially four different quadrants that an ITR can fall into, but some quadrants should not be of interest or may not be feasible to achieve. The decision rules can thus be classified as in Figure 1.1.

When identifying the ITR optimizing ICER, we need to take into account which quadrants the alternative ITRs fall into. Obviously, the ITRs falling into Q2 quadrant are among the most desirable, which may not be feasible in certain circumstances. Additionally, ITRs that attain lower effectiveness should not be considered, even if they could lead to reduced costs. In the second problem, we will assume the reference ITR, typically assigning the standard care to the patient population, has a low benefit and a low cost. To facilitate the computation and interpretation, we propose a modified criterion, termed as winsorized ICER (wICER). Specifically, we use incremental winsorized costs that are guaranteed to be nonnegative in defining the ICER. This modification enables us to focus on the ITRs residing in Q1 and Q2 quadrants, which are of the major interests in identifying the most cost-effective ITR.

It is worth noting that our proposed framework does not require additional pre-specified parameters such as thresholds for risk constraints, or weights in the utility function. To our knowledge, there has been no work on estimating the ITR that optimizes a ratio-type objective function. We employ Dinkelbach's algorithm to transform a fractional program into an equivalent parametric program that is easy to handle [18]. Specifically, the resulting parametric program [21], which formulates the optimization problem as a function of a parameter, essentially maximizes a composite outcome defined by the optimal parameter. Dinkelbach's establishment of the relationship between fractional and parametric program enables us to derive a theoretical optimal rule of the ratio-type problem. We then propose two estimation methods that are guided by the theoretical optimal rule: regression-based approach [67] and outcome-weighted learning based approach [99]. The regression-based method models the conditional mean of the outcome given a set of covariates and treatment, and select the treatment with the larger conditional mean. Outcome-weighted learning based method estimates the optimal ITR from a weighted classification perspective, where weights are defined by the benefit and cost in our situation.

1.3 Stabilized Dynamic Surveillance Rules

Active surveillance is a disease management strategy that closely monitors a patient's condition without intervention unless there are indications of a worsening condition. Such a strategy can reduce the overtreatment of disease by delaying intervention in patients who were diagnosed with low-risk disease and providing treatments only when a more severe malignancy is identified. Dynamic surveillance rules (DSRs) are sequential surveillance decision rules that can adapt over time according to a patient's evolving characteristics. In the setting of Canary Prostate Active Surveillance Study(PASS) What is PASS?sorry just added the full study name, they can provide s a formal decision rule for the personalized subsequent monitoring schedule to tailor the intensity of active surveillance, identifying those men among whom surveillance can be safely modulated.

The DSR can be derived in the form of a time-dependent binary decision rule on whether an intervention procedure (e.g., biopsies or surgery) should be taken at a future time τ scheduled by a fixed surveillance protocol, given the patient is event-free up to a visit time (landmark time) s. The procedure typically proceeds by estimating the dynamic risk, the updated τ_0-year risk for an adverse event based on a patient's information accumulated up to t, and then constructing the surveillance rules via comparing the risk with a pre-specified risk threshold. Partly conditional models [58], and joint models [85, 84] can be used for dynamic risk predictions. However, the identification of an appropriate risk threshold needs some deliberation in this setting. In addition, the derived rule relies on the aptness of the underlying regression model for longitudinal and time-to-event data. We develop methods that can improve on the robustness of model-based decision rules by considering model-free reinforcement learning algorithms [81]. Such approaches have been adapted in the dynamic treatment regime literature, but not yet been considered in the setting of deriving the followup schedule of a monitoring test.

One important hurdle in searching for a DSR is the identification of a clinically relevant objective function that captures the clinical consequences important to patients. The optimal DSR indicating follow-up schedules should maximize the clinical benefit while adjusting for the associated risk, e.g., overtreatment. Here we consider an average risk-adjusted clinical benefit (RACB) performance measure. It weighs the importance of high true positive fraction (TPF) against low false positive fraction (FPF) at each stage. The RACB function is in the same spirit as the notion of net benefit

in decision theory [57, 87]. It is often used as a clinical validity measure of a medical tests, but has seldom been considered as an objective function for optimization. Recently, Wang et al. [91] considered using the RACB function to search for a clinical decision rule for the binary outcome with baseline data. We extend the criterion used in [91] for the binary outcome to the time-dependent setting with repeated measurements. The criterion is clinically meaningful by balancing the benefit and risk of the DSR over the course of monitoring. To our knowledge, this is the first time such a measure is adopted for the active surveillance setting.

For active surveillance that involves a potentially large number of landmark times, a decision rule with formulations varying by landmark times may be difficult to implement in clinical practice. Furthermore, the baseline time could be hard to define as the enrollment times for patients may be different between the cohort for developing the rule and the target cohort the rule is applied to. Therefore a time-varying DSR would also be challenging to generalize. Indeed, there has been growing interest in developing shared decision rules across stages, especially in the area of dynamic treatment regimes. For example, [12] developed shared-Q-learning for deriving dynamic treatment regimes with shared parameters. They formulated the decision rules as linear functions of time-varying covariates, and the coefficients are assumed to be the same across decision points. Recently, [89] proposed the shared-parameter G-estimation, [98] developed censored shared-Q-learning and censored shared-O-learning method, which allow for censored outcomes. Potential generalizations of these approaches require specific objective functions for the active surveillance setting.

We focus on developing new methods of estimating coefficient parameters of biomarkers indexing the DSRs that are shared across landmark times, aiming to optimize the average RACBs over time. We term DSRs with shared parameters as stabilized DSRs. In particular, we propose two methods to estimate the stabilized DSRs that are easy to implement using slightly modified standard statistical software. The first method is a two-step modeling approach, termed as shared modeling (SM). We estimate the optimal decision rules for each individual at every stage via regression modeling, and then estimate the stabilized DSRs via a classification procedure with the estimated time-varying decision rules as the response. The second approach is termed as optimization with surrogate function (OSF). It proceeds by optimizing the estimator of the average RACB, where a surrogate function is utilized to facilitate computation. OSF does not model the outcomes, and hence does not rely on any underlying model assumptions. We establish the asymptotic properties of the estimated

coefficient parameters of biomarkers indexing the DSRs from both methods.

Chapter 2

A GENERAL FRAMEWORK FOR FUNCTIONALLY INFORMED SET-BASED ANALYSIS: APPLICATION TO A LARGE-SCALE COLORECTAL CANCER STUDY

2.1 Introduction

Single variant analysis in genome-wide association studies (GWAS) has been successful in identifying thousands of variants associated with various diseases and traits [8]. However, these variants all together explain only a fraction of heritability, suggesting that many variants remain to be discovered. Until now, most of these discoveries have been mainly driven by increases in sample size. The gain from substantially increasing sample size is diminishing, but incorporation of functional knowledge about the genome will likely play a critical role in informing discovery of novel loci as well as understanding the pathways in which the genetic loci may be involved.

Research for integrating functional knowledge into GWAS has been active recently. This is in part due to success of large collaborative projects such as the Genotype-Tissue Expression (GTEx) project [54] and the Encyclopedia of DNA Elements (ENCODE) [15], which have generated extensive knowledge about functions of genetic variants that can be used for aggregating and weighting genetic variants. Widely available GWAS summary statistics for individual variants has made it possible to leverage these functional information, leading to many more discoveries of novel genetic loci. For example, PrediXcan[22, 5] and TWAS [27] test the association between genetically predicted gene expression levels and phenotypes. A comprehensive review and comparison of various methods can be found in Barbeira et al. (2018) [5]. The TWAS-like analysis can also be framed as a class of Mendelian randomization [9, 6], in which under some assumptions the mediator effect of gene expression can be estimated by the inverse variance weighted ratios of regression coefficients of genetic variants for the phenotype and those for the gene expression. All of these methods also apply to other types of mediators including methylation and lifestyle variables (e.g., smoking) that may be regulated by genetic variants.

These approaches could be considered as a type of set-based association test, in which the

predictor is the weighted sum of a set of genetic variants with weights being the effect sizes on gene expression. However, these methods do not take into account the potential effects of genetic variants beyond their effects on expression of a specific gene. Complex trait loci typically map to regions of the genome clustered with regulatory elements, which in turn have combinatorial effects on the expression of several target genes [17, 23]. Variants may have functional effects on more than one gene through their disruption of multiple regulatory elements [17]. Consequently, these approaches likely only capture part of the total effect of expression quantitative trait loci (eQTL).

We recently proposed a Mixed effects Score Test (MiST), which formulates the association of mediators (fixed effects), while allowing for effects of individual variants on disease risk directly adjusting for mediators (random effects) [80, 79]. Thus, MiST can increase power if some variants individually influence disease risk through other functional mechanisms besides mediators (e.g., gene expression). Another advantage of MiST is that the test statistics for the mediation and direct effects are independent, providing a flexible framework for optimally combining the two components to achieve the maximal power. However, the test statistics of MiST were derived from individual-level data, which cannot be applied if there is difficulty in accessing individual-level data. To maximize power for detecting novel genetic association, it is desired to conduct association analysis using GWAS summary statistics, facilitating pooling data across studies and consortia.

In this paper, we propose forming the test statistics of MiST based on summary statistics, which we term as `sMiST`. There are several novel contributions: 1) simultaneous testing of multiple mediators (e.g., gene expression and methylation); 2) testing of the variance component of the direct effects of genetic variants independent of the mediation effects; 3) combining the test statistics of both mediation and direct effects to form a single overall test that can capture information from both mediation and direct effects; 4) conditional testing of mediation and direct effects, adjusting for multiple other genetics variants. For example, one may perform conditional testing to examine whether a finding is novel conditional on known loci. When there is only one mediator, the test statistic for testing the association of the mediator under the assumption of no direct effects has the same form as PredXcan and TWAS [5, 27] and the Mendelian randomization two-stage estimator [10, 6]. Our method also avoids the direct inversion of the covariance matrix of genotypes as in the Mendelian randomization approach for dealing with correlated variants [6], therefore, it can work on genes with varying degrees of correlation structures, without any variant pruning. We show that our

method of combining summary statistics gives p-values that are consistent with those constructed from individual level data, and that it is much more efficient computationally. We applied sMiST to a large-scale GWAS of colorectal cancer using summary statistics, and identified three novel loci that are located 1MB outside of known CRC loci regions, as well as one additional secondary novel locus.

2.2 Methods

MiST framework

Consider an outcome Y, which can be continuous or binary. We are interested in the association of a set of P variants $G = (G_1, \ldots, G_P)$ with outcome Y. Assume there are K mediating variables $M = (M_1, M_2, \ldots, M_K)^T$, with which G are associated and $K < P$; here the superscript T is for transpose. Let X be a vector of confounders including the intercept. The confounders may include study, age, sex, and principle components to account for population structure in the data. A generalized linear model can be used to assess the association of M and G while adjusting for confounders X

$$g\{\mathrm{E}(Y|X, M, G)\} \quad = \quad X^T\eta + \sum_{k=1}^{K} M_k\gamma_k + \sum_{p=1}^{P} \delta_p G_p, \tag{2.1}$$

where $g(\cdot)$ is a logit function if Y is binary and an identity function if Y is continuous. The regression coefficients η, $\gamma = (\gamma_1, \ldots, \gamma_K)^T$, and $\delta = (\delta_1, \ldots, \delta_P)^T$ are the effects of the confounders, K mediators, and direct effects of G, respectively. To obtain estimators for γ and δ, ideally the measurements of genotypes G, mediators M, and outcome Y are collected on the same set of individuals. However,GWAS usually have very large sample sizes because of their need to detect modest genetic effects; as such, collecting mediators M such as gene expression and methylation on all individuals in GWAS can be costly and logistically difficult.

As M is not measured, it is instructive to examine $\mathrm{E}(Y|X, G)$ by integrating out the unmeasured M under the true model (2.1) [33]. If g is linear, it is straightforward to see that $\mathrm{E}(Y|X, G) = X^T\eta + \sum_{k=1}^{K} \mathrm{E}(M_k|G, X)\gamma_k + \sum_{p=1}^{P} \delta_p G_p$. This suggests that if there is a model that can predict M_k well using G, we can use this model to impute the missing M_k by $\mathrm{E}(M_k|G, X)$.

If g is logit, there is no closed form for $E(Y|X,G)$ but we can approximate $g\{\mathrm{E}(Y|X,G)\} \approx \{X\eta + \mathrm{E}(M|G,X)\gamma + \sum_{p=1}^{P}\delta_p G_p\}/\phi$, where $\phi = \{1+\gamma^T \mathrm{cov}(M|G,X)\gamma/1.7^2\}^{1/2}$ [11]. Despite the parameters are attenuated by $1/\phi$ under this model, testing of null association for the mediation with $\mathrm{E}(M|G,X)$and direct effects with $\{G_p, p=1,\ldots,P\}$ is equivalent to testing γ and δ's $= 0$ in model (2.1). For simplicity, we used the same notation $\{\gamma,\delta\}$ for the attenuated parameters in the following models.

Specifically, we fit a linear regression model to the mediators:

$$\mathrm{E}(M_k|X,G) \quad = \quad X^T\eta + \sum_{p=1}^{P} W_{pk}G_p, \qquad k=1,\ldots,K, \tag{2.2}$$

where W_{pk} is the weight or regression coefficient of pth variant associated with the kth mediator. Here, to avoid introducing too many non-critical notation, we use η to denote generically the regression coefficients for confounders X and they may not be same as η for confounders in other models. The weight W_{pk} is set to 0 if the pth variant is not associated with kth mediator. In some situations, some variants that are associated with mediators M are not part of the set $\{G_p, p=1,\ldots,P\}$. We can expand $\{G_p, p=1,\ldots,P\}$ to include these variants but set the corresponding δ's in model (2.1) to 0. Now plugging (2.2) in (2.1), we obtain

$$g\{\mathrm{E}(Y|X,M,G)\} \quad = \quad X^T\eta + \sum_{k=1}^{K}\widehat{M}_k\gamma_k + \sum_{p=1}^{P}\delta_p G_p, \tag{2.3}$$

where $\widehat{M}_k = \sum_{p=1}^{P} W_{pk}G_p$ for $k=1,\ldots,K$. To obtain the weights $\{W_{pk}, p=1,\ldots,P,\, k=1,\ldots K\}$, we can use a reference dataset that has both genotyping and mediator data. The dataset needs not overlap with the GWAS data. For example, PrediXcan uses genetic variants and gene expression data from GTEx and other studies to build a genetically predicted gene expression linear regression model for each gene [22].

As the number of mediators K is typically small, we assume γ as fixed effects. On the other hand, the number of genetic variants P can be large. An omnibus χ^2 test with P degrees of freedom may not be powerful. Instead, we assume that $\delta_p, p=1,\ldots,P$, follow an arbitrary distribution with

mean 0 and variance τ^2. Thus, we test the overall null

$$H_0 : \gamma = 0 \text{ and } \tau^2 = 0.$$

If the test rejects the null hypothesis at a pre-specified significance level, it suggests there is evidence against the null total effects of genetic variants G on Y. We note that model (2.3) can also be formulated by a hierarchical model as shown in Su et al. (2018) [79], where in a generalized linear model of G and Y, the main effects of G are further modeled by incorporating the functional information of the genetic variants such as weights in predicting gene expression.

Summary statistics-based mixed effects score test (sMiST)

Su et al. [79] proposed the Mixed effects Score Test (MiST) to test nullity of the fixed effects γ and variance component τ^2 using individual level data. Here we introduce a method that requires only summary statistics to perform the tests for $H_0 : \gamma = 0$ and $\tau^2 = 0$. Following the convention, assume we have the summary statistics at hand:

- Standard GWAS output: marginal regression coefficients $\{\widehat{\beta}_p^*, \text{se}(\widehat{\beta}_p^*), p = 1, 2, ..., P\}$ from

$$g\{E(Y|X, G_p)\} = X\eta + G_p\beta_p^*, \qquad p = 1, \ldots, P,$$

- Covariance of the genotypes, $\text{cov}(G)$.

The summary statistics can also be replaced by score statistic $\widetilde{U}_p$ and variance $\widetilde{V}_p$ with $\widehat{\beta}_p^* \approx \widetilde{V}_p^{-1}\widetilde{U}_p$ and $\text{se}(\widehat{\beta}_p^*) \approx \widetilde{V}_p^{-1/2}$. When the variants are rare or less frequent, score statistics are numerically more reliable than the estimates of marginal regression coefficients, because score statistics are calculated under the null. The covariance $\text{cov}(G)$ can be obtained from an internal random subset of control samples or an external reference database. In the latter case, the the reference data should match as close as possible to the underlying population for the summary statistics to avoid false positives [5].

Based on the summary statistics, we derive the test statistics for the overall mediation effects $\gamma = 0$, as well as individual mediator effects $\gamma_k, k = 1, \ldots, K$ under $\tau^2 = 0$. In addition, we derive

the test statistics for $\tau^2 = 0$, conditional on $\widehat{M}$. By conditioning on $\widehat{M}$, the test statistic for τ^2 is independent of the test statistic for γ [79]. We can then straightforwardly combine the two test statistics by using the p-value-based Fisher's or minP combination procedure. Alternatively, we can also use data-driven weighted combination methods as in MiST: optimally weighted linear combination and adaptively weighted linear combination, neither of which requires individual level data. We termed the summary statistics-based combined mixed effects test as `sMiST`.

In theory, p-values derived from summary statistics and p-values derived from individual-level data are asymptotically equivalent under the null if there are no confounders and the estimate of cov(G) is accurate, the latter of which is important especially if the genotype data are from an external dataset that differs from the data that generate the summary statistics.

2.3 Results

2.3.1 Identifying novel genes associated with CRC risk using sMiST

We analyzed a large GWAS of colorectal cancer (54,454 cases and 64,163 controls) [34]. We considered the mediation effect of gene expression and downloaded the estimates of genetic effects on gene expression from the PredictDB Data Repository (`http://predictdb.org/`). We controlled the overall type I error at 0.05, allocating 0.04 for genome-wide discovery and 0.01 for conditional analysis to identify novel loci while adjusting for known CRC loci. Specifically, we tested 8,893 genes and used a Bonferroni correction to account for multiple testing, which yields a significance level at the gene level $0.04/8893 = 4.5 \times 10^{-6}$. For the conditional analysis, we set the significance level at the gene level to be 0.01 divided by the number of significant genes from the genome-wide discovery.

A total of 90 genes reached the genome-wide significance level of 4.5×10^{-6} using optimally weighted linear combination of sMiST (S1 Table). To evaluate whether these genes are novel for CRC, we performed conditional analysis adjusting for the CRC known loci [34] on the same chromosome using sMiST. We constructed a weight matrix $W_{Q+P,Q+1}$ such that the first Q columns are 1 on the diagonal corresponding to known loci and 0 everywhere else, and the last column is 0 for the first Q rows and weights of P variants used in predicting gene expression for the remaining P rows. We arranged summary statistics for the Q known loci and the P variants as a vector. It is

straightforward to see that the adjusted p-value for the predicted gene expression conditioning on the known loci is as if each of the known loci were a "mediator".

After adjusting for the CRC known loci risk, four genes remain significant at $0.01/90 = 1.1\text{x}10^{-4}$ (Table 1), three of which have no known loci within 1Mb of transcription start and end sites of the gene. For all four genes, the main association signal comes from the variance component of the random effects of the SNPs, not from the predicted gene expression. A further examination of marginal association along with eQTL weights shows that variants with the larger weights in predicting gene expression do not have evidence for association (*NT5DC2* and *VPREB3*). For *PLD6* and *ANKRD10*, variants that up-regulate (or down-regulate) gene expression have incosistent direction of association with outcome, yielding non-significant p-values for the predicted gene expression (S1-S4 Fig). The odds ratio estimates are close to 1 and their 95% confidence intervals cover 1 (S2 Table). On the other hand, for these genes, several variants do show association with disease risk, for which the variance component test is powerful to detect when the signals are sparse in a set-based test.

Table 2.1. Novel CRC associated genes and secondary genes.

Novel genes: 0 known loci within 1Mb

Gene Info				Unadjusted P-value[1]			Adjusted P-value[1]		
Gene	R^2	N SNPs	chr	Pred Exp	Var Comp	sMiST	Pred Exp	Var Comp	sMiST[2]
NT5DC2	0.35	52	3	0.96	1.92e-06	3.96e-06	0.95	2.03e-06	4.38e-06
PLD6	0.25	36	17	0.25	1.42e-06	2.89e-06	0.29	9.12e-07	1.99e-06
VPREB3	0.04	12	22	0.99	1.41e-06	3.19e-06	0.99	1.41e-06	3.19e-06

Novel secondary genes: $\geq$ 1 known loci within 1Mb

Gene Info				Unadjusted P-value[1]			Adjusted P-value[1]		
Gene	R^2	N SNPs	chr	Pred Exp	Var Comp	sMiST	Pred Exp	Var Comp	sMiST
ANKRD10	0.06	36	13	0.48	1.13e-06	2.36e-06	0.43	2.39e-05	5.45e-05

[1] The unadjusted and adjusted p-values are without and with adjusting for the known CRC loci that are on the same chromosome of the gene.

[2] The column names are as follows. R^2 is the variation of gene expression explained by eQTLs from the PrediXcan model; N SNPs is the number of variants in the gene; chr is the chromosome #; Pred Exp is the p-value for predicted gene expression; Var Comp is the p-value for the variance component; sMiST is the combined p-value of predicted gene expression and variance component tests using optimally weighted linear combination.

Next, we conducted a sequential analysis to explore whether the significance of each identified genes is mainly driven by only one variant or a subset of the variants. We first selected the most

marginally significant variant after adjusting for known loci. Then we included known loci and also this most significant variant in sMiST to evaluate the association. If the p-value from either the predicted gene expression or variance component was < 0.05, we continued the process and selected the next most significant variant, adjusting for known loci and previously included variants, until neither the predicted gene expression nor variance component p-value reached significance at 0.05. The association of all of these genes is driven by two or more variants (S3 Table). In particular, for gene *ANKRD10*, 8 variants are associated with CRC risk. All of these highlight the power of set-based association testing that incorporates functional information.

2.3.2 Performance of `sMiST` *in simulation*

We evaluated the performance of summary statistics-based `sMiST` in testing the mediation and variance components. We examined the type I error of sMiST by generating Y assuming both $\gamma = 0$ and $\tau^2 = 0$. The type I error for sMiST as well as for the mediation and variance component tests is well kept (S4 Table). Importantly, we would like to examine how closely sMiST p-values are compared with the p-values from MiST that were calculated based on individual level data, which we treat as the gold standard. This is because an essential property of summary statistics-based test statistics is that they should agree well with the test statistics obtained as if individual level data were available. We selected three different genes due to their different genetic structures. As the performance of sMiST is similar for all three genes, we only present the results for the *CXCR1* gene here. Gene *CXCR1* has 42 variants with several clusters of high correlation. Details of simulation are provided in Methods and Materials.

Impact of confounding

As the asymptotic equivalence between sMiST and individual-level data based MiST holds when there are no confounders, we examined extensively the impact of confounders on sMiST. We calculated $\text{cov}(G)$ using the same genotyping data as for generating the outcome. The robustness of $\text{cov}(G)$ estimated from smaller sample size and external data will be assessed in the section of "Performance of sMiST in real data analysis". For *CXCR1*, there is one known locus outside the gene, which is highly correlated with the predicted gene expression (mediation) with correlation of -0.66. We thus

created a confounding variable by summing this known locus and other independent genetic variants weighted by their marginal effect sizes. We varied the number of independent variants added to the confounding variable to yield the correlation between the confounder and predicted gene ranging from 0.1 to 0.4, representing moderate to high correlation. We also varied the effect size of the confounder, β, from 0.3 to 0.9 for modest to strong effect.

We considered 4 general scenarios:

1. Complete null,

2. Null mediation effect and non-zero variance component,

3. Non-zero mediation effect and null variance component, and

4. Non-zero for both mediation effect and variance component.

Fig 2.1 shows the scatter plots of $-\log10$(p-values) for the mediation effect (top) and variance component (bottom) of sMiST and individual-level data based MiST, when the correlation between confounder and predicted gene expression is 0.25, and $\beta = 0.6$. It is clear that the points fall on the 45 degree line, suggesting sMiST provides virtually identical results to the individual level data based MiST for both mediation and variance components under all four scenarios. In fact, sMiST performs very well compared with MiST even when the correlation is as high as 0.4 and β is 0.9 (S7 Fig).

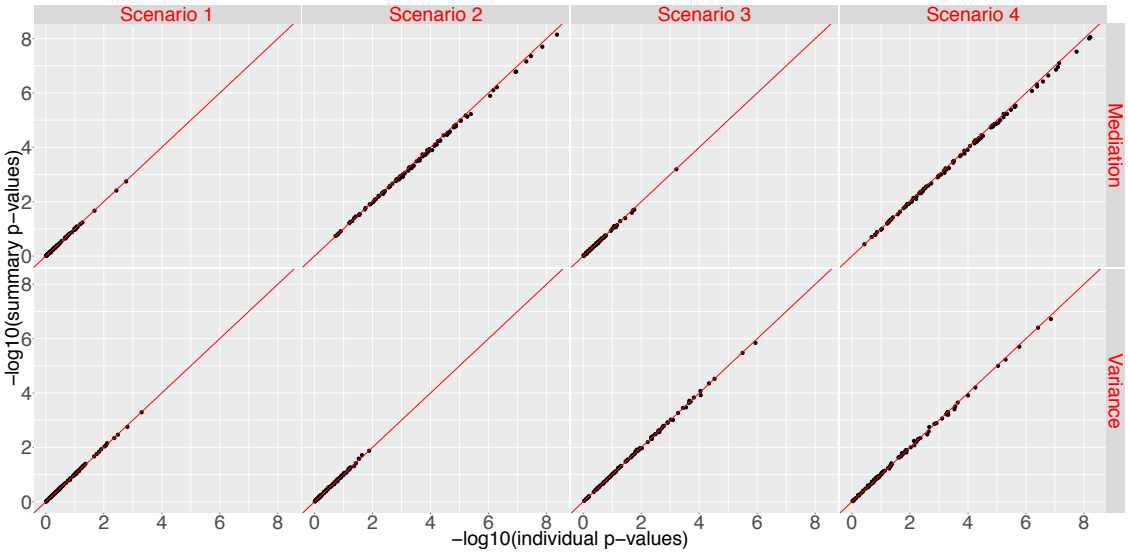

Fig 2.1. Scatter plots of −log10(p-values) for testing the mediation effect and variance component for sMiST compared with individual level data based MiST in the presence of confounding.

Performance of sMiST with multiple mediators

Our method can be generalized to instances when there are multiple mediators. To illustrate, we generated two correlated mediators. One mediator was predicted gene expression of of *CXCR1*, and the other "mediator" is the known CRC locus outside of the gene, which is in nearly perfect correlation with one of the variants in *CXCR1*. This is to mimic the scenario for testing the joint and conditional effect of predicted gene expression and known locus. We combined the genotype data of *CXCR1* and of the known CRC locus into a mega-genotype $n \times (P+1)$ matrix, where n is the number of subjects and P is the number of eQTLs in the *CXCR1* gene. We assigned a $(P+1) \times 2$ weight matrix of the form (W_1, W_2), where $W_1 = (w_1, \ldots, w_P, 0)^T$ and $W_2 = (0, \ldots, 0, 1)^T$. Here the weight is again from the the PredictDB Data Repository.

We present the p-value for testing the joint mediation effect and the p-value for the variance component, as well as the individual p-values associated with each component. sMiST again shows virtual identical p-values with individual-level data based p-values for both the joint mediation effect and individual mediator's effect conditional on the other mediator (Fig 2.2).

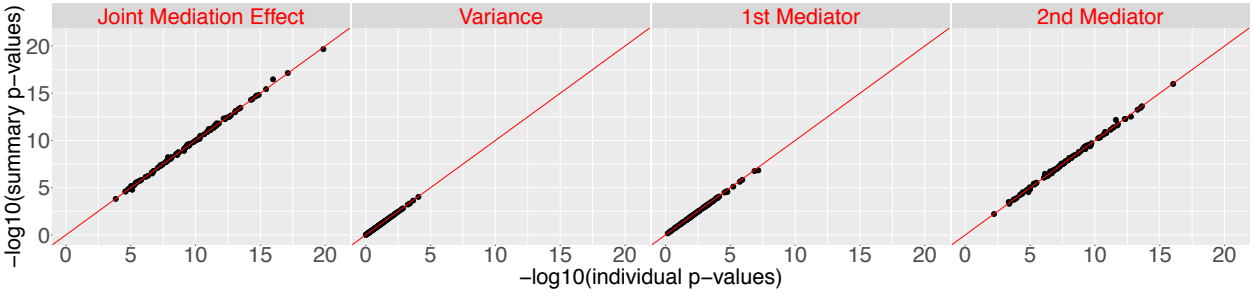

Fig 2.2. Performance of sMiST when there are two mediators.

2.3.3 Performance of sMiST with rare variants

We compared the performance of summary statistics based sMiST with individual level data based MiST for rare variants with MAF from 0.1% to 1.0%. We calculated sMiST using $\{\widehat{\beta}_p^*, \text{se}(\widehat{\beta}_p^*)\}$ denoted by sMiST-Wald and score statistics $\{\widetilde{U}_p, \widetilde{V}_p\}$ denoted by SMiST-Score. We also calculated sMiST using the standardized score test statistics to address the situation that only the z statistics $\{Z_p, p = 1, \ldots, P\}$ from score or likelihood ratio tests and the directions of the effects are available. In this situation, we replaced $\widehat{\beta}_p^*$ by $\text{sign}(\beta_p^*)Z_p$, $\text{se}(\widehat{\beta}_p^*)$ by 1, and the covariance of the genotypes by the correlation of the genotypes, where sign is 1 if β_p^* is > 0, -1 if β_p^* is < 0, and 0 otherwise. We denote this by sMiST-Standardized Score.

Fig 2.3 showed the comparison of these sMiST test statistics with MiST under the null and alternative hypothesis. It is clear that sMiST-Wald yields many outliers for both the mediation and variance components with p-values near 1 whereas the corresponding individual level data based MiST p-values range from 0 to 1. In contrast, the sMiST-Score agrees very well with MiST on both the mediation and variance component p-values under the null. Under the alternative, the mediation p-values still agree very well with MiST mediation p-values. For the variance component, while it generally agrees, sMiST-Score p-values are slightly inflated. sMiST-Standardized Score p-values also fall on the 45 degree line compared with MiST under the null and alternative; however, they have greater variation. Under the alternative, the p-values for mediation effects are slighly more conservative whereas the p-values for the variance component are slightly anti-conservative.

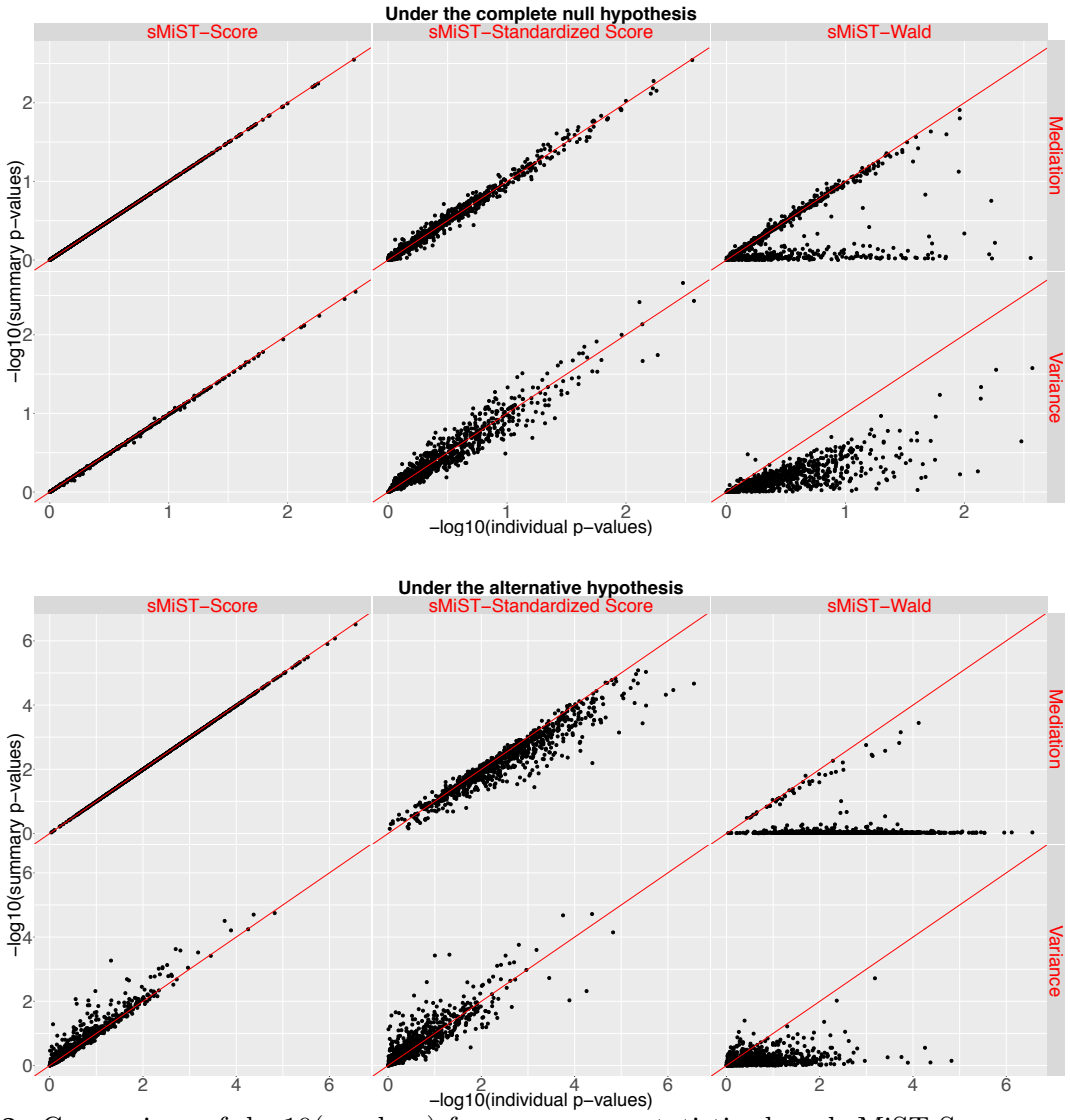

Fig 2.3. Comparison of -log10(p-values) from summary statistics based sMiST-Score, sMiST-Standardized Score, and sMiST-Wald vs. individual level data based MiST under the complete null hypothesis (top panel) and under the alternative hypothesis (bottom panel)

2.3.4 Additional Simulation Results

We assessed the power of sMiST and its comparison with MiST under a wide range of scenarios: (1) varying strength of the association of G with M with $R^2 = 0.05$, 0.2, and 0.8; (2) varying proportion of associated variants in the direct effects: Prop=0.1, 0.2, 0.4, 0.6, and 0.8; and (3) mis-specification of the model for M given G where the true link function is log but the linear link is used to fit the

model. As expected, as R^2 increases, the power for the mediation effect increases, while the power for the direct effect stay the same (S5 Table). As the proportion of variants with direct effects increases, the power for mediation effect is constant but the power for the direct effects increases. As a result, the power for the total effect of mediation and direct effects increases under both scenarios.

When the relationship of G and M is mis-specified, the power for the mediation effect is reduced substantially when $R^2 = 0.05$ but not as much when $R^2 = 0.2$ and 0.8 (S6 Table). Interestingly, testing of direct effects can pick up some of the power loss for mediation effects due to model mis-specification. The power for the total effects under model misspecification is nearly the same as the power when the model is correctly specified when $R^2 \geq 0.2$ or the proportion of variants with direct effects ≥ 0.6.

2.3.5 Performance of sMiST in real data analysis

An important input to sMiST or any summary statistics-based test statistics is the covariance matrix of the genetic variants. Instead of focusing on one or few genes, we evaluated the impact of the covariance matrix based on genome-wide real data analyses of GECCO studies for which we have individual level data for both outcomes and genotypes. Thus, we can directly compare the summary statistics-based test sMiST with the individual-level data based test MiST for a broad spectrum of genetic architecture and weight distribution in calculating predicted expression.

We obtained the summary statistics of marginal association log-odds ratio estimates and standard errors from GECCO data for sMiST to calculate the p-values for the mediator effect and variance component. In addition, using the individual level data, we obtained the mediation and variance component p-values using MiST, and we treated these p-values as the gold standard for sMiST to be compared with.

In reality, the LD structure is often not available from the same source where the summary statistics are generated; hence external reference population are used to provide the estimated LD matrix on the variants. To evaluate our proposed method under such situation, we conduct a genome-wide analysis with summary level information from two different cohorts, GWAS summary statistics from GECCO and LD matrices calculated from CORECT. We compare the p-values of fixed effects and variance components from our method to those obtained from MiST based on

individual level data in GECCO. From the scatter plots of the two sets of p-values as presented in Fig 2.4, we observe that the p-values on fixed effects and variance components from our method are comparable to the results from *MiST* using individual level data. The patterns of points aligning around the line of equality validate the proposed method under the situations when LD information from a similar external reference population is leveraged.

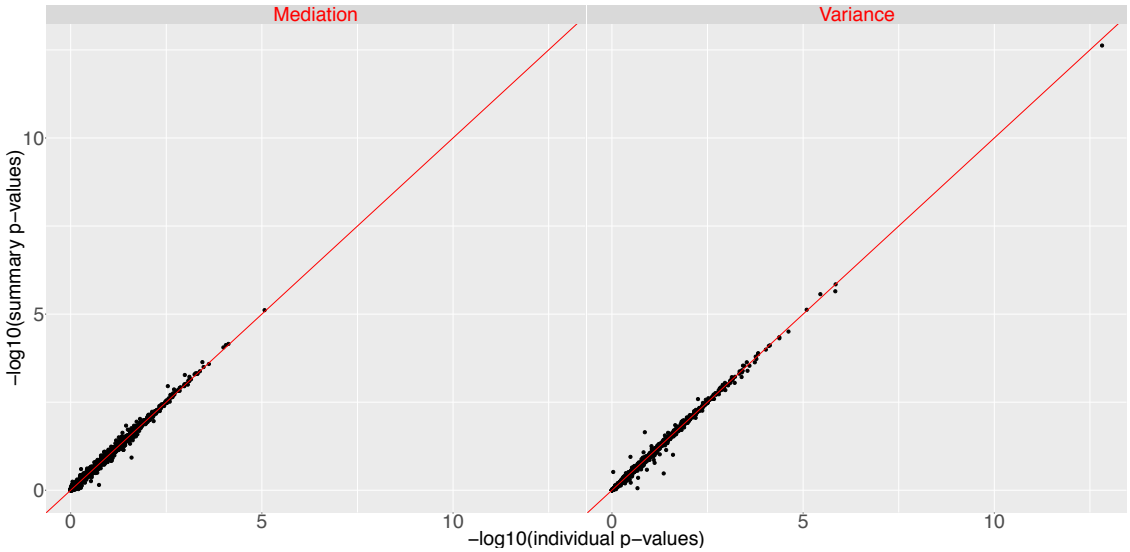

Fig 2.4. Comparison of sMiST using summary statistics from GECCO and LD matrices from CORECT with MiST with individual level data in GECCO

We then assessed the impact of the sample size of genotyping data needed for calculating the covariance matrix. We randomly sampled different sizes of sub-samples from GECCO and estimated the covariance of genotypes from the sub-samples. Fig 2.5a shows the scatter plots of $-$log10(p-values) of mediation and variance components obtained from sMiST with the covariance matrix based on $n = 1,000, 5,000$, and 10,000 samples, respectively, as compared with p-values from MiST. The p-values for sMiST and MiST generally fall on the 45 degree line; however, as the sample size becomes smaller, there are more and more outliers for the variance component test, where sMiST yields much smaller p-values compared to MiST. Upon close examination, these genes have an extreme correlation structure: all variants are in nearly perfect correlation with each other. For these extreme genes, the covariance estimates from small samples can be even more singular or perfectly singular. Although our method does not directly invert the whole covariance matrix for

the mediation test, for the variance component testing it still involves inverting $W^T \text{cov}(G) W$ while projecting out the mediation component. Therefore, in the situation of nearly singular matrix, it can be numerically unstable.

To avoid this numerical problem, we regularized the correlation matrix of G by adding λI, where I is the identity matrix, as in the ridge regression. Following the asymptotic consistency results of Knight and Fu (2000) [38] for penalized regression, we chose λ based on sample size (n) used in calculating the covariance matrix: $\lambda = \frac{1}{\sqrt{n}\log(n)}$, such that the parameter estimates are consistent as n increases. We performed the regularization for all genes, since for a gene that is of moderation correlation structure, its covariance matrix is insensitive to the regularization. Fig 2.5b shows the scatter plots of regularized sMiST compared to MiST and it is clear that all outliers are gone even when $n = 1,000$, and the regularization has minimal impact on the overall performance of sMiST. There are some points below the 45 degree line for the variance component test, suggesting sMiST may be slightly conservative. However, these generally occur when the p-values are large. When the p-values are small where they matter, sMiST even with regularization matches very well with MiST.

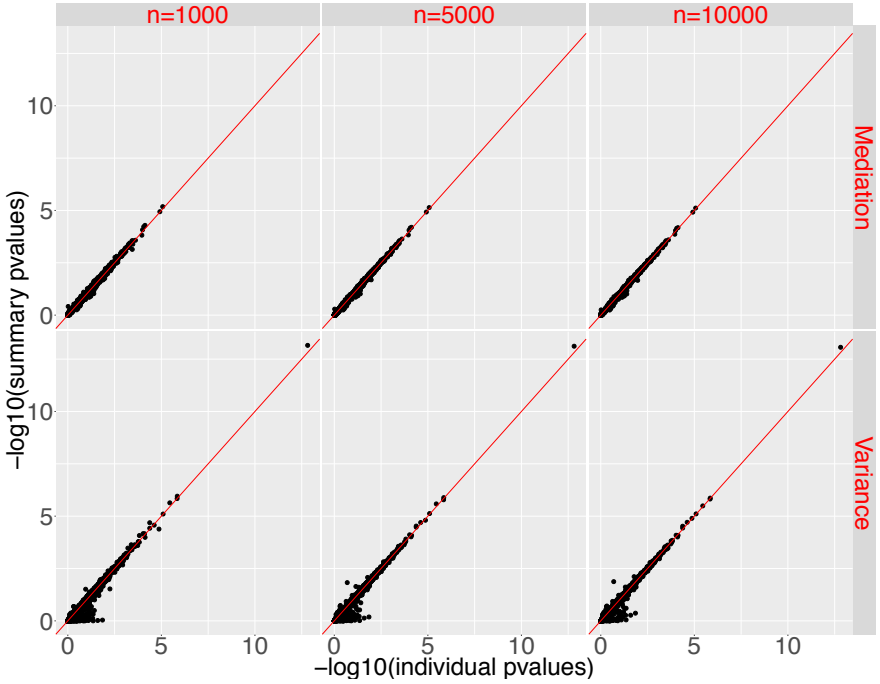

(a) Genotype covariance estimation without regularization

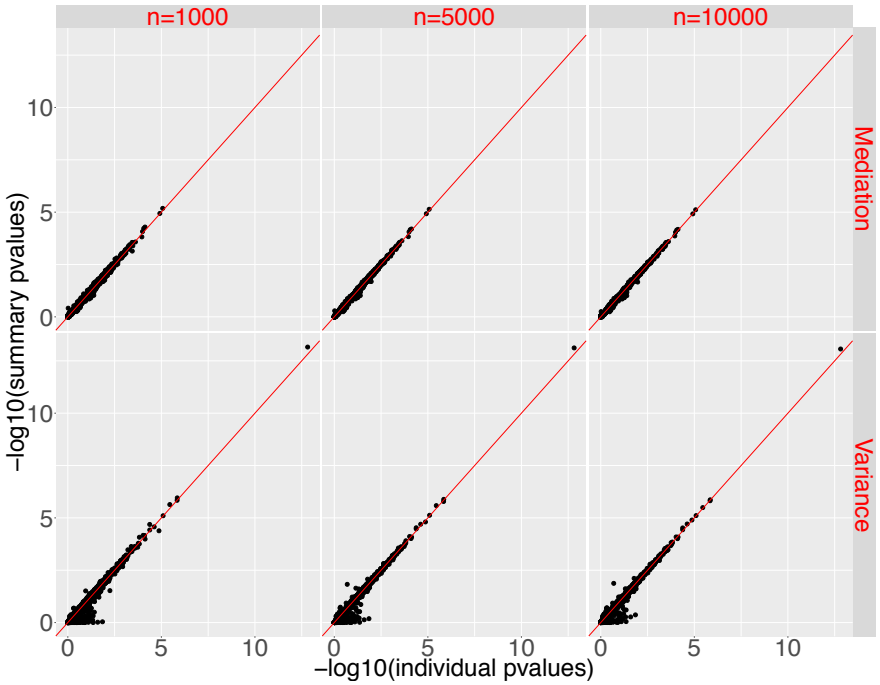

(b) Genotype covariance estimation with regularization

Fig 2.5. Effect of sample sizes in calculating the genotype covariance matrix on the mediation and variance component p-values for sMiST without regularization (top panel) and with regularization (bottom panel)

2.3.6 Comparison of sMiST with S-PrediXcan and TWAS

We compared the p-values for the predicted gene expression from sMiST (sMiST-mediation) as well as the two popular summary statistics-based methods S-PrediXcan [5] and TWAS [27] with the p-values calculated based on individual level data from GECCO, as described as in the previous section (Fig 2.6). The -log10(p-value)s fall around the 45 degree line for all methods, suggesting these summary statistics-based methods generally agree with individual level data-based p-values. Both sMiST and S-PrediXcan, which are nearly perfectly correlated with each other (S8 Fig), have a higher correlation with individual-level data based p-values than TWAS. Both sMiST and S-PrediXcan have the same estimator $\widehat{\gamma} = W^T \text{Cov}(G) W)^{-1} W^T D \widehat{\beta}^*$ but with slightly different variance estimator, where S-PrediXcan uses summary statistics, se$(\widehat{\beta}_p^*)$ and the MAF of the pth SNP, to approximate the variance of the outcome while sMiST approximates the correlation of β^* by the correlation matrix of genotypes. TWAS takes the weighted sum of Z statistics, which differs from S-PrediXcan and sMiST-mediation by a factor of the proportion of the phenotype explained by a SNP's genotype[5, 27]. In general, this factor is close to 1; hence, we do not expect substantial difference between TWAS and S-PrediXcan and sMiST-mediation as shown in Fig 2.6.

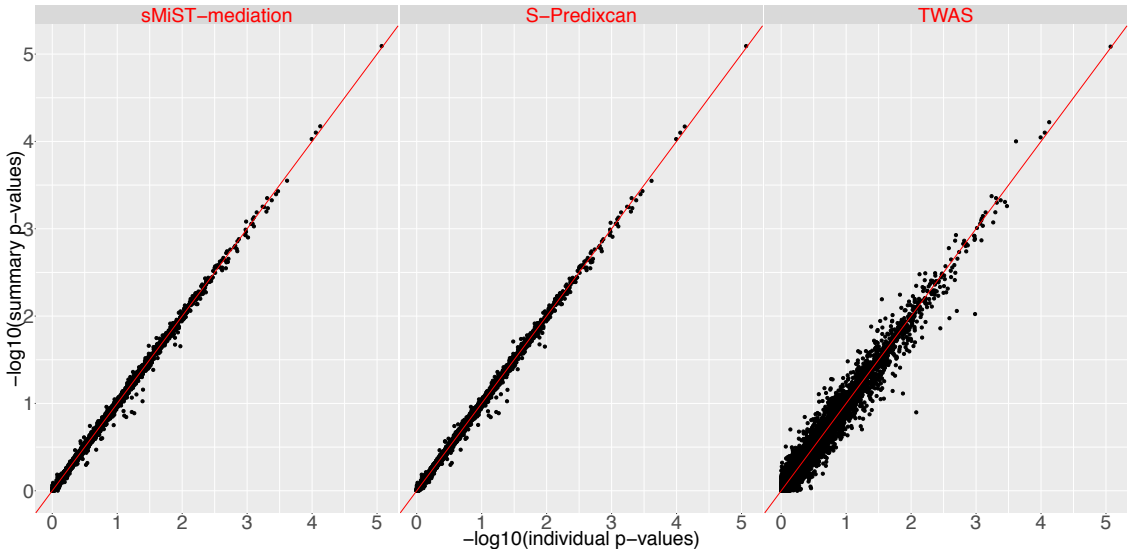

Fig 2.6. Scatter plots of −log10(p-values) from summary statistics-based methods sMiST mediation, S-PrediXcan, and TWAS vs. −log10(p-values) based on individual level data.

2.4 Discussion

We proposed a versatile set-based approach using summary statistics, sMiST, for testing the total effect of multiple mediators and direct effect. The computational time for sMiST is much faster than individual-level data based MiST. For example, for a dataset of 10,000 cases and 10,000 controls, MiST takes 0.955 seconds but sMiST takes only 0.022 seconds to calculate the p-value. sMiST also provides p-value for each mediator in the presence of other mediators under the assumption of $\tau^2 = 0$ and p-value for direct effects conditional on all the mediators. When there is evidence for mediator effect, we may further perform co-localization analysis using methods proposed previously [101, 24, 29, 93] to examine whether any specific genetic variant is pleiotropic to both the mediator and disease risk.

We offer a few observations from our extensive simulation and real data-based studies. Generally speaking, larger sample sizes lead to better estimates of the covariance matrix, and thus better alignment with results from individual level data. With growing external genotyping databases, having a large enough sample size to calculate the covariance is generally not a problem. To prevent numerical problems for genes with extreme correlation structures, we applied regularization for all genes, irrespective of correlation structures, in the hope that the regularization will minimize the numerical instability for genes with extreme correlation structures, while having minimal impact on other genes. Using this approach, we can mitigate bias that may arise due to high LD regions with a sample size as low as 1000. However, this regularization could potentially lower the power of our method, and yield slightly more conservative results. Such negative impact will be diminished, as our regularization is a function of sample size and it approaches 0 as the sample size increases.

Under all four scenarios, weaker correlation between confounder and fixed effects leads to better alignment between individual-level mediation effect p-values and summary-based mediation effect p-values, while the effect size of confounder does not affect the performance much. In particular, when the correlation is at the highest (0.4), summary statistics based mediation effect p-values can be somewhat over-conservative. The performance of the direct effect is not affected because of the orthogonalization of mediator and genotype in the data generation.

Generally, sMiST gains power by testing for the total association of mediation and direct effects compared to testing for only the mediation effect. However, when there is no direct effect, sMiST

may lose some power due to testing an additional parameter of variance component that has null effect. More powerful combination methods can be employed to combine the test statistics for mediation and variance component to mitigate this impact[79]. These combination methods rely on only the p-values or test statistics and can be applied to sMiST. When the direct effect has a different sign than the mediated effect (inconsistent mediator) [56], the power for testing mediation effect and sMiST can be considerably reduced; however,if the direct effect is sufficiently strong, the power for mediation can approach to 1 (S7 Table). Under this situation, one needs to be cautious about the interpretation of mediation. Methods have been proposed to test the inconsistent mediation effect for one variable (here, one genetic variant) [75]. However, there lacks research for testing inconsistent mediation effect with multiple genetic variants. It is probably unlikely that a mediator is inconsistent with all genetic variants in practical situations. Nevertheless, it is a topic that warrants future research.

From our application of sMiST to CRC GWAS data, we identified three novel genes contributing to CRC risk that were not previously identified in the single variant analysis of the same dataset. *NT5DC2* has been shown to markedly reduce the expression of Fyn, a Src family proto-oncogene and has been implicated in glioblastoma[26], though not yet linked to CRC susceptibility. Of interest there are a couple of other nearby genes in the region, *NISCH* and *SEMA3G*, which share gene-linked regulatory elements, are expressed in T cells, and have been shown to play a role in CRC [2, 36]. For *VPREB3*, the protein encoded by this gene is thought to be involved in B-cell maturation, and may play a role in assembly of the pre-B cell receptor. A nearby gene, *CABIN1*, plays an important role in the T-cell receptor-mediated signal transduction pathway. Expression of this gene has previously been associated with CRC recurrence [46]. *PLD6* is a phospholipase of the outer mitochondrial membrane and acts as a regulator of mitochondrial shape by facilitating mitochondrial fusion [14]. Interestingly, a previous study showed that depletion of *PLD6* prevents *MYC* repression of *ANKRD1* and several other target oncogenes of YAP/TAZ. It has been hypothesized that mitochondrial dynamics, influenced in part by *PLD6*, might be an integral part of *MYC*-induced anabolic metabolism [78]. For *ANKRD10*, it is in a region dense with cancer-related genes (*CDKN2A CDKN2B*) and thus it is not surprising there may be multiple variants with independent regulatory effets. There is no report about the function of this gene; however, its paralog *ANKRD6* recruits CKI-epsilon to the beta-catenin degradation complex and

allows efficient phosphorylation of beta-catenin, thereby inhibiting beta-catenin/Tcf signals [73]. As such, *ANKRD10* may have similar function in regulation of the Wnt pathway as *ANKRD6*.

It is of great interest to study the effect of interplay between mediation variables M and genetic variants G on the phenotypes. Huang et al. (2014)[33] derived $g(E(Y|G,X)$ under the interaction model by integrating out M and found that the model depends not only on the linear terms of confounders X and G's but also on the cross-product between X and G's and the second order of G's. Conceptually the proposed sMiST using summary statistics can be extended to study the interaction effect. However, the currently available summary statistics on marginal association do not permit modeling of interaction effects. Summary statistics on pairwise interaction among G as well as interaction between X and G will be needed in order to study the interaction effect of mediation.

2.5 Methods and Materials

2.5.1 Ethics Statement

This study uses the summary statistics of genome-wide association studies for colorectal cancer, and the de-identified genotyping data from GECCO, CCFR and CORECT. The study was approved by the Institutional Review Board at the Fred Hutchinson Cancer Research Center in Seattle, WA under file numbers 3995 and 6501.

2.5.2 Derivation of `sMiST`

Assume that there are no confounders. We first focus on linear regression model. Consider a study of n independent individuals. Let Y be a $n \times 1$ vector of outcomes, G a $n \times P$ matrix of P variants for the n individuals, W a $P \times K$ matrix with W_{pk} being the regression coefficient of pth variant for the kth mediator, and D is a diagonal matrix of cov(G). Further, let $\widehat{\beta}^* = (\widehat{\beta}^*_1, \ldots, \widehat{\beta}^*_P)^T$. For simplicity, we center G and Y so that the intercept is 0. It is easy to see that

$$n^{1/2}(\widehat{\beta}^* - \beta^*) = (\frac{D}{n})^{-1} n^{-1/2} \{\sum_{i=1}^{n} G_{i1}(Y_i - G_{i1}\beta^*_1), \ldots, \sum_{i=1}^{n} G_{iP}(Y_i - G_{iP}\beta^*_P)\}^T,$$

where β^* is the limit of $\widehat{\beta}^*$. As n for GWAS typically is very large, under regularity conditions, by the continuous mapping theorem and the central limit theorem, $n^{1/2}(\widehat{\beta}^* - \beta^*)$ converges to a multivariate normal distribution with mean 0 and covariance of $\widehat{\beta}^*$. Under $\tau^2 = 0$, the estimator for the mediation effect is

$$\begin{aligned}\widehat{\gamma} &= \{W^T \text{cov}(G) W\}^{-1} W^T G Y \\ &= \{W^T \text{cov}(G) W\}^{-1} W^T D (D^{-1} G Y) \\ &= \{W^T \text{cov}(G) W\}^{-1} W^T D \widehat{\beta}^*.\end{aligned}$$

We can obtain $\text{cov}(\widehat{\gamma})$ as

$$\text{cov}(\widehat{\gamma}) = \{W^T \text{cov}(G) W\}^{-1} W^T D \text{cov}(\widehat{\beta}^*) D^T W \{W^T \text{cov}(G) W\}^{-1},$$

where

$$\text{cov}(\hat{\beta}^*) = \begin{bmatrix} \text{se}(\hat{\beta}_1^*) & & \\ & \ddots & \\ & & \text{se}(\hat{\beta}_P^*) \end{bmatrix} \text{cor}(G) \begin{bmatrix} \text{se}(\hat{\beta}_1^*) & & \\ & \ddots & \\ & & \text{se}(\hat{\beta}_P^*) \end{bmatrix}.$$

Here $\text{cor}(G)$ is the correlation matrix of G, which is the exact correlation of $\widehat{\beta}^*$ under the null but an approximation under the alternative. Then, the test statistic for the mediation effect is

$$U_\gamma = \widehat{\gamma}^T \text{cov}(\widehat{\gamma})^{-1} \widehat{\gamma}.$$

Under $H_0 : \gamma = 0$ and $\tau^2 = 0$, $U_\gamma \sim \chi^2_K$. The test statistic for the kth mediator $\gamma_k = 0$ is $\widehat{\gamma}_k / \text{se}(\widehat{\gamma}_k) \sim N(0, 1)$ for $k = 1, \ldots, K$, where $\text{se}(\widehat{\gamma}_k)$ is the square root of the kth diagonal element of $\text{cov}(\widehat{\gamma})$.

For the variance component test, we derive the test statistic under $\tau^2 = 0$. By this, the variance component test adjusts for the mediator effect, and is independent of U_γ (Su et al. 2018) [79]. When combining the two test statistics using e.g., weighted linear combination, if they were correlated, the search space for the weight would be restricted. Independent test statistics can circumvent such restriction. Further, due to the non-conventional distribution for the variance component test, having independent test statistics can avoid the complex correlation structure and make it

straightforward to derive the distribution of the combined test statistics. This is very useful, as it allows us to calculate p-values fast in a genome-wide search. Further, there are many methods to combine independent test statistics including popular p-values-based Fisher's and Tippett's combinations and data-adaptive combinations, which can be readily applied to our independent test statistics for mediation effect and variance component [48, 79].

The key to deriving the variance component test statistic conditioning on $\widehat{M}$ is that, as opposed to using $\widehat{\beta}_p^*$, we derive the summary statistics for each of P genetic variants $\widehat{\alpha}_p^*$ by conditioning out $\widehat{M}_k, k = 1, \ldots, K$, which are given by

$$\widehat{\alpha}_p^* = A \begin{bmatrix} \widehat{\beta}^* \\ \widehat{\beta}_p^* \end{bmatrix}, \quad \text{and} \quad A = (0, 0, ..., 0, 1) C^{-1} \begin{bmatrix} W^T D & 0 \\ 0 & D_p \end{bmatrix},$$

where D_p is the pth diagonal entry of D, and C is a $(K+1)\times(K+1)$ matrix with $C_{jk} = W_j^T \text{cov}(G) W_k$ with W_j and W_k the jth and kth columns of W, and $C_{(K+1).} = C_{.(K+1)}^T = [\text{cov}(G)_{p.} W, D_p]$. The covariance of $\widehat{\alpha}^*$ can then be straightforwardly obtained as $\text{cov}(\widehat{\alpha}^*) = A\text{cov}(\widehat{\beta}^*)A^T$. The test statistic for the variance component is

$$U_{\tau^2} \quad = \quad U_{\alpha^*}^T U_{\alpha^*},$$

where $U_{\alpha^*} = \widehat{\alpha}^* / \text{var}(\widehat{\alpha}^*)$. Under the null, the variane component test U_{τ^2} follows a mixture of χ_1^2 with the mixture weighting as the eigenvalues of matrix $D_{\alpha^*} R^* D_{\alpha^*}$, where D_{α^*} is a diagonal matrix with $1/\text{se}(\widehat{\alpha}^*)$, and R^* is the correlation matrix of $\widehat{\alpha}^*$, both of which can be easily obtained from $\text{cov}(\widehat{\alpha}^*)$.

Under the logistic regression model, by the Taylor's expansion, we have $\widehat{\gamma} - \gamma = (W^T G^T \Delta G W)^{-1} W^T G^T (Y - \mu) + o_p(n^{-1/2})$, where Δ is a diagonal matrix of $\mu(1-\mu)$ and $\mu = \text{E}(Y|G)$. Here G is centered. For simplicity of presentation, we omit any differences in the order of $o_p(n^{-1/2})$ because for the $\sqrt{n}$ asymptotic normality, these differences will be 0. Assume Δ is constant on the diagonal, we can reorganize $\widehat{\gamma} - \gamma = (W^T G^T G W)^{-1} W^T D (D\Delta)^{-1} G^T (Y - \mu) = \{W^T \text{cov}(G) W\}^{-1} W^T D (\widehat{\beta}^* - \beta^*)$. When the effects are modest, $\gamma \approx \{W^T \text{cov}(G) W\}^{-1} W^T D \beta^*$. As a result, $\widehat{\gamma} = \{W^T \text{cov}(G) W\}^{-1} W^T D \widehat{\beta}^*$, which has the exactly same form as $\widehat{\gamma}$ under the linear model. Under the null, $U_\gamma \sim \chi_K^2$. We note that Δ is constant under the null. However, even when the null does not hold, Hu et al. (2013)[31]

shows Δ does not strongly depend on covariates. Our extensive simulation also shows the proposed test statistics perform well under this approximation. Similar to the derivation for $\widehat{\gamma}$, we can also obtain the test statistic for the variance component under the logistic regression model, which has the same form as the variance component test under the linear model.

When there are confounders, the derivation for test statistics using summary statistics becomes complicated. Under the liner model, $\widehat{\gamma}$ is the weighted sum of XY and W^TGY with the weight as the corresponding elements in the inverse of the covariance matrix of (X, W^TG). If the effects of confounders are 0 or X and G are independent, then $\widehat{\gamma}$ only depends on G and the above test statistics are the same. If the effects of confounders are not 0 and X and G are correlated, $\widehat{\gamma}$ will depend on X; however, we observe our proposed test statistics hold very well based on our extensive simulations and real data analysis, suggesting that our test statistics are robust even in the presence of confounders.

2.5.3 Datasets

Summary statistics (log-odds ratio estimates and standard errors of genome-wide genetic variants) were obtained from a meta-analysis of GWAS studies from three large consortia, including: the Genetics and Epidemiology of Colorectal Cancer Consortium (GECCO), the Colon Cancer Family Registry (CCFR), and the Colorectal Cancer Transdisciplinary Study (CORECT) [34]. In total, the consortia have 54,454 cases and 64,163 controls of European Ancestry. The genotyping data were imputed to the Haplotype Reference Consortium [59] with ∼40 million variants. The linkage disequilibrium or covariance of the genotypes was calculated using individual level data from GECCO ($n = 26,554$). The details of study designs, genotyping QC, association and meta-analysis can be found elsewhere [34]. We downloaded the weights or regression coefficients of cis (< 1Mb from gene start or end) regulatory variants associated with gene expression for whole blood from the PredictDB Data Repository (`http://predictdb.org/`). The regression coefficients were estimated from a regularized linear regression model with elastic-net penalty [22]. The models were developed using a reference dataset of genotype and whole blood transcriptome data from 922 normal individuals from Depression Genes and Networks [7]. We considered genes of which the predictive $R^2 > 0.01$ in the gene expression model, resulting in 8,893 genes. Using regulatory information derived from

whole blood is relevant for studying susceptibility to CRC for two primary reasons. First, a subset of the immune-relevant cell types present in whole blood are relevant to CRC risk. In particular, T-cell populations of the intestine play a critical role in orchestrating the careful balance between immune activation and tolerance at the mucosal layer. Second, whole blood is the largest reference transcriptome dataset. As many tissues and cell types share common heritability in gene expression, in some cases whole blood models are preferred for building robust predictive models because of their large sample size.

2.5.4 Performance of `sMiST` *in simulation*

We selected three genes (*CXCR1*, *C18orf32*, and *ARHGAP11A*) from the eQTL database from the PredictDB Data Repository. Both *CXCR1* and *C18orf32* are of moderate size (∼40 genetic variants), while *ARHGAP11A* is larger set (92 variants). In terms of the LD structure, both *C18orf32* and *ARHGAP11A* show largely independence or weak correlation among variants; however, *CXCR1* contains several clusters of variants that are nearly perfectly correlated.

We used the GWAS genotyping data from GECCO as the template ($n = 26,554$), and generated the disease status under the generalized linear regression model (2.1) with logit link. We set the intercept to be -3, yielding about 5% baseline disease probability. We generated the mediator $M = cB + \epsilon$, where $B = \sum_{p=1}^{P} w_p G_p$ was the genetically predicted gene, and $\epsilon \sim N(0, \sigma^2)$. Here, c and σ^2 were set such that variation of M explained by G is 0.05, 0.20, and 0.80, while keeping the variance of M constant, which we set to be 1.5. The weights $\{w_p, p = 1, \ldots, P\}$ were obtained from the PredictDB Data Repository. The effect of the mediator M was set to be $\log(2)$. Further, we let the random effects $\delta_p \sim N(0, 0.05)$. To mimic the individual variant contributions that were not explained by predicted gene expression, we took the residuals from regressing the sum of direct effect $\sum_{p=1}^{P} \delta_p I_p G_p$ on B where I_p is 1 if pth variant has a direct effect and 0 otherwise, and added the residuals as direct effects to the model. The proportion of variants with direct effects was set to be 0.1, 0.2, 0.4, 0.6, 0.8, and 1.0. To save space, for most simulations presented in the main text, we set $R^2 = 0.05$ and all variants have direct effects unless otherwise noted. Results for other parameter settings are provided in S4 – S7 Table. For each simulation setting, we generated 1000 simulated data sets, each set consisting of 1000 cases and 1000 controls.

Implementation

We implemented `sMiST` using R programming language. The software is available for download at https://research.fhcrc.org/hsu/en/software.html.

Supporting information

S1 Fig. Gene *NT5DC2* (a) forest plot of marginal association of genetic variants in *NT5DC2*; (b) forest plot of conditional association adjusting for predicted gene expression; (c) pairwise linkage disequilibrium (LD) R^2. The p-values < 0.05 are labeled on the left margin in (a) and (b). The weights used in calculating gene expression are labeled on the right margin in (b).

S2 Fig. Gene *VPREB3* (a) forest plot of marginal association of genetic variants in *VPREB3*; (b) forest plot of conditional association adjusting for predicted gene expression; (c) pairwise linkage disequilibrium (LD) R^2. The p-values < 0.05 are labeled on the left margin in (a) and (b). The weights used in calculating gene expression are labeled on the right margin in (b).

S3 Fig. Gene *PLD6* (a) forest plot of marginal association of genetic variants in *PLD6*; (b) forest plot of conditional association adjusting for predicted gene expression; (c) pairwise linkage disequilibrium (LD) R^2. The p-values < 0.05 are labeled on the left margin in (a) and (b). The weights used in calculating gene expression are labeled on the right margin in (b).

S4 Fig. Gene *ANKRD10* (a) forest plot of marginal association of genetic variants in *ANKRD10*; (b) forest plot of conditional association adjusting for predicted gene expression; (c) pairwise linkage disequilibrium (LD) R^2. The p-values < 0.05 are labeled on the left margin in (a) and (b). The weights used in calculating gene expression are labeled on the right margin in (b).

S5 Scatter plots of -log10(p-values) of sMiST (Y-axis) and MiST (X-axis) for mediation and variance component for gene *CXCR1* under various confounding situations.

S6 Fig. Pairwise comparison of $-\log 10$(p-values) between sMiST-mediation, S-PrediXcan, and TWAS.

S1 Table. Summary of OR (odds ratio) estimate, 95% CI (confidence interval) and p-value of predicted gene expression for the novel loci.

S2 Table. Sequential Analysis Results of the novel loci.

S3 Table. Type 1 error of sMiST and MiST with varying R^2 and proportion of

variants with direct effects (Prop) for gene *CXCR1*.

S4 Table. Power performance of sMiST vs. MiST with varying R^2 and proportion of variants with direct effects (Prop) for gene *CXCR1*.

S5 Table. Power performance of sMiST vs. MiST under model misspecification with varying R^2 and proportion of variants with direct effects for gene *CXCR1*.

S6 Table. Power performance of sMiST vs. MiST under inconsistent mediator, when $R^2 = 0.05$ and the proportion of variants with direct effects is 0.80 for gene *CXCR1*.

2.6 Supplementary Materials

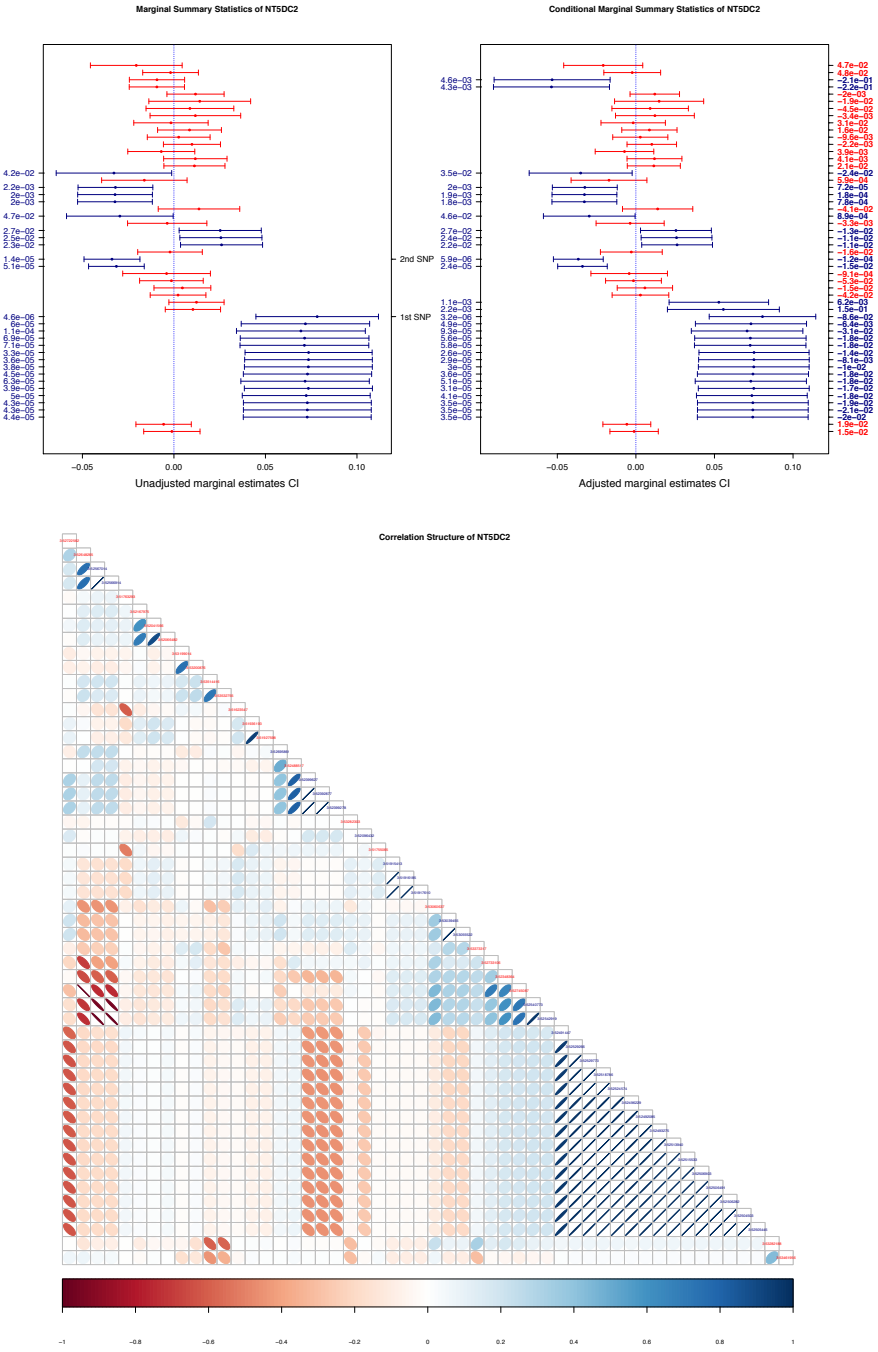

Fig S1. Gene *NT5DC2*: (a) forest plot of marginal association of genetic variants in *NT5DC2*; (b) forest plot of conditional association adjusting for predicted gene expression; (c) pairwise linkage disequilibrium (LD) R^2. The p-values < 0.05 are labeled on the left margin in (a) and (b). The weights used in calculating gene expression are labeled on the right margin in (b)

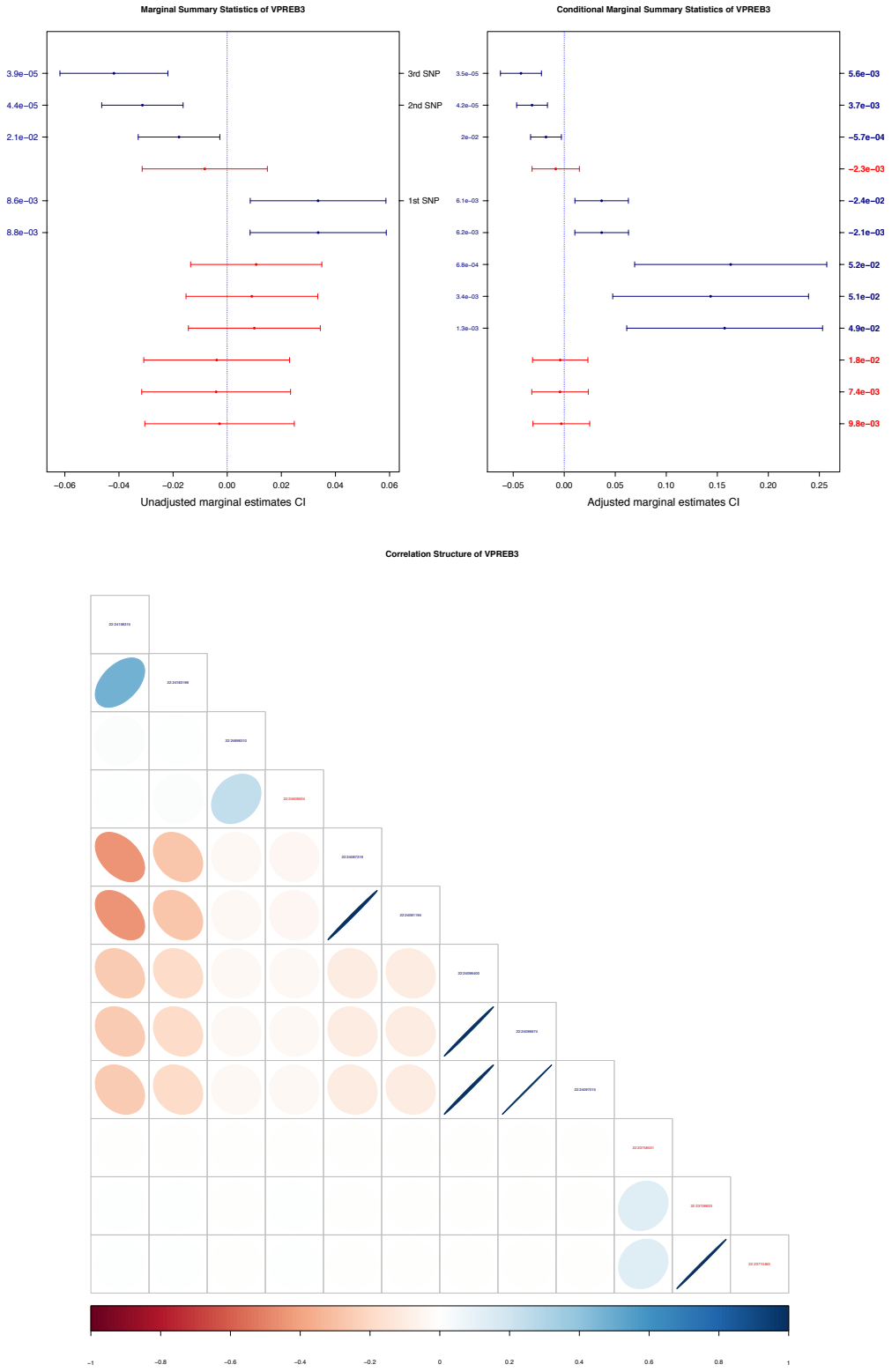

Fig S2. Gene *VPREB3*: (a) forest plot of marginal association of genetic variants in *VPREB3*; (b) forest plot of conditional association adjusting for predicted gene expression; (c) pairwise linkage disequilibrium (LD) R^2. The p-values < 0.05 are labeled on the left margin in (a) and (b). The weights used in calculating gene expression are labeled on the right margin in (b).

Fig S3. Gene *PLD6*: (a) forest plot of marginal association of genetic variants in *PLD6*; (b) forest plot of conditional association adjusting for predicted gene expression; (c) pairwise linkage disequilibrium (LD) R^2. The p-values < 0.05 are labeled on the left margin in (a) and (b). The weights used in calculating gene expression are labeled on the right margin in (b).

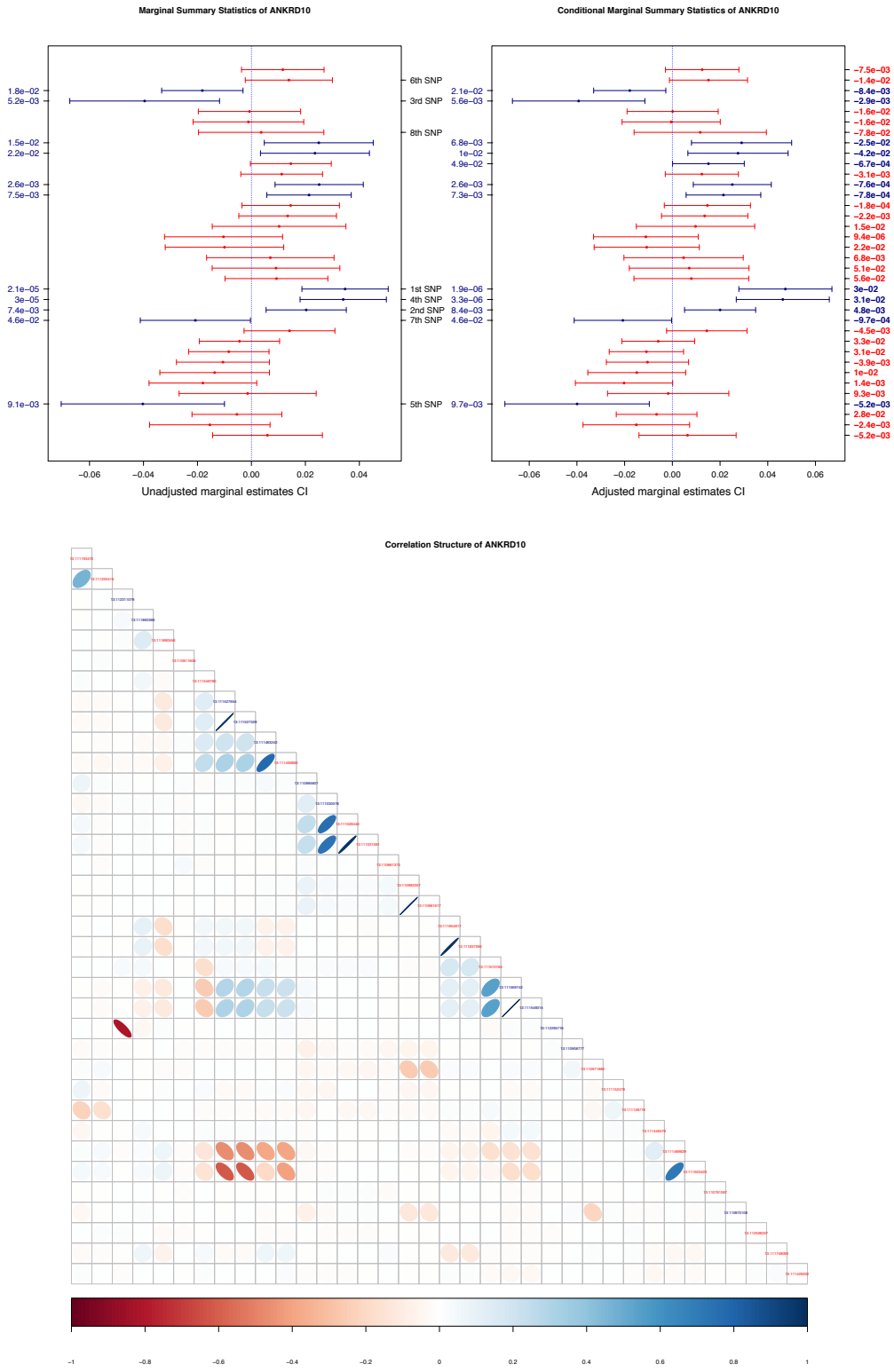

Fig S4. Gene *ANKRD10*: (a) forest plot of marginal association of genetic variants in *ANKRD10*; (b) forest plot of conditional association adjusting for predicted gene expression; (c) pairwise linkage disequilibrium (LD) R^2. The p-values < 0.05 are labeled on the left margin in (a) and (b). The weights used in calculating gene expression are labeled on the right margin in (b).

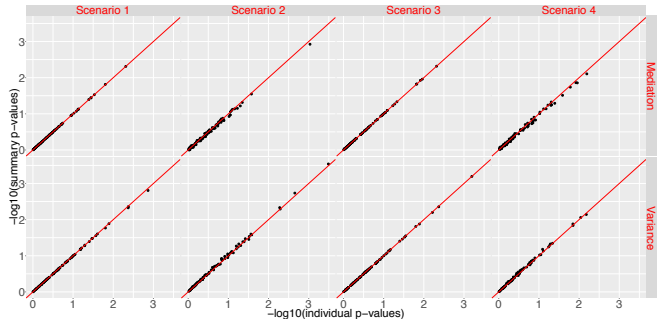

(a) S1: complete null

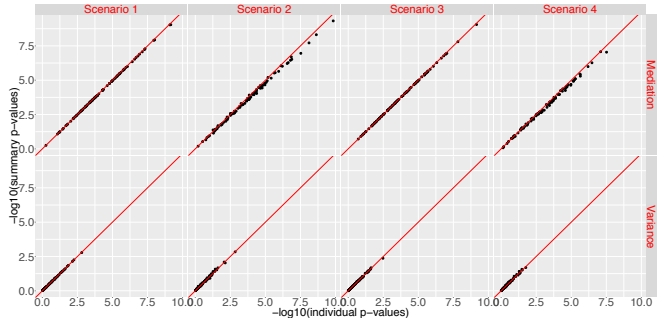

(b) S2: mediation null, variance component alternative

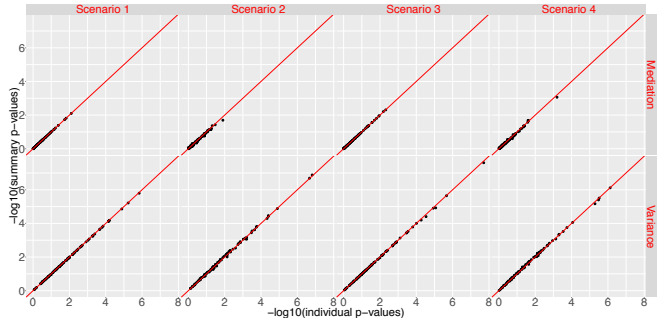

(c) S3: mediation alternative, variance component null

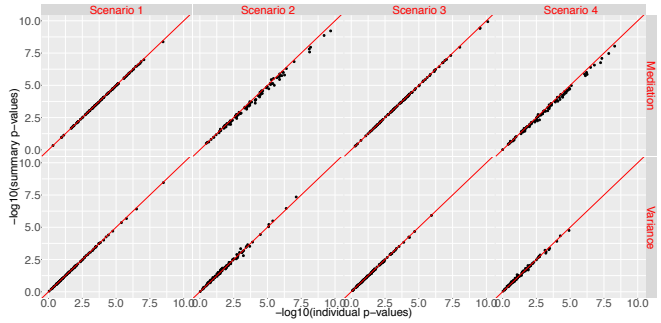

(d) S4: both mediation and variance component alternative

Fig S5. Scatter plots of -log10(p-values) of sMiST (Y-axis) and MiST (X-axis) for mediation and variance component for gene *CXCR1* under various confounding situations. Scenario (1) cor(X, M) = 0.1 and effect of X = 0.3; (2) cor(X, M) = 0.4 and effect of X = 0.3; (3) cor(X, M) = 0.1 and effect of X = 0.9; (4) cor(X, M) = 0.4 and effect of X = 0.9.

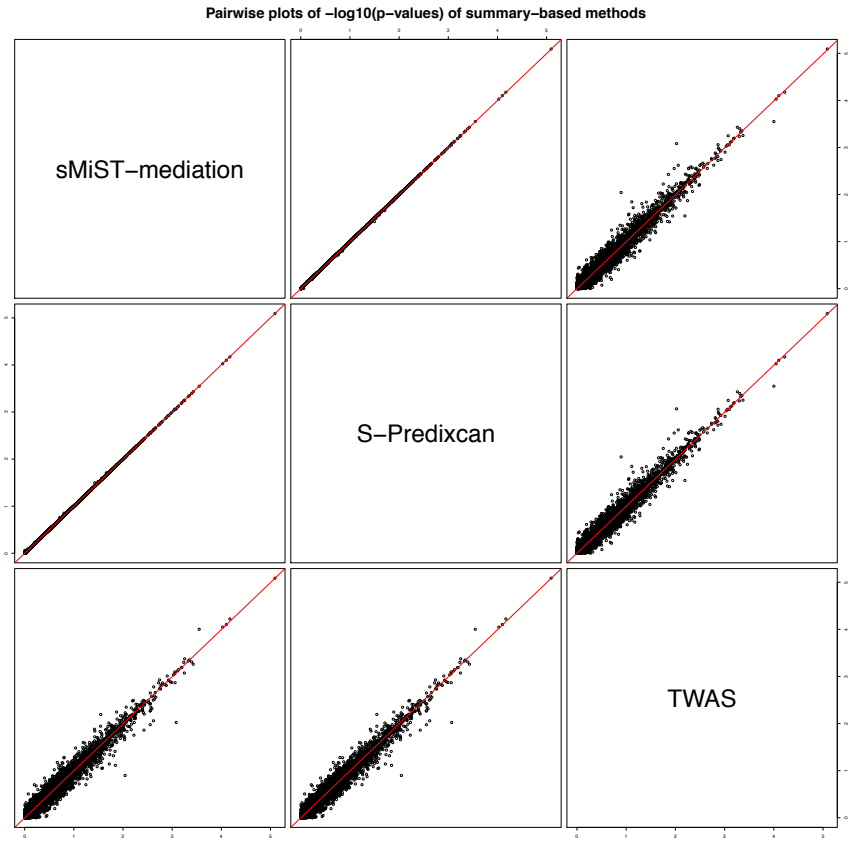

Fig S6. Pairwise comparison of $-\log 10$(p-values) between sMiST-mediation, S-PrediXcan, and TWAS.

Table S1. Summary of OR (odds ratio) estimate, 95% CI (confidence interval) and p-value of predicted gene expression for the three novel loci (*NT5DC2, PLD6, VPREB3, VPREB*) and 1 novel secondary locus (*ANKRD10*).

Novel genes: No known loci within 1Mb									
Gene Info				**Unadjusted**			**Adjusted**		
Gene	R^2	N SNPs	chr	OR	95% CI	p-value	OR	95% CI	p-value
NT5DC2	0.35	52	3	1.00	[0.97,1.03]	0.96	1.00	[0.97,1.05]	0.95
VPREB3	0.04	12	22	1.00	[0.85,1.17]	0.99	~	~	~
PLD6	0.25	36	17	1.03	[0.98,1.10]	0.25	1.03	[0.97,0.94]	0.29
Novel secondary genes: $\geq$ 1 known loci within 1mb									
Gene Info				**Unadjusted**			**Adjusted**		
genename	R^2	N SNPs	chr	OR	95% CI	p-value	OR	95% CI	p-value
ANKRD10	0.06	36	13	1.04	[0.94,1.15]	0.48	1.04	[0.94,1.04]	0.43

Table S2. Sequential Analysis Results of the 3 novel loci (*NT5DC2, PLD6, VPREB3, VPREB*) and 1 novel secondary locus (*ANKRD10*). "Pred.Exp p-value" is the p-value for predicted gene expression. "Random p-value" is the p-value for the variance component of the random effects, after adjusting for genetic variants in "SNPs adjusted sequentially".

SNPs adjusted sequentially	Pred.Exp p-value	Random p-value
NT5DC2	0.95	2.03e-06
3:52491447_C/A	0.40	3.12e-03
3:53039455_G/A	0.08	0.23
PLD6	0.29	9.12e-07
17:17140683_A/G	0.13	9.05e-04
17:17141330_T/G	0.13	8.92e-04
17:16883680_G/A	0.8	0.49
VPREB3	0.99	1.41e-06
22:24087319	0.43	1.70e-04
22:24183198	0.84	0.04
22:24898310	0.93	0.41
ANKRD10	0.43	2.39e-05
13:111559742_G/A	0.04	0.05
13:112295716_G/A	0.02	0.55
13:111860386_A/G	0.02	0.63
13:111549315_C/T	0.02	0.63
13:110970108_T/C	0.02	0.73
13:111220415_C/T	0.05	0.87
13:110908777_T/G	0.05	0.94
13:111549790_C/T	0.17	0.94

Table S3. Type 1 error of sMiST and MiST with varying R^2 and proportion of variants with direct effects (Prop)† for gene *CXCR1*.

		Mediation		Variance		Fisher's Combination	
R^2	Prop	MiST	sMiST	MiST	sMiST	MiST	sMiST
0.050	0.200	0.044	0.044	0.052	0.052	0.056	0.056
0.200	0.200	0.044	0.044	0.052	0.052	0.056	0.056
0.800	0.200	0.044	0.044	0.052	0.052	0.056	0.056
0.050	0.400	0.043	0.043	0.046	0.045	0.056	0.054
0.200	0.400	0.043	0.043	0.046	0.045	0.056	0.054
0.800	0.400	0.043	0.043	0.046	0.045	0.056	0.054
0.050	0.600	0.051	0.051	0.054	0.052	0.045	0.045
0.200	0.600	0.051	0.051	0.054	0.052	0.045	0.045
0.800	0.600	0.051	0.051	0.054	0.052	0.045	0.045
0.050	0.800	0.052	0.052	0.047	0.044	0.057	0.056
0.200	0.800	0.052	0.052	0.047	0.044	0.057	0.056
0.800	0.800	0.052	0.052	0.047	0.044	0.057	0.056

$^\dagger \gamma = b = 0$

Table S4. Power performance of sMiST vs. MiST with varying R^2 and proportion of variants with direct effects (Prop)† for gene *CXCR1*.

		Mediation		Variance		Combined	
R^2	Prop	MiST	sMiST	MiST	sMiST	MiST	sMiST
Varying R^2							
0.050	0.400	0.167	0.167	0.534	0.530	0.536	0.534
0.200		0.689	0.689	0.502	0.501	0.826	0.822
0.800		0.770	0.770	0.520	0.512	0.878	0.877
Varying prop of variants with direct effects							
0.200	0.100	0.681	0.681	0.173	0.172	0.641	0.640
	0.200	0.711	0.712	0.306	0.300	0.739	0.739
	0.400	0.689	0.689	0.502	0.501	0.826	0.822
	0.600	0.678	0.680	0.737	0.732	0.909	0.907
	0.800	0.705	0.705	0.850	0.848	0.949	0.946

$^\dagger\gamma = 0.1, b = 1.7$

Table S5. Power performance of sMiST vs. MiST under model misspecification with varying R^2 and proportion of variants with direct effects† for gene *CXCR1*.

		Mediation		Variance		Combined	
R^2	Prop	True	Misspec	True	Misspec	True	Misspec
0.050	0.200	0.763	0.494	0.216	0.323	0.774	0.591
0.200	0.200	0.793	0.744	0.294	0.301	0.806	0.772
0.800	0.200	0.775	0.769	0.315	0.305	0.814	0.802
0.050	0.400	0.782	0.515	0.410	0.547	0.840	0.763
0.200	0.400	0.787	0.731	0.504	0.535	0.878	0.862
0.800	0.400	0.771	0.751	0.563	0.548	0.880	0.864
0.050	0.600	0.759	0.460	0.568	0.712	0.885	0.835
0.200	0.600	0.773	0.707	0.724	0.738	0.925	0.898
0.800	0.600	0.767	0.740	0.734	0.726	0.927	0.918
0.050	0.800	0.773	0.457	0.658	0.807	0.919	0.889
0.200	0.800	0.763	0.702	0.795	0.809	0.947	0.940
0.800	0.800	0.775	0.755	0.810	0.806	0.956	0.948

†$\gamma = 0.1, b = 1.7$

Table S6. Power performance of sMiST vs. MiST under inconsistent mediator, when $R^2 = 0.05$ and the proportion of variants with direct effects is 0.80 for gene *CXCR1*.

	Mediation		Variance		Combined	
Model	MiST	sMiST	MiST	sMiST	MiST	sMiST
$\gamma = 0.25, b = 0$	0.705	0.705	0.042	0.042	0.597	0.596
$\gamma = 0.25, b = -0.5 * \gamma * c$	0.238	0.238	0.045	0.045	0.182	0.181
$\gamma = 0.25, b = -2.5 * \gamma * c$	0.954	0.954	0.033	0.033	0.909	0.908

Chapter 3

ESTIMATING INDIVIDUALIZED TREATMENT REGIMES TO OPTIMIZE INCREMENTAL COST EFFECTIVENESS RATIO

3.1 Introduction

Medical decision making can be complex, which requires considerations of multiple factors, such as differential patient responses to various treatments, anticipated risks and benefits of alternative intervention strategies. Specifically, there has been growing interest in developing individualized treatment regimes (ITRs), which recommend treatments based on patients' characteristics [67, 99, 100]. However, the goal of these methods is typically to maximize the expected benefit of a single clinical outcome if followed by the whole population.

While maximizing treatment efficacy is the primary goal, evaluations of costs and/or risks associated with the treatments are also important. There have been developments on constructing ITRs, taking into account both efficacy and risk outcomes. An existing body of literature focuses on constructing a utility function that jointly models efficacy and toxicity, and estimate an optimal ITR to maximize the utility function. These approaches construct an objective function, defined as the utility of benefits and toxicity, and estimate an optimal strategy to maximize the posterior expected mean of the objective function [30, 32, 47, 55, 83]. Lizotte et al. [53] proposed to constructed a linear combination of the competing outcomes as a composite primary outcome, and Laber et al. [43] proposed to construct set-valued treatment regimes that avoids eliciting trade-offs between outcomes, and can output multiple candidate treatments when there does not exist a treatment that is uniformly the best across all outcomes. There are also methods focusing on estimating the optimal ITR to maximize the clinical benefit while directly imposing a constraint on the risk [92, 95]. However, all of these approaches either require joint modeling of the efficacy and safety outcomes, or require a pre-specification of threshold value on the risk constraint.

To account for the benefit-cost tradeoff, incremental cost-effectiveness ratio (ICER) is commonly used in health economics to assess the economic value of an intervention, compared with the

alternative [61, 88, 60]. Existing statistical literature mainly focused on estimation and confidence interval (CI) construction for the ICER in order to compare the cost effectiveness of different arms [13, 35, 61, 64]. In this paper, we generalize the notion of ICER as the criterion to evaluate the quality of the ITRs. Having a single criterion to optimize avoids partial orderings and the subsequent non-uniqueness associated with set-valued and other multi-objective regimes. However, to the best of our knowledge, such a metric has not been proposed for a specified ITR, which is more complex than comparing two pre-specified interventions.

To define the ICER of an ITR, we first set the reference treatment regime, and derive the ratio of the change in the expected efficacy over the change in the expected cost over the whole population, when switching the reference to the ITR of interest. Therefore, different ITRs will exhibit varying ICERs, and our goal is to identify the one leading to the most desirable ICER. However, because the ICER characterizes the incremental costs and benefits, it is not trivial to identify an ITR that optimizes this criterion. As shown in Figure 3.1, there are potentially four different quadrants that an ITR can fall into, but some quadrants should not be of interest or may not be feasible to achieve. The decision rules can thus be classified as below

Fig 3.1. Cost-effectiveness plane

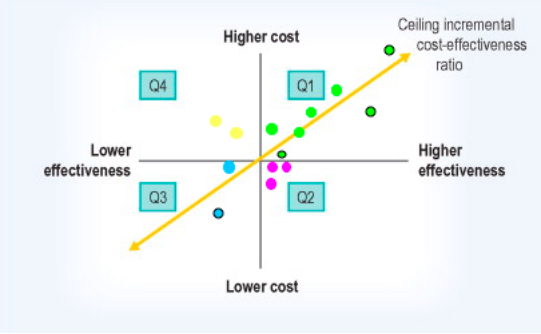

- Q1 quadrant: ITRs achieve higher benefits at higher costs.
- Q2 quadrant: ITRs achieve higher benefits at lower costs.
- Q3 quadrant: ITRs achieve lower benefits at lower costs.

- Q4 quadrant: ITRs achieve lower benefits at higher costs.

When identifying the ITR optimizing ICER, we need to take into account which quadrants the alternative ITRs fall into. Obviously, the ITRs falling into Q2 quadrant are among the most desirable, which may not be feasible in certain circumstances. Additionally, ITRs that attain lower effectiveness should not be considered, even if they could lead to reduced costs. In this paper, we will assume the reference ITR, typically assigning the standard care to the patient population, has a low benefit and a low cost. To facilitate the computation and interpretation, we propose a modified criterion, termed as winsorized ICER (wICER). Specifically, we use incremental winsorized costs that are guaranteed to be nonnegative in defining the ICER. This modification enables us to focus on the ITRs residing in Q1 and Q2 quadrants, which are of the major interests in identifying the most cost-effective ITR.

It is worth noting that our proposed framework does not require additional pre-specified parameters such as thresholds for risk constraints, or weights in the utility function. To the best of our knowledge, there has been no work on estimating the ITR that optimizes a ratio-type objective function. We employ Dinkelbach's algorithm to transform fractional program, where the objective function is a ratio of two non-linear functions, into an equivalent parametric program that is easy to handle [18]. Specifically, the resulting parametric program [21], which formulates the optimization problem as a function of a parameter, essentially maximizes a composite outcome defined by the optimal parameter. Dinkelbach's establishment of the relationship between fractional and parametric program enables us to derive a theoretical optimal rule of the ratio-type problem. We then propose two estimation methods that are guided by the theoretical optimal rule: regression-based approach [67] and outcome-weighted learning based approach [99]. The regression-based method models the conditional mean of the outcome given a set of covariates and treatment, and select the treatment with the larger conditional mean. Outcome-weighted learning based method estimates the optimal ITR from a weighted classification perspective, where weights are defined by the benefit and cost in our situation.

The manuscript is organized as follows: we introduce the statistical frame and provide the theoretical form of the individualized treatment rule that maximizes the ratio-type problem in section 2. We propose two estimation approaches in estimating optimal ITRs in section 3. We

conduct extensive simulation results of our proposed methods and compare them with existing approaches that optimize benefits or costs only while ignoring the other outcome in section 4. Lastly, we apply our approaches to Multicenter Automatic Defibrillator Implantation Trial with Cardiac Resynchronization Therapy (MADIT-CRT) study, a randomized trial in section 5.

3.2 Statistical Framework

3.2.1 Notation

In our paper, the benefit of interest is survival time, and the cost of interest is medical cost. We define $\tilde{T}$ to be the survival time, and τ to be the end of the study; because there is no information about survival beyond τ, we use $T = \min(\tau, \tilde{T})$ as the benefit outcome of interest. We denote R as the cost outcome. We denote $X = (X_1, \ldots, X_p)^T \in \mathbb{R}^p$ to be baseline characteristics, and denote $A \in \{-1, 1\}$ as the binary treatment assigned. We assume that data are collected from a randomized clinical trial, so that the probability of assigning treatments is known. An ITR, say d, is a function from $\mathbb{R}^p$ into the space of treatments $\{-1, 1\}$; under the rule d, a patient with covariates $X = x$ is assigned with the treatment $d(x)$. To later define the optimal ITR, we use the framework of potential outcomes [70]. Let $T(a)$ denote the potential outcome under treatment $a \in \{-1, 1\}$ and define $T(d) = \sum_{a\in\{-1,1\}} T(a)I\{A = d(X)\}$ to be the potential outcome under d. Under the standard assumptions, including 1) consistency, the actually observed outcomes and potential outcomes are consistent: $T(A) = T$; 2) positivity, there exists $\rho > 0$ such that $\rho < P(A = a|X)$ for each $a \in \{1, -1\}$ with probability one; and 3) no unmeasured confounders, conditional on covariates X, the potential outcomes are independent of A, the treatment that has been actually received, which is automatically held in randomized clinical trial. These assumptions are common and well studied, with more details can be found in [72]. It can be shown that the expected outcomes under the ITR d are given as

$$E^d(T) = E\left\{\frac{TI\{A = d(X)\}}{p(A|X)}\right\} \quad \text{and} \quad E^d(R) = E\left\{\frac{RI\{A = d(X)\}}{p(A|X)}\right\}. \tag{3.1}$$

We denote d^s as the ITR that serves as a reference, for example, the ITR that recommends standard of care to all patients, i.e., $d^s(X) = -1$, for any X.

3.2.2 ICER and Its Optimization

The ICER of an ITR d relative to the reference ITR is defined as

$$ICER(d) = \frac{E^d(R) - R_0}{E^d(T) - T_0},$$

where constants T_0 and R_0 are the expected benefit and expected cost of the reference treatment regime. There could be potentially many alternative ITRs that exhibit varying expected efficacy and costs. As discussed in Section 1, we are interested to identify the cost-effective ITRs among the Q1 and Q2 quadrants in Figure 3.1, which include ITRs leading to improved effectiveness compared to the reference ITR. Among ITRs in Q1, a natural optimization problem of finding a d can be framed as

$$\min_d \quad \frac{E^d(R) - R_0}{E^d(T) - T_0} \text{ subject to } E^d(T) - T_0 > 0,\ E^d(R) - R_0 > 0. \tag{3.2}$$

The ITR that optimizes (3.2) is denoted by d_{ICER}.

However, extreme values in the numerator of (3.2) could lead to numerical unstable performances of the ratio optimization problem. Additionally, ITRs in Q2 are excluded for the optimization of (3.2), but they are also of interest in practice. This motivates us to optimize a new unified metric that covers ITRs in both quadrants, while avoiding numerical instabilities of (3.2). We propose to maximize the inverse of the winsorized ICER (wICER), defined as

$$\max_d \quad \frac{E^d(T) - T_0}{E^d(\mathbf{R}) - R_0} \tag{3.3}$$

where $\mathbf{R} = \max(R, R_0)$. We term it as the inverse winsorized ICER (iwICER). By truncating R at R_0, $E^d(\mathbf{R}) - R_0$ is guaranteed to be non-negative for any d. Subsequently, by considering the optimization problem (3.3), the constraint in (3.2) is no longer needed, given any rules with negative incremental benefits cannot be selected as it would attain a negative ratio of $iwICER$.

Unlike original ICER, iwICER is a sufficient metric that can be used to compare all alternative ITRs, without additional information about which quadrants of the original ICER they fall into. Further, the metric of iwICER ensures that the optimization of (3.3) to be numerically stable by providing a buffer against potentially extreme values of $E^d(R) - R_0$.

Let d^* be the optimizer of (3.3), which maximizes the benefit gain, given one unit increase in winsorized cost, compared to the standard care. Note that it is not known whether d^* actually falls in Q1 or Q2. If d^* falls in Q2, (3.3) and (3.2) are not directly comparable. If d^* falls in Q1, it is by nature more conservative, compared to d_{ICER} that solves (3.2), by the fact that $ICER(d^*) \geq ICER(d_{\text{ICER}})$. Particularly, the following proposition shows that if d^* falls in Q1, we establish the equivalence between (3.3) and an optimization problem under the worst case-scenario, and the equivalence of (3.2) and an optimization problem under the best case-scenario.

Proposition 3.2.1. *If d^* falls in Q1, the optimization problem of (3.3) is equivalent to*

$$\min_{d\in D} \max_{\theta\in\Theta} \frac{E^d(\max(R,\theta)) - R_0}{E^d(T) - T_0}. \tag{3.4}$$

The optimization problem of (3.2) is equivalent to the following problem

$$\min_{d\in D} \min_{\theta\in\Theta} \frac{E^d(\max(R,\theta)) - R_0}{E^d(T) - T_0}, \tag{3.5}$$

where $D = \{d:\ E^d(T) - T_0 > 0, E^d(R) - R_0 > 0\}$, and $\Theta = \{\theta : \theta \leq R_0\}$.

The proof of Proposition (3.2.1) is provided in the appendix. Proposition (3.2.1) indicates that if d^* falls in Q1, finding the optimal ITR under the winsorized ICER metric can be thought of identifying the best decision rule under the worst case scenario, while optimizing under the original objective (3.2) is to identify the best decision rule under the best case scenario. Admittedly, the numerical stability of solving (3.3) is at the cost of its conservative nature.

3.2.3 Theoretical Optimal ITR

In this section, we derive the form of the theoretical optimal ITR, $d^*(X)$, that maximizes iwICER(d). We define $\delta_T(x) = E(T|A=1, X=x) - E(T|A=-1, X=x)$ and $\delta_{\mathbf{R}}(x) = E(\mathbf{R}|A=1, X=x) - E(\mathbf{R}|A=-1, X=x)$.

Theorem 3.2.2. *If $d^* \in S \subset \mathbf{D} = \{d:\ E^d(T) - T_0 > 0\}$, where S is a subset of the feasible set that is compact and connected, then the optimal treatment rule maximizing*

$$iwICER(d) = \frac{E^d(T) - T_0}{E^d(\mathbf{R}) - R_0}$$

is $d^*(X) = sgn\{f^*(X)\}$, *where* $f^*(X) = \delta_T(X) - \alpha^*\delta_{\mathbf{R}}(X)$, *and* α^* *solves the equation*

$$F(\alpha) = \max_{d\in\mathbf{D}}\{E^d(T) - \alpha E^d(\mathbf{R})\} - T_0 + \alpha R_0 = 0 \tag{3.6}$$

The proof follows from that of Dinkelbach's paper [18] and is deferred in the appendix. The theorem, which is essentially an application of Dinkelbach's algorithm, transforms the original fractional problem into solving a sequence of parametric programs (parametrized by α) until finding the optimal α^*. For a given α, the parametric program solves for $\max_{d\in\mathbf{D}}\{E^d(T) - \alpha E^d(\mathbf{R})\}$, which is equivalent to maximizing a composite outcome $T - \alpha\mathbf{R}$. We identify the optimal weight α^* by finding the root to (3.7). Interestingly, the proof of the theorem shows that α^* is equal to $\max_{d\in\mathbf{D}}$ iwICER(d).

Note that $E^d(T-\alpha\mathbf{R}) = E[E(T-\alpha\mathbf{R}|X, A = 1)I\{d(X) > 0\} + E(T-\alpha\mathbf{R}|X, A = -1)I\{d(X) < 0\}]$, and subsequently, the optimal ITR that maximizes $T - \alpha\mathbf{R}$ is $\text{sgn}(\delta_T(X) - \alpha\delta_{\mathbf{R}}(X))$. Therefore, (3.6) is equivalent to the following

$$\begin{aligned} & E[\{E(T|X, A = 1) - \alpha E(\mathbf{R}|X, A = 1)\}I\{\delta_T(X) - \alpha\delta_{\mathbf{R}}(X) > 0\} \\ + \quad & \{E(T|X, A = -1) - \alpha E(\mathbf{R}|X, A = -1)\}I\{\delta_T(X) - \alpha\delta_{\mathbf{R}}(X) < 0\}] \\ - \quad & T_0 + \alpha R_0 = 0. \end{aligned} \tag{3.7}$$

3.3 Estimation of the Optimal Treatment Rules

In this section, we propose two methods to estimate the optimal treatment rule d^* using the collected data: ICER-RM (regression-based) and ICER-O-learning (outcome-weighted learning based).

Let C denote the censoring time, which could go beyond τ, the study time. We assume that C and T are continuous, and independent. The observed data consists of n independent identically distributed subjects, $\{\mathcal{T}_i = T_i \wedge C_i, \mathcal{R}_i = R_i \wedge \tilde{R}_i^{C_i}, \Delta_i = I(T_i \le C_i), X_i, A_i\}$, $i = 1, ..., n$, where $\Delta = I(T \le C)$ denotes the censoring indicator, $\tilde{R}_i^{C_i}$ denotes the accumulated cost until censoring time C_i. We assume that $\pi(a; X) = pr(A = a|X)$ is strictly bounded away from zero with probability 1 for each value of a.

3.3.1 Regression Modeling based Method (ICER-RM)

We first introduce the regression modeling method to estimate $d^*(X)$, which we term as ICER-RM. Motivated by (3.7), we first estimate $E(T|X, A = j)$ and $E(\mathbf{R}|X, A = j), j = \pm 1$, as well as $\delta_T(X)$ and $\delta_{\mathbf{R}}(X)$ using the empirical data. Then the estimated optimal ITR for optimizing iwICER(d) is $\hat{d}(X) = \text{sgn}\{\hat{\delta}_T(X) - \hat{\alpha}\hat{\delta}_{\mathbf{R}}(X)\}$, where $\hat{\alpha}$ is obtained by solving

$$\begin{aligned} & F_n(\alpha) = \frac{1}{n}\sum_{i=1}^{n}[\{\hat{E}(T_i|X_i, A_i = 1) - \alpha\hat{E}(\mathbf{R}_i|X_i, A_i = 1)\}I\{\hat{\delta}_T(X_i) - \alpha\hat{\delta}_{\mathbf{R}}(X_i) > 0\} \\ + \quad & \{\hat{E}(T_i|X_i, A_i = -1) - \alpha\hat{E}(\mathbf{R}_i|X_i, A_i = -1)\}I\{\hat{\delta}_T(X_i) - \alpha\hat{\delta}_{\mathbf{R}}(X_i) < 0\}] \\ - \quad & \hat{T}_0 + \alpha\hat{R}_0 = 0 \end{aligned}$$

We can impose parametric models to obtain $\hat{\delta}_T(X)$ and $\hat{\delta}_{\mathbf{R}}(X)$. When the benefit and cost outcomes are subject to censoring, we adopt the technique of inverse probability censored weighting (IPCW) in estimating the required quantities. Let $S_c(t) = pr(C > t)$ denote the survival function for the censoring time. We weigh each non-censored observed survival and cost outcomes by the inverse of the probability of not being censored. The censoring weights can be estimated by the Kaplan-Meier estimator. We denote the estimator of S_c by $\hat{S}_c$. Assume that $E(T|X, A) = \Phi(X, A)\theta$, where $\Phi(X, A) = (1, X, A, XA)$. Let $\hat{\boldsymbol{\mathcal{R}}}_i = \max(\mathcal{R}_i, \hat{R}_0)$. We solve for

$$\begin{aligned} \hat{\theta}_T &= \text{argmin}_\theta \sum_{i=1}^{n} \frac{\{\mathcal{T}_i - \Phi(X, A)\theta\}^2\Delta_i}{\hat{S}_c(\mathcal{T}_i)} \\ \hat{\theta}_{\mathbf{R}} &= \text{argmin}_\theta \sum_{i=1}^{n} \frac{\{\hat{\boldsymbol{\mathcal{R}}}_i - \Phi(X, A)\theta\}^2\Delta_i}{\hat{S}_c(\mathcal{T}_i)}. \end{aligned}$$

Subsequently, $\hat{E}(T|X, A = j) = \Phi(X, A = j)\hat{\theta}_T$ and $\hat{E}(\mathbf{R}|X, A = j) = \Phi(X, A = j)\hat{\theta}_{\mathbf{R}}$. Similarly, we can obtain

$$\begin{aligned} \hat{T}_0 &= \frac{1}{n}\sum_{i=1}^{n} \frac{\mathcal{T}_i\Delta_i I(A_i d^s(X_i) > 0)}{P(A_i|X_i)\hat{S}_c(\mathcal{T}_i)} \\ \hat{R}_0 &= \frac{1}{n}\sum_{i=1}^{n} \frac{\mathcal{R}_i\Delta_i I(A_i d^s(X_i) > 0)}{P(A_i|X_i)\hat{S}_c(\mathcal{T}_i)}, \end{aligned} \tag{3.8}$$

where $d^s(X_i) = -1, i = 1, \ldots, n$.

3.3.2 Outcome-weighted Learning Based Approach (ICER-O-learning)

The second approach is motivated by the form of (3.6), which indicates that if we estimate the value of $\max_{d\in D}\{E^d(T) - \alpha E^d(\mathbf{R})\}$ for each specific α, the optimal α^* can be solved accordingly. We propose to estimates $d_\alpha = \text{argmax}_{d\in D}\{E^d(T) - \alpha E^d(\mathbf{R})\}$ under the framework of outcome-weighted learning (OWL). Combined with (3.1), we notice that maximizing $E^d(T) - \alpha E^d(\mathbf{R})$ is equivalent to minimizing

$$E\left\{\frac{(T - \alpha\mathbf{R})I\{A \neq d(X)\}}{p(A|X)}\right\}, \tag{3.9}$$

which can be viewed as a weighted classification error, with weights proportional to $(T-\alpha\mathbf{R})/P(A|X)$.

The empirical objective of minimizing (3.9) is equivalent to

$$\min_f \frac{1}{n}\sum_{i=1}^{n}\left\{\frac{(\mathcal{T}_i - \alpha\boldsymbol{\mathcal{R}}_i)\Delta_i I(A_i f(X_i) < 0)}{P(A_i|X_i)S_c(\mathcal{T}_i)}\right\} \tag{3.10}$$

Again we can use Kaplan-Meier estimator, denoted as $\hat{S}_c$, to estimate S_c, $\hat{R}_0$ to estimate R_0, and $\hat{\boldsymbol{\mathcal{R}}}_i = \max(\mathcal{R}_i, \hat{R}_0)$ to estimate $\boldsymbol{\mathcal{R}}_i$. To handle the potential negative weights in $\mathcal{T}_i - \alpha\mathcal{R}_i$, we follow [52], and solve the follwoing objective that is equivalent to (3.10).

$$\min_f \frac{1}{n}\sum_{i=1}^{n}\left\{\frac{|\mathcal{T}_i - \alpha\boldsymbol{\mathcal{R}}_i|\Delta_i I(A_i^* f(X_i) < 0)}{P(A_i|X_i)S_c(\mathcal{T}_i)}\right\} \tag{3.11}$$

where $A_i^* = A_i\text{sgn}(\mathcal{T}_i - \alpha\boldsymbol{\mathcal{R}}_i)$.

Due to the nonconcave and discontinuous 0-1 indicator function, direct optimization of (3.11) is computationally difficult. A common strategy in machine learning literature is to replace this indicator function with a convex surrogate function. Denote the convex surrogate function as $\phi(t)$. Therefore, for a given α, we denote $\hat{f}_\alpha(X_i)$ to be the optimizer of

$$\min_f \frac{1}{n}\sum_{i=1}^{n}\left\{\frac{(\mathcal{T}_i - \alpha\hat{\boldsymbol{\mathcal{R}}}_i)\Delta_i\phi(A_i^* f(X_i))}{P(A_i|X_i)\hat{S}_c(\mathcal{T}_i)}\right\} \tag{3.12}$$

Furthermore, we introduce the regularization parameter λ_n to penalize the complexity of the

decision function to avoid overfitting. The empirical surrogate objective is

$$\min_f \frac{1}{n}\sum_{i=1}^{n}\left\{\frac{W_{\alpha,i}\phi(A_i^* f(X_i))}{P(A_i|X_i)}\right\} + \lambda_n\|f\|^2, \tag{3.13}$$

where $W_{\alpha,i} = (\mathcal{T}_i - \alpha\hat{\boldsymbol{\mathcal{R}}}_i)\Delta_i/\hat{S}_c(\mathcal{T}_i)$, and $\|f\|$ is some norm for f. In this paper, for easy interpretability and computational efficiency, we only consider linear decision function $f(X_i) = \beta_0^\alpha + X_i^T\beta^\alpha$, and $\|f\| = \|\beta^\alpha\|$. We introduce slack variable ϵ_i following the usual SVM. The optimization problem can be written as min $\gamma\sum_{i=1}^n W_{\alpha,i}\epsilon_i + \|\beta^\alpha\|^2$ subject to $\epsilon_i \geq 0$ and $A_i^*(X_i^T\beta^\alpha + \beta_0^\alpha) \geq 1 - \epsilon_i$, where γ is a tuning parameter. By introducing Lagrange multipliers k_i and μ_i , we obtain the Lagrangian

$$\frac{1}{2}\|\beta^\alpha\|^2 + \gamma\sum_{i=1}^{n} W_{\alpha,i}\epsilon_i - \sum_{i=1}^{n} k_i\{A_i^*(X_i^T\beta^\alpha + \beta_0^\alpha) - (1-\epsilon_i)\} - \sum_{i=1}^{n}\mu_i\epsilon_i,$$

where $k_i, \mu_i \geq 0$. By taking derivatives with respect to β^α, β_0^α, and ϵ_i, we have $0 = \sum_{i=1}^n k_i A_i^*$, $\beta^\alpha = \sum_{i=1}^n k_i A_i^* X_i$, and $k_i = \gamma W_{\alpha,i} - \mu_i$. The dual problem is thus

$$\max_k \sum_{i=1}^{n} k_i - 1/2\sum_{i=1}^{n}\sum_{j=1}^{n} k_i k_j A_i^* A_j^* X_i^T X_j,$$

subject to $0 \leq k_i \leq \gamma W_{\alpha,i}$, and $\sum_{i=1}^n k_i A_i^* = 0$. We denote $\hat{k}$ to be the solution to the dual problem, and obtain $\hat{\beta}^\alpha = \sum_{i=1}^n \hat{k}_i A_i^* X_i$, and $\hat{\beta}_0^\alpha$ is solved using margin points subject to Karush–Kuhn–Tucker conditions $\hat{k}_i\{A_i^*(X_i^T\hat{\beta}^\alpha + \hat{\beta}_0^\alpha) - (1-\hat{\epsilon}_i)\} = 0$, where $\hat{k}_i > 0$, and $\hat{\epsilon}_i = 0$. Thus, for a particular α, we have the estimated optimal rule by outcome weighted learning as $\hat{f}_\alpha(X_i) = X_i^T\hat{\beta}^\alpha + \hat{\beta}_0^\alpha$.

We then estimate $\hat{\alpha}$ to be the root of $F_n(\alpha) = 0$, where

$$F_n(\alpha) = \frac{1}{n}\sum_{i=1}^{n}\left\{\frac{\mathcal{T}_i\Delta_i I(A_i\hat{f}_\alpha(X_i) > 0)}{P(A_i|X_i)\hat{S}_c(\mathcal{T}_i)}\right\} - \alpha\frac{1}{n}\sum_{i=1}^{n}\left\{\frac{\hat{\boldsymbol{\mathcal{R}}}_i\Delta_i I(A_i\hat{f}_\alpha(X_i) > 0)}{P(A_i|X_i)\hat{S}_c(\mathcal{T}_i)}\right\} - \hat{T}_0 + \alpha\hat{R}_0 = 0,$$

where $\hat{T}_0$ and $\hat{R}_0$ are defined in (3.8).

3.4 Simulation Studies

We simulated 10 independent and identically distributed covariates X_1, ..., X_{10} from a uniform $(0, 1)$ distribution, and treatment A from {1, -1} with probability 0.5. In the first scenario, the survival

time followed an accelerated failure time model, where T was the minimum of $\tau = 2.5$ and $\tilde{T}$, with $\tilde{T}$ generated from

$$\log(\tilde{T}) = -0.2 - 0.5X_1 + 0.5X_2 + 0.5X_3 + (0.1X_1 + 0.6X_2 - 0.1X_3 - 0.3) * A + \epsilon_T,$$

$\epsilon_T \sim N(0, 0.4)$. The censoring time C was generated from a uniform $(0, 6)$, yielding around 20% censoring rate. The cost outcome R was generated from

$$R = 2 + X_1 + 2(X_2 + X_5 - 1.2X_1 - 0.2) * A + \epsilon_R,$$

$\epsilon_R \sim N(0, 0.4)$. In this setting, the optimal ITR for maximizing $E^d(T)$, denoted by d_T^*, is linear with $d_T^*(X) = \text{sgn}(0.1X_1 + 0.6X_2 - 0.1X_3 - 0.3)$; and the optimal ITR for minimizing $E^d(R)$, denoted by d_R^*, is also linear with $d_R^*(X) = -\text{sgn}(X_2 + X_5 - 1.2X_1 - 0.2)$.

In the second scenario, the survival time T is the minimum of $\tau = 3$ and $\tilde{T}$, where $\tilde{T}$ is generated from

$$\lambda_{\tilde{T}}(t|A, X) = \lambda_{\tilde{T}_0}(t) \exp\{0.6X_1 - 0.8X_2 + (-0.1 - 0.4X_1^2 - 0.3X_2 + 0.6X_3)A\},$$

and $\lambda_{\tilde{T}_0}(t) = 2t$. The censoring time is generated from a uniform $(0, 4)$. The censoring percentage is around 40 percent. Similar to [3, 97, 13], we considered four types of costs that could occur for each patient: initial cost, annual fixed cost, annual random cost, and termination cost. The total cost is the sum of the initial cost, (annual fixed cost + annual random cost) $\times\, T$, and termination cost. These costs for standard care ($A = -1$) are sampled from $U[1000, 2000]$, $U[2000, 3500]$, $U[0, 400]$, $2000R_t$, and for experimental care ($A = 1$) are sampled from $U[2000, 3000]$, $U[4000, 5500]$, $U[0, 400]$, and $2000R_t$, respectively, where R_t is generated from

$$6 + X_1 + (3X_7^2 + 0.2X_8^2 - 0.3 - 3X_1 + X_2) \times A + \epsilon_R,\ \epsilon_R \sim N(0, 1).$$

We divided total cost by 10000, so that R is approximate at the same scale as T.

To evaluate the performance of the proposed methods including ICER-RM, and ICER-O-learning, we included methods that only optimize one single outcome while ignoring the other outcome for comparison. We denote T-RM to be the regression based method with the goal to maximize the

survival time, and T-O-Learning to be the OWL based analogue. We denote **R**-RM to be the regression based method with the goal to minimize the risk outcome, and **R**-O-Learning to be the OWL based analogue. Additionally, we included the ITR that recommends experimental care to all, denoted as d^e, as a benchmark.

For each scenario, the sample sizes for the training data sets were taken to be equal to 400 and 1500, and the simulations were repeated 100 runs for each sample size. We developed the ITRs using different methods on the training data, and evaluated these resulting rules on an independent validation data set of size 10,000. Specifically, we computed the mean ratio outcome (iwICER) had the whole population followed the estimated ITR on the validation set. We also calculated the empirical average of incremental values in the survival time, the cost and the winsorized cost for the estimated ITRs. We summarized the results in Tables 1 and 2 for the first and the second scenario respectively.

The oracle values under the optimal ITR for each scenario were presented for comparison. For the ICER-RM method, we applied weighted least squares on the non-censored survival and cost data separately, with weights derived from the Kaplan-Meier estimator. For the ICER-O-Learning method, we first calculated the weights defined in (3.13) and solved the weighted classification problem, which can be implemented using the R package 'DynTxRegime'.

The results show that the proposed methods outperform the competitors. The estimated ITRs of the proposed methods not only attain higher values of iwICER, but also yield high values of the incremental benefits and small values of the incremental costs. Experimental care applied to all, however, achieves high values of the incremental benefits at the cost of high values of the incremental costs. In Scenario 1, although the data generation $\log(\tilde{T})$ is generated from a linear model, a linear regression to T, which is truncated at τ, might be slightly misspecified. However, we can see from simulation results in Table 1 that the average outcome of ICER-RM is very close to the oracle value of 0.544 as sample size increases. ICER-RM performs slightly better than ICER-O-learning in terms of the iwICER value. Conversely, in Scenario 2, since the data generation mechanism is complex, the ICER-O-learning method outperforms the other methods due to its robustness.

n	Method	iwICER(d)	$E^d(T) - T_0$	$E^d(\mathbf{R}) - R_0$	$E^d(R) - R_0$	Accuracy
	Optimal	0.544	0.145	0.267	-0.331	1.000
	Experimental	0.296	0.267	0.903	0.777	0.492
400	ICER-RM	**0.478(0.027)**	0.151(0.040)	0.318(0.094)	-0.254(0.153)	0.863(0.041)
	ICER-O-learning	0.453(0.031)	0.139(0.038)	0.308(0.088)	-0.274(0.138)	0.850(0.037)
	T-RM	0.320(0.018)	0.314(0.009)	0.984(0.059)	0.851(0.089)	0.509(0.037)
	T-O-learning	0.322(0.019)	0.300(0.016)	0.935(0.070)	0.775(0.107)	0.531(0.040)
	R-RM	0.168(0.034)	0.024(0.005)	0.143(0.008)	-0.513(0.008)	0.796(0.010)
	R-O-learning	0.162(0.127)	0.044(0.035)	0.280(0.080)	-0.321(0.117)	0.717(0.071)
1500	ICER-RM	**0.511(0.015)**	0.148(0.021)	0.289(0.042)	-0.302(0.068)	0.900(0.015)
	ICER-O-learning	0.498(0.027)	0.143(0.029)	0.285(0.055)	-0.311(0.085)	0.893(0.020)
	T-RM	0.323(0.009)	0.320(0.005)	0.992(0.030)	0.869(0.044)	0.509(0.019)
	T-O-learning	0.327(0.012)	0.316(0.008)	0.968(0.040)	0.823(0.058)	0.527(0.022)
	R-RM	0.177(0.020)	0.025(0.003)	0.142(0.005)	-0.515(0.005)	0.798(0.005)
	R-O-learning	0.170(0.109)	0.031(0.020)	0.186(0.025)	-0.457(0.033)	0.772(0.041)

Table 3.1. Estimated average iwICER(d) (sd) in Scenario 1

n	Method	iwICER(d)	$E^d(T) - T_0$	$E^d(\mathbf{R}) - R_0$	$E^d(R) - R_0$	Accuracy
	Optimal	0.589	0.157	0.266	0.084	1.000
	Experimental	0.201	0.134	0.641	0.584	0.363
400	ICER-RM	0.400(0.097)	0.119(0.033)	0.299(0.054)	0.134(0.074)	0.750(0.081)
	ICER-O-learning	**0.413(0.107)**	0.122(0.035)	0.297(0.051)	0.130(0.070)	0.761(0.085)
	T-RM	0.333(0.083)	0.144(0.037)	0.437(0.071)	0.321(0.095)	0.618(0.091)
	T-O-learning	0.325(0.094)	0.140(0.040)	0.433(0.071)	0.316(0.094)	0.615(0.095)
	R-RM	0.039(0.106)	0.007(0.019)	0.175(0.013)	-0.021(0.015)	0.667(0.033)
	R-O-learning	0.153(0.120)	0.050(0.040)	0.326(0.055)	0.177(0.076)	0.568(0.089)
1500	ICER-RM	0.516(0.045)	0.148(0.021)	0.287(0.034)	0.113(0.045)	0.849(0.041)
	ICER-O-learning	**0.523(0.042)**	0.152(0.021)	0.292(0.040)	0.120(0.054)	0.851(0.044)
	T-RM	0.415(0.049)	0.187(0.020)	0.455(0.051)	0.342(0.067)	0.679(0.063)
	T-O-learning	0.413(0.063)	0.186(0.023)	0.455(0.055)	0.342(0.074)	0.674(0.079)
	R-RM	0.009(0.073)	0.002(0.012)	0.162(0.009)	-0.036(0.010)	0.673(0.015)
	R-O-learning	0.072(0.126)	0.017(0.031)	0.210(0.037)	0.028(0.044)	0.643(0.053)

Table 3.2. Estimated average iwICER(d) (sd) in Scenario 2

3.5 A Real Data Example: MADIT-CRT

The Multicenter Automatic Defibrillator Implantation Trial with Cardiac Resynchronization Therapy (MADIT-CRT) study is a randomized clinical trial, where patients are randomized into either the implantable cardiac defibrillator (ICD) arm or the CRT with an ICD (CRT–ICD) arm. There are 503 patients in the ICD arm and 748 in the CRT–ICD arm. The results of the trial showed that the CRT–ICD reduces the risk of the occurrence of heart failure (HF), especially in patients with a left bundle branch block conduction disturbance. However, the average costs of CRT–ICD are higher, and therefore the cost effectiveness analysis is worth conducting. We used the HF-free

survival time as the benefit measure, and restricted both survival and cost to a 4-year time horizon. The censoring percentage is more than 80% for this study. Following [13], we discounted both survival and cost at a 3% annual rate and then spread out evenly in the interval. We considered 6 baseline covariates, including New York Heart Association functional class I/II heart failure (NYHA), with 0 = no heart failure, 1 = heart failure, gender (0 = male, 1 = female), age, race (0 = Caucasians, 1 = non-Caucasians), diabetes (0 = no diabetes, 1 = diabetes), and left bundle branch block conduction disturbance (LBBB), with 0 = no LBBB, 1 = LBBB. To compare the performance of estimated ITRs from various methods, we considered the following metrics: the median iwICER, the median change in HF-free survival time, the median change in winsorized cost, and the median change in original cost. We randomly split the full data into a training set and a testing set, with a 1:1 ratio, where ITRs were developed on the training set, and evaluated on the testing set. This procedure was repeated 100 times, and the average performance metrics are reported.

Table 3 shows that the estimated ITR by optimizing the HF-free survival time while ignoring the cost achieve a similar iwICER as the proposed methods. The results indicate that for this example, ITRs that maximize efficacy do not lead to significantly higher costs. Conversely, the ITR that recommends experimental treatment to all patients leads to a lower expected iwICER. Lastly, we ranked variable importance using the magnitude of the coefficients of the estimated linear treatment rule of all methods, by using the full data. The results of variable importance are summarized in Table 4. The variable LBBB plays an important factor in optimizing the iwICER and the efficacy.

Method	iwICER(d)	$E^d(T) - T_0$	$E^d(\mathbf{R}) - R_0$	$E^d(R) - R_0$
ICER-RM	0.357(1.012)	0.300(0.445)	1.012(0.768)	0.201(0.711)
ICER-O-learning	**0.423(1.751)**	0.401(0.395)	1.009(0.678)	0.196(0.651)
T-RM	0.367(1.090)	0.272(0.413)	0.906(0.724)	0.094(0.672)
T-O-learning	0.423(1.766)	0.399(0.410)	0.968(0.685)	0.181(0.655)
R-RM	0.219(6.125)	-0.049(0.524)	0.645(0.899)	-0.103(0.835)
R-O-learning	0.184(3.006)	-0.053(0.434)	0.530(0.706)	-0.104(0.682)
Experimental	0.227(0.247)	0.203(0.182)	0.911(0.245)	0.318(0.414)

Table 3.3. Median of estimated iwICER(d) in MADIT-CRT

	ICER-RM	ICER-O-learning	T-RM	T-O-learning	**R**-RM	**R**-O-learning
LBBB	1	1	1	1	4	2
Diabetes	2	3	5	4	1	1
Gender	3	2	3	3	3	4
NYHA	4	5	2	2	2	5
Race	5	4	4	5	5	3
Age	6	6	6	6	6	6

Table 3.4. Real data analysis: ranking of covariates based on average standardized effects

3.6 Discussion

We proposed new methods to optimize the ICER. We work on a novel metric, winsorized ICER, where the winsorization procedure on the cost data provides numerical stability in optimization procedure, and ensures the resulting incremental changes in cost to be nonnegative. By considering the winsorized cost in the objective, we can obtain a desirable ITR that has great improvements in benefit while keeping original cost under control. While the optimal ITR that maximizes iwICER may be considered conservative, the proposed metric does not require pre-specification of additional parameters. We developed two methods to estimate the optimal ITRs in optimizing the winsorized ICER: ICER-RM and ICER-O-learning. ICER-RM uses parametric models to estimate the conditional mean of the outcome given a set of covariates and treatment, and select the treatment with the larger conditional mean. ICER-O-learning estimates the optimal ITR from a weighted classification perspective, where weights are defined by the benefit and cost in our situation. ICER-O-learning in general is more robust to model mis-specifications, while ICER-RM is computationally more efficient.

We have adopted Dinkelbach's algorithm of translating a fractional program into an equivalent parametric program that is easy to handle [18]. Such framework is flexible to accomodate more complicated methods in solving the parametric program. However, the computational burden associated with more complicated methods needs to be taken into account. Note that in ICER-RM, the linearity of expectation property guarantees the regression-based ITR that optimizes $T - \alpha\mathbf{R}$ to be a linear combination of T-RM and **R**-RM, and therefore the estimation procedures only involve estimations of T-RM and **R**-RM separately. On the other hand, ICER-O-learning requires

performing a sequence of estimation procedures for O-learning-based ITRs that optimize $T - \alpha\mathbf{R}$ before finding the optimal α^*. It is important to develop efficient method to accelerate the algorithm. Additionally, it is of interest to develop a general framework that allows for a multi-stage decision setting with potentially high dimensional covariates.

3.7 Appendix

3.7.1 Proof of Proposition (3.2.1)

Proof. We first note that (3.3) is equivalent to $\max_{d\in D} \{E^d(T) - T_0\}/\{E^d(max(R, R_0)) - R_0\}$, given the maximizer of (3.3) must be in the set D. Given any fixed $d \in D$, we have

$$\max_{\theta\in\Theta} E^d(\max(R, \theta)) = E^d(\max(R, R_0))$$

$$\max_{\theta\in\Theta} \{E^d(\max(R, \theta)) - R_0\}/\{E^d(T) - T_0\} = \{E^d(\max(R, R_0)) - R_0\}/\{E^d(T) - T_0\}$$

$$E^d(T) - T_0 > 0$$

$$E^d(\max(R, R_0)) - R_0 > 0$$

Thus, $\max_{d\in D}\{E^d(T) - T_0\}/\{E^d(max(R, R_0)) - R_0\}$ is equivalent to minimizing its inverse, which is $\min_{d\in D}\{E^d(max(R, R_0)) - R_0\}/\{E^d(T) - T_0\}$. The proof of the equivalence between (3.2) and (3.5) is similar, after observing $\min_{\theta\in\Theta} E^d(\max(R, \theta)) = E^d(max(R, -\infty)) = E^d(R), \forall d \in D$. □

3.7.2 Proof of Theorem (3.2.2)

The proof of Theorem (3.2.2) directly follows from that of [18]. We define $N(d) = E^d(T) - T_0$, and $D(d) = E^d(\mathbf{R}) - R_0$. Our proposed objective can be formulated as

$$\max_{d\in S} \quad \frac{N(d)}{D(d)} \tag{3.14}$$

We consider another related problem

$$\max_{d\in S} \quad \{N(d) - qD(d)\}, \tag{3.15}$$

where $q \in \mathbb{R}$. We would want to prove $q^* = \frac{N(d^*)}{D(d^*)} = \max_{d\in S} \frac{N(d)}{D(d)}$ iff $F(q^*) = \max_{d\in S} \{N(d) - q^*D(d)\} = 0$.

Proof. Part 1 In part 1, we prove if $q^* = \frac{N(d^*)}{D(d^*)} = \max_{d\in S} \frac{N(d)}{D(d)}$, then $F(q^*) = \max_{d\in S} \{N(d) - q^*D(d)\} = 0$. We let d^* to be solution to (3.14). We then have $N(d^*)/D(d^*) = q^* \geq N(d)/D(d), \forall d \in$

S. Given $D(d) > 0, \forall d \in S$, we have

$$\begin{aligned} N(d) - q^* D(d) &\leq 0, \forall d \in S \\ N(d^*) - q^* D(d^*) &= 0 \end{aligned} \tag{3.16}$$

From (3.16) we see that $F(q^*) = \max_{d \in S} \{N(d) - q^* D(d)\} = 0$, and d^* is an maximizer of $\max_{d \in S} \{N(d) - q^* D(d)\}$.

Part 2 In part 2, we prove if $F(q^*) = \max_{d \in S} \{N(d) - q^* D(d)\} = 0$, then $q^* = \frac{N(d^*)}{D(d^*)} = \max_{d \in S} \frac{N(d)}{D(d)}$. We let d^* to be a solution to (3.15) such that $N(d^*) - q^* D(d^*) = 0$. The definition of (3.15) implies that $N(d) - q^* D(d) \leq N(d^*) - q^* D(d^*) = 0, \forall d \in S$. Therefore, we have

$$\begin{aligned} N(d) - q^* D(d) &\leq 0, \forall d \in S \\ N(d^*) - q^* D(d^*) &= 0 \end{aligned} \tag{3.17}$$

From (3.17) we have $q^* \geq N(d)/D(d), \forall d \in S$, that is q^* is the maximum of problem (3.16). Given that $N(d^*)/D(d^*) = q^*$, we can conclude d^* is a solution for (3.14). Therefore, d^* that solves (3.15), with $q = q^*$, also solves (3.14). □

The above theorem does not guarantee the uniqueness of d^*.

Chapter 4

CONSTRUCTING STABILIZED DYNAMIC SURVEILLANCE RULES FOR OPTIMAL MONITORING SCHEDULE

4.1 INTRODUCTION

Active surveillance is a disease management strategy that closely monitors a patient's condition without intervention unless there are indications of a worsening condition. Such a strategy can reduce the overtreatment of disease by delaying intervention in patients who were diagnosed with low-risk disease and providing treatments only when a more severe malignancy is identified. In the Canary Prostate Active Surveillance Study (PASS), men with clinically localized prostate cancer who have chosen to manage their cancers using active surveillance are followed prospectively [51]. The patients undergo serial monitoring with serum prostate specific antigen (PSA), clinical examinations, and surveillance biopsies [62]. However, repeated biopsies and frequent measurements of PSA could be burdensome and expensive for the patients and it is well recognized that such a one-size-fits-all approach, managing all prostate cancers with the same schedule, makes little clinical or biological sense [16]. Dynamic surveillance rules (DSRs) are sequential surveillance decision rules that can adapt over time according to a patient's evolving characteristics. In the setting of PASS, they can provide s a formal decision rule for the personalized subsequent monitoring schedule to tailor the intensity of active surveillance, identifying those men among whom surveillance can be safely modulated.

The DSR can be derived in the form of a time-dependent binary decision rule on whether an intervention procedure (e.g., biopsies or surgery) should be taken at a future time τ scheduled by a fixed surveillance protocol, given the patient is event-free up to a visit time (landmark time) s. The procedure typically proceeds by estimating the dynamic risk, the updated τ_0-year risk for an adverse event based on a patient's information accumulated up to t, and then constructing the surveillance rules via comparing the risk with a pre-specified risk threshold. Flexible modeling approaches such as the joint models [85, 84] and Partly conditional models [58] can be used for

dynamic risk predictions. However, the identification of an appropriate risk threshold needs some deliberation in this setting. In addition, the derived rule relies on the aptness of the underlying regression model for longitudinal and time-to-event data. We develop methods that can improve on the robustness of model-based decision rules by considering model-free reinforcement learning algorithms [81] . Such approaches have been adapted in the dynamic treatment regime literature, but not yet been considered in the setting of deriving the followup schedule of a monitoring test.

One important hurdle in searching for a DSR is the identification of a clinically relevant objective function that captures the clinical consequences important to patients. For example, a surveillance biopsy for prostate cancer has the immediate benefit of identifying patients who have progressed or are at higher risk of progression, which indicate more intensive monitoring or surgery might be needed. However, it may also lead to the harm of treating low-risk patients for whom the procedure is not necessary. The optimal DSR indicating follow-up schedules should therefore maximize the clinical benefit while adjusting for the associated risk, e.g., overtreatment. Here we consider an average risk-adjusted clinical benefit (RACB) performance measure. It weighs the importance of high true positive fraction (TPF) against low false positive fraction (FPF) at each stage. The RACB function is in the same spirit as the notion of net benefit in decision theory [57, 87]. It is often used as a clinical validity measure of a medical tests, but has seldom been considered as an objective function for optimization. [91] considered using the RACB function to search for a clinical decision rule for the binary outcome with baseline data. We extend the criterion used in [91] for the binary outcome to the time-dependent setting with repeated measurements. The criterion is clinically meaningful by balancing the benefit and risk of the DSR over the course of monitoring. To the best of our knowledge, this is the first time such a measure adopted for the active surveillance setting.

For active surveillance that involves a potentially large number of landmark times, a decision rule with formulations varying by landmark times may be difficult to implement in clinical practice. Furthermore, the baseline time could be hard to define as the enrollment times for patients may be different between the cohort for developing the rule and the target cohort the rule is applied to. Therefore a time-varying DSR would also be challenging to generalize. Indeed, there has been growing interest in developing shared decision rules across stages, especially in the area of dynamic treatment regimes. For example, [12] developed shared-Q-learning for deriving dynamic treatment regimes with shared parameters. They formulated the decision rules as linear functions of time-

varying covariates, and the coefficients are assumed to be the same across decision points. Recently, [89] proposed the shared-parameter G-estimation. [98] developed censored shared-Q-learning and censored shared-O-learning method, which allow for censored outcomes. Potential generalizations of these approaches require with specific objective functions for the active surveillance setting.

We focus on developing new methods of estimating coefficient parameters of biomarkers indexing the DSRs that are shared across landmark times, aiming to optimize the average RACBs over time. We term DSRs with shared parameters as stabilized DSRs. In particular, we propose two methods to estimate the stabilized DSRs that are easy to implement using slightly modified standard statistical software. The first method is a two-step modeling approach, termed as shared modeling (SM). We estimate the optimal decision rules for each individual at every stage via regression modeling, and then estimate the stabilized DSRs via a classification procedure with the estimated time-varying decision rules as the response. The second approach is termed as optimization with surrogate function (OSF). It proceeds by optimizing the estimator of the average RACB, where a surrogate function is utilized to facilitate computation. OSF does not model the outcomes, and hence does not rely on any underlying model assumptions. We establish the asymptotic properties of the estimated coefficient parameters of biomarkers indexing the DSRs from both methods. Simulation results show that the proposed methods have superior performances, especially under small sample sizes. The methods are further applied to the PASS study.

The manuscript is organized as follows: we first explain the time-varying property of DSR, and introduce the notion of stabilized DSR in Section 2. We propose two new approaches in estimating stabilized DSRs in Section 3, followed by the asymptotic properties of the proposed methods in Section 4. The results of simulation studies evaluating the proposed methods are presented in Section 5. In Section 6, we illustrate our methods with a biomarker study from the PASS. We end the paper with a discussion in Section 7.

4.2 STATISTICAL FRAMEWORK

4.2.1 Notation

Let T denote the survival time. The longitudinal time-varying biomarkers is denoted by $\boldsymbol{X} = \{X(s_1), ..., X(s_m)\}$, measured at times $\boldsymbol{s} = \{s_1, ..., s_m\}$, where $X(s_j)$ is the jth measurement

observed at time s_j, $j = 1, ..., m$, $m \leq J$, and J is the maximum number of time index. The observed covariate information consists of $\boldsymbol{H} = \{\boldsymbol{X}, \boldsymbol{s}\}$. At time $u \geq 0$, the history of the covariate process is $\boldsymbol{H}(u) = \{\boldsymbol{X}(u), \boldsymbol{s}(u)\}$, where $\boldsymbol{X}(u) = \{X(s_j) : 0 \leq s_j \leq u\}$, and $\boldsymbol{s}(u) = \{s_j, s_j < u\}$.

4.2.2 Time-varying DSR

Denote the DSR that informs whether to come for a surveillance visit within the coming τ_0 months at time u as $\mathcal{R}_u^{\tau_0}(\boldsymbol{X}(u))$, which uses the covariate information up to time u as input, and takes value in $\{0, 1\}$. We drop superscript τ_0 in the rest of the paper for notation convenience. At any time u, the true positive fraction, $\text{TPF}_u(\mathcal{R}_u)$, is defined as

$$\text{TPF}_u(\mathcal{R}_u) = P\{\mathcal{R}_u(\boldsymbol{X}(u) = 1 | 0 < \tilde{T}_u \leq \tau_0\},$$

and false positive fraction, $\text{FPF}_u(\mathcal{R}_u)$, is defined as

$$\text{FPF}_u(\mathcal{R}_u) = P\{\mathcal{R}_u(\boldsymbol{X}(u) = 1 | \tilde{T}_u > \tau_0\},$$

where $\tilde{T}_u = T - u$ denote the residual event time. While the u-indexed TPF_u FPF_u, $\mathcal{R}_u$ are time-specific and continuous over u, we are mainly interested in the performances of $\mathcal{R}_{s_j}(\boldsymbol{X}(s_j))$, with the corresponding metrics TPF_{s_j} and FPF_{s_j}, at landmark times $j = 1, ..., J$. We simply use index j instead of s_j for time-specific notations in the rest of the paper.

At the jth time index, $\text{TPF}_j(\mathcal{R}_j)$ reflects the gain of the time-specific rule, the extent to which individuals in need of a followup are being identified; and $\text{FPF}_j(\mathcal{R}_j)$ reflects the cost of the rule in terms of over-treating individuals who should be spared the procedure. A time-specific RACB function for $\mathcal{R}_j$ is defined as $\phi_j(\mathcal{R}_j) = \text{TPF}_j(\mathcal{R}_j) - \xi\text{FPF}_j(\mathcal{R}_j)$, where ξ is the pre-specified weight to balance the relative importance of TPF and FPF based on clinical and other practical considerations. We aim at optimizing the global average objective, formulated as

$$\Phi(\boldsymbol{\mathcal{R}}) = \frac{1}{J}\sum_{j=1}^{J} \phi_j(\mathcal{R}_j),$$

where $\boldsymbol{\mathcal{R}} = \{\mathcal{R}_1, ...\mathcal{R}_J\}$. It is straightforward to show that

$$\begin{aligned}\phi_j(\mathcal{R}_j) &= P\{\mathcal{R}_j(X(s_j)) = 1 | 0 < \tilde{T}_j \leq \tau_0\} - \xi P\{\mathcal{R}_j(X(s_j)) = 1 | \tilde{T}_j > \tau_0\} \\ &= E\left(I[\mathcal{R}_j(X(s_j)) = 1] V_j\{X(s_j)\}\right),\end{aligned}$$

where

$$V_j(X(s_j)) = \frac{P\{\tilde{T}_j \leq \tau_0 | X(s_j), \tilde{T}_j > 0\}}{P(\tilde{T}_j \leq \tau_0)} - \xi \frac{P\{\tilde{T}_j > \tau_0 | X(s_j)\}}{P(\tilde{T}_j > \tau_0)}.$$

The optimal decision rule at the jth time is

$$\mathcal{R}_j^*(X(s_j)) = I\left[V_j(X(s_j)) \geq 0\right].$$

Subsequently, $\boldsymbol{\mathcal{R}}^* = \{\mathcal{R}_1^*, ...\mathcal{R}_J^*\}$ optimizes $\Phi(\boldsymbol{\mathcal{R}})$.

4.2.3 Stabilized DSR

In general, $\mathcal{R}_j^*$ could vary for different time points s_j, which could be challenging to implement in the current clinical practices for active surveillance. We therefore focus on stabilized and interpretable DSRs that are linear combinations of $h(X(s_j))$ and $B(s_j)$, denoted as $S\{h(X(s_j)), B(s_j)\}$. Here, $h(X(s_j))$ is a function of $X(s_j)$. $B(s_j)$ is a function of s_j, which could be simply j, assuming a linear effect of measurement time, $\log(s_j)$ or spline basis function of s_j, capturing the potentially nonlinear effect of measurement time. If there is no clear evidence of time effect, $B(s_j)$ could be removed, or set to 0. The goal is to identify the optimal stabilized DSR that maximizes $\Phi(\boldsymbol{\mathcal{R}})$.

4.3 ESTIMATING STABILIZED DSR FROM CENSORED DATA

We propose two methods to estimate the stabilized DSR from longitudinal data that are subject to censoring. Let C denote the censoring time. The data are collected from n independent and identically distributed patient trajectories, where for subject i, we observe $Y_i = \min(T_i, C_i)$, and $\Delta_i = I(T_i \leq C_i)$.

4.3.1 Shared modeling (SM)

One way to construct stabilized DSR is to directly model $V_j\{X(s_j)\}$ by specifying a shared parameter structure across time points [12], and the rule can derived based on the fitted model. We impose a model as $P(V_j \geq 0|\boldsymbol{H}(s_j)) = g(\mathbb{X}_j^T\beta^g)$, where $\mathbb{X}_j = \{1, h(X(s_j)), B(s_j)\}$, and β^g is shared between different stages. Here, we choose to model the binary counterpart of $V_j(X(s_j))$ instead of $V_j(X(s_j))$ on a continuous scale, which is less sensitive to the outliers and could lead to a higher classification accuracy.

However, $V_j\{X(s_j)\}$s are unknown, and need to be estimated. Hence, the proposed SM approach includes two steps. In the first step, we impose a working model for $P\{\tilde{T}_j \leq \tau_0|X(s_j), \tilde{T}_j > 0\}$. The model has the formation of

$$P\{\tilde{T}_j \leq \tau_0|X(s_j), \tilde{T}_j > 0\} = g(\boldsymbol{h}(X(s_j))^T\theta_j),$$

where $g(.)$ is a known, strictly increasing, differentiable function, and $\boldsymbol{h}(X(s_j)) = (1, h(X(s_j)))$. Under the prospective longitudinal setting, $\tilde{T}_j \leq \tau_0$ are not always observed due to censoring for any time point s_j. We proposed to use the inverse probability of censoring weights (IPCW) to account for longitudinal data with censored events. Let $\widehat{G}_j(\cdot)$ be the Kaplan-Meier estimator for $G_j(\cdot)$, the survival function of C among subjects with $Y_i \geq s_j$. The time-dependent estimator $\hat{\theta}_j$ can be solved through the following weighted estimating equation

$$U(\theta_j) = \frac{1}{n_j}\sum_{i=1}^{n_j} \hat{w}_{ij}h(X_i(s_{ij}))\{I(Y_i \leq \tau_0 + s_{ij}) - g(\boldsymbol{h}(X_i(s_{ij}))^T\theta_j)\},$$

where $\hat{w}_{ij} = \{I(Y_i \leq \tau_0 + s_{ij})\Delta_i + I(Y_i > \tau_0 + s_{ij})\}/\widehat{G}_{Y_i\wedge(s_{ij}+\tau_0)}$. Weighted logistic regression can be used in estimating $\hat{\theta}_j$. Subsequently, we can estimate $V_{ij}(X_i(s_{ij}))$ with

$$\widehat{V}_{ij}(X_i(s_{ij})) = \frac{g(\boldsymbol{h}(X_i(s_{ij}))^T\widehat{\theta}_j)}{\sum_{i=1}^{n_j} g(\boldsymbol{h}(X_i(s_{ij}))^T\widehat{\theta}_j)/n_j} - \xi\frac{1 - g(\boldsymbol{h}(X_i(s_{ij}))^T\widehat{\theta}_j)}{1 - \sum_{i=1}^{n_j} g(\boldsymbol{h}(X_i(s_{ij}))^T\widehat{\theta}_j)/n_j}.$$

Provided with the estimated $\widehat{V}_j(X(s_j))$, in the second step, we impose a model on $P(\widehat{V}_j > 0|H(s_j)) = g(\mathbb{X}_j^T\beta^g)$, where $\mathbb{X}_j = \{1, h(X(s_j)), B(s_j)\}$. Logistic regression using Generalized Estimating Equations (GEE) accounting for clustering can be used to estimate $\hat{\beta}^g$. The working

correlation matrix can be case-specific, but in general, independence working correlation suffices. The estimated stabilized rule $\widehat{S}(h(X_i(s_{ij})), B(s_{ij})) = I(\mathbb{X}_{ij}^T \hat{\beta}^g > 0)$.

4.3.2 Optimization with surrogate function (OSF)

We propose a second method to identify a stabilized DSR by directly optimizing an estimator of $\Phi_{RACB}(S)$,

$$\widehat{\Phi}(S) = \frac{1}{J}\sum_{j=1}^{J}\frac{1}{n_j}\sum_{i=1}^{n_j}\left[I\{S(\mathbb{X}_{ij}) = 1\}\left(\widehat{W}_{1,ij} - \xi\widehat{W}_{2,ij}\right)\right], \tag{4.1}$$

where

$$\widehat{W}_{1,ij} = \frac{I(Y_i \le \tau_0 + s_{ij})\Delta_i/\widehat{G}_j(Y_i)}{(\sum_{i=1}^{n_j}\{I(Y_i \le \tau_0 + s_{ij})\Delta_i/n_j\widehat{G}_j(Y_i)}, \widehat{W}_{2,ij} = \frac{I(Y_i > \tau_0 + s_{ij})/\widehat{G}_j(\tau_0 + s_{ij})}{\sum_{i=1}^{n_j}\{I(Y_i > \tau_0 + s_{ij})/n_j\widehat{G}_j(\tau_0 + s_{ij})}.$$

Maximizing (4.1) is equivalent to to minimizing

$$\frac{1}{J}\sum_{j=1}^{J}\frac{1}{n_j}\sum_{i=1}^{n_j}\left[I\{A_{ij}S(\mathbb{X}_{ij}) \ne 1\} \mid \widehat{W}_{1,ij} - \xi\widehat{W}_{2,ij} \mid\right],$$

where $A_{ij} = \text{sign}(\widehat{W}_{1,ij} - \xi\widehat{W}_{2,ij})$, $S(\mathbb{X}_{ij}) = I(\mathbb{X}_{ij}^T\beta^\phi > 0)$, and $\beta^\phi = (\beta_0^\phi, {\beta_1^\phi}^T)^T$. Since $\widehat{\Phi}(S)$ involves indicators from all time points, it is difficult to directly optimize $\widehat{\Phi}(S)$ over β^ϕ. We will replace a surrogate function ϕ for the indicator. In this paper, we use the hinge loss, $\phi(v) = \max(1 - v, 0)$. Furthermore, we introduce the regularization parameter λ to penalize the complexity of the decision function to avoid overfitting. Thus, we minimize the empirical surrogate objective

$$\min_{\beta^\phi}\sum_{j=1}^{J}\sum_{i=1}^{n_j}\left[\phi(A_{ij}\mathbb{X}_{ij}^T\beta^\phi) \mid \frac{1}{n_j}\widehat{W}_{1,ij} - \xi\frac{1}{n_j}\widehat{W}_{2,ij} \mid\right] + \lambda\|\beta_1^\phi\|^2. \tag{4.2}$$

We introduce slack variable ϵ_{ij} following the techniques applied in support vector machine (SVM), our problem becomes

$$\min_{\beta^\phi,\epsilon}\kappa\sum_{j=1}^{J}\sum_{i=1}^{n_j}\left[\epsilon_{ij}\left|\frac{1}{n_j}\widehat{W}_{1,ij} - \xi\frac{1}{n_j}\widehat{W}_{2,ij}\right|\right] + \frac{1}{2}\|\beta_1^\phi\|^2. \tag{4.3}$$

subject to $A_{ij}\mathbb{X}_{ij}^T\beta^\phi \ge 1 - \epsilon_{ij}, \epsilon_{ij} \ge 0$, where κ is a tuning parameter. After introducing Lagrange

multipliers, the Lagrange function becomes:

$$\kappa\sum_{j=1}^{J}\sum_{i=1}^{n_j}\left[\epsilon_{ij}\left|\frac{1}{n_j}\widehat{W}_{1,ij}-\xi\frac{1}{n_j}\widehat{W}_{2,ij}\right|\right]+\frac{1}{2}\|\beta_1^{\phi}\|^2-\sum_{j=1}^{J}\sum_{i=1}^{n_j}a_{ij}\{A_{ij}\mathbb{X}_{ij}^T\beta^{\phi}-(1-\epsilon_{ij})\}-\sum_{j=1}^{J}\sum_{i=1}^{n_j}\mu_{ij}\epsilon_{ij},$$

where $a_{ij}\geq 0, \mu_{ij}\geq 0$. Taking derivatives with respect to β_0^{ϕ}, β_1^{ϕ} and ϵ_{ij}, we have $\beta_1^{\phi}=\sum_{j=1}^{J}\sum_{i=1}^{n_j}a_{ij}A_{ij}\mathbb{X}_{[ij,-1]}$, where $\mathbb{X}_{[,-1]}$ denotes the design matrix without the first column of 1s corresponding to the intercept, $\sum_{j=1}^{J}\sum_{i=1}^{n_j}a_{ij}A_{ij}=0$, and $a_{ij}=\kappa \mid \widehat{W}_{1,ij}/n_j-\xi\widehat{W}_{2,ij}/n_j \mid -\mu_{ij}$. Plugging these equations back into the Lagrange function, we obtain the dual problem

$$\max_a\sum_{j=1}^{J}\sum_{i=1}^{n_j}a_{ij}-\frac{1}{2}\sum_{j=1}^{J}\sum_{i=1}^{n_j}\sum_{l=1}^{J}\sum_{k=1}^{n_l}a_{ij}a_{kl}A_{ij}A_{kl}\langle\mathbb{X}_{[ij,-1]},\mathbb{X}_{[kl,-1]}\rangle,$$

subject to $0\leq a_{ij}\leq\kappa \mid \widehat{W}_{1,ij}/n_j-\xi\widehat{W}_{2,ij}/n_j \mid, \sum_{j=1}^{J}\sum_{i=1}^{n_j}a_{ij}A_{ij}=0$. The above can be solved by quadratic programming. Finally, we obtain that $\hat{\beta}_1^{\phi}=\sum_{j=1}^{J}\sum_{i=1_{\hat{a}_{ij}>0}}^{n_j}\hat{a}_{ij}A_{ij}\mathbb{X}_{[ij,-1]}$, and $\hat{\beta}_0^{\phi}$ can be solved using the margin points $(\hat{a}_{ij}>0,\hat{\epsilon}_{ij}=0)$, subject to the complementary slackness condition. Subsequently, the estimated stabilized DSR is $I(\mathbb{X}_{ij}^T\hat{\beta}^{\phi}>0)$.

We recommend using the 'owl' function in package 'DynTxRegime' on the comprehensive R network (cran.org), where reward is $\mid \widehat{W}_{1,ij}/n_j-\xi\widehat{W}_{2,ij}/n_j \mid *P(A_{ij})$, and regime is A_{ij}, for easy implementation of the algorithm.

4.4 INFERENCE

In this section, we provide asymptotic properties of the proposed methods, under the following assumptions:

A1. $n_j=O(n),\forall j\in\{2,..J\}$;

A2. With probability at least $1-\delta$, we have $\|\hat{\theta}_j-\theta_j\|_2<c_1(\delta)n^{-1/2},\forall j\in\{1,..J\}$.

A3. There exists at least one covariate (including the intercept) with a nonzero coefficient with its conditional distribution given the other covariates is absolutely continuous. For identifiability purpose, we set its absolute value to be 1.

Denote β^{g^*} to be the root of $M(\beta^g) = 0$, the specific form of which is provided in the appendix, and β^{ϕ^*} as

$$\beta^{\phi^*} = \text{argmin} \frac{1}{J} \sum_{j=1}^{J} \mathbb{E}\left[\phi(\mathbb{X}_j^T \beta^\phi)\} \left(W_{1,ij} - \xi W_{2,ij}\right)\right],$$

where the expectation is with respect to $\mathbb{X}_j$. We establish the consistency of the estimators: $\hat{\beta^g} \xrightarrow{p} \beta^{g^*}$, $\hat{\beta^\phi} \xrightarrow{p} \beta^{\phi^*}$.

Asymptotic Normality: $\sqrt{n}(\hat{\beta^g} - \beta^{g^*}) \to N(0, \Sigma_g)$, $\sqrt{n}(\hat{\beta^\phi} - \beta^{\phi^*}) \to N(0, \Sigma_\phi)$. The forms of Σ_g and Σ_ϕ are provided in the appendix.

The proofs are provided in the appendix.

The theorems indicate that the asymptotic distributions are well-defined for both $\hat{\beta}^g$ and $\hat{\beta}^\phi$. We note that in general, β^{g^*} and β^{ϕ^*} differ from the true parameter β^{opt}, which is the oracle parameter indexing the optimal DSRs that are shared across landmark times. We show in the supplement that under certain scenarios, with one example presented in the simulation studies, we have $\beta^{g^*} = \beta^{\text{opt}}$. For the OSF method, in order to have $\beta^{\phi^*} = \beta^{\text{opt}}$, we have to ensure $E\{X^T\beta^{\phi^*}|X^T\beta\}$ is linear in $X^T\beta$, which is satisfied when the covariates X are elliptically symmetric, for example, if $\mathbb{X}$ follows the normal distribution. In longitudinal studies, repeated measures are often correlated within each cluster, and typically violate this condition. However, as we shown in the simulation studies, the OSF method is robust to possible assumption violation.

4.5 SIMULATION STUDIES

4.5.1 Data generation

We conducted simulation studies to compare our proposed approaches and some existing methods. In scenario 1 was a simplified setting where the model in SM method was correctly specified, and the optimal global average objective of $\Phi(\boldsymbol{\mathcal{R}})$ can be obtained. Scenario 2 was a more realistic data generation, and due to its complexity, no oracle value of $\Phi(\boldsymbol{\mathcal{R}})$ can be obtained. In Scenario 1,we set $J = 5$, then there were up to 5 measurements per subject taken at $s_j = 6(j-1)$, for $j = 1, \ldots, 5$, and $\tau_0 = 6$. We generated two biomarkers $X_{j,1}$ and $X_{j,2}$, measured at $j = \{1, 2, ..J\}$ from a multivariate normal distribution, which has a mean equals to 1, and an exchangeable covariance matrix, with diagonal entries equaling to 1, and off-diagonal entries

equaling to 0.7. We generated a binary event indicator variable $Q_j|X_{j1}, X_{j2} \sim Bernoulli(\mu_j)$, where $\mu_j = exp(\theta_{0j} + \theta_{1j}X_{j1} + \theta_{2j}X_{j2})/\{1 + exp(\theta_{0j} + \theta_{1j}X_{j1} + \theta_{2j}X_{j2})\}$, $\forall j \in \{1, 2, .., J\}$. If $Q_{im} = 1$ for certain patient i, $m \in \{1, 2, .., J\}$, indicating an event occurs within time τ_0 from s_m, we removed subsequent information at the jth visit, $\forall j > m$, and generate $T_i = s_{im} + v_1 * \tau_0$, $v_1 \sim Uniform(0, 1)$. If $Q_{ij} = 0$ for patient i, $\forall j \in \{1, 2, .., J\}$, indicating no event occurs within time τ_0 from s_J, we let $T_i = s_{iJ} + v_2 * \tau_0$, $v_2 \sim Uniform(1, 10)$. Lastly, we generated a censoring indicator $C \sim Uniform(0, 150)$ so that the censoring percentage is around 15 % .

Let $P_{1j} = P(Q_j = 1|Q_m = 0, \forall m < j)$, $P_{0j} = 1 - P_{1j}$, $\forall j \in \{1, 2, .., J\}$, where P_{1j} varies as j varies. It can be shown that the explicit form of time-dependent optimal DSR $b_j^* = (b_{0j}^*, b_{1j}^*, b_{2j}^*) = (\theta_{0j} - g^{-1}\{\frac{\xi}{P_{0j}}(\frac{1}{P_{1j}} - \frac{\xi}{P_{0j}})^{-1}\}, \theta_{1j}, \theta_{2j})$ [91]. Let $\theta_{1j} = 1$ and $\theta_{2j} = -3$. In this case, the global optimal rule $\mathcal{R}_j^*$ consists of time-invariant biomarker coefficients, but potentially time-variant intercepts as b_{0j}^* is a function of not only θ_{0j}, but also P_{0j}. We fix $b_{0j}^* = b_0^*$ by varying θ_{0j}, i.e., the intercepts of the time-dependent rules were also fixed, we obtained $\Phi(S^*) = \Phi(\boldsymbol{\mathcal{R}}^*)$. However, if we additionally constrain $b_{0j}^* = b_0^*, \forall j \in \{1, ..., J\}$ by varying θ_{0j} at each j, meaning that the intercepts of the time-dependent rules are fixed, we can have $\Phi(S^*) = \Phi(\boldsymbol{\mathcal{R}}^*)$, where $\mathcal{R}_j^*(\{1, X_{ij,1}, X_{ij,2}\}) = b_0^* + \theta_1 X_{ij,1} + \theta_2 X_{ij,2}$, and $S^*(\mathbb{X}_{ij}) = \mathbb{X}_{ij}^T \beta^*$, where $\mathbb{X}_{ij} = \{1, X_{ij,1}, X_{ij,2}\}$, and $\beta^* = \{b_0^*, \theta_1, \theta_2\}$. More details on the data generation are provided in the appendix.

In Scenario 2, we set $J = 5$ and assumed a linear mixed effects model with measurement errors for the biomarkers Z_1 to Z_4. We generated Z_k, $k = 1, ..., 4$, by $Z_{i,k}(u) = W_{i,k}(u) + e_{i,k}(u)$, where $W_{i,k}(u) = a_{0i,k} + a_{1i,k} log(u/v_1)$. The random components $a_{i,k} = (a_{0i,k}, a_{1i,k})$ were generated as a bivariate normal with mean= $(-0.1, -1.0)^T$, and covariance matrix $M = (0.83^2 \ -0.005; -0.005 \ 0.13^2)$. The measurement errors $e_{i,k}(u)$ are generated from $N(0, 0.1)$.

Failure time was assumed to follow a proportional hazards model with hazard rate function as $\lambda(u) = \lambda_0(u) \exp(-0.7W_2(u) + 0.8W_3(u) - 1.3W_4(u))$, with a Weibull baseline hazard: $\lambda_0(u) = v/v_1(u/v_2)^{v-1}$. We set $v_1 = 30$, scale $v_2 = 15$, and shape $v = 1.4$. Therefore, theoretically the survival time and optimal DSR should not depend on covariate Z_1. Censoring time was generated from a uniform distribution $\sim Uniform(0, 150)$, resulting in about 30% censoring.

4.5.2 Performance Comparisons

In both scenarios, we considered sample sizes of 400 and 1500. We independently generated a validation dataset with 60000 observations. The experiment is performed 100 times repeatedly. In each replicate, we calculate the mean outcomes for different methods in the validation dataset had the whole population followed the estimated DSR. We present the results of $\xi = 0.75$ in the main text, and the results of $\xi = 1$ and $\xi = 4/3$ are in the supplement. To our knowledge, there is no existing method that aims specifically at solving our problem. Nevertheless, we consider an approach that adapts the existing longitudinal regression models thus can be easily implemented as a comparison with our novel learning-based methods. Specifically, we fit flexible partly conditional (PC) GLM models [58] to obtain an estimate of the conditional probability of the event within τ_0 given event-free survival and covariate information up to time s. To have a uniform cutoff point across all landmark times, we do a grid search of [0,1], with step size 0.01, on the training set, to select the optimal cutoff p^* that maximizes the global average RACB. The resulting decision rule derived from revised PC-GLM has the same non-intercept coefficients as PC-GLM, while adjusting intercept to be $\beta_0^{\text{PC-GLM}} - log(p^*/(1-p^*))$. In addition to the DSR derived from the generalized linear model (GLM) form of the PC-GLM with a uniform cutoff , we also compare the performance of the proposed methods with the methods that derive time-dependent DSRs instead ($\Phi_{RACB}(s)$ verus $\Phi_{RACB}(\mathcal{R})$). In addition, we compare the proposed methods to the ones deriving the optimal DSRs that can vary over time. In particular, the analog for the SM method in deriving the time-dependent DSRs is simply its first step, which we term as "unshared modeling". The analog for the OSF method is to consider stage-specific parameters instead of shared parameters in the algorithm, which we term as "unshared OSF". We report the performance of tie. In scenario 1, we are able to derive a closed form of global optimal stabilized rule S^*, which is applied on the validation set. $\Phi_{RACB}(S^*)$ is thus our gold standard.

Results for coefficients of the stabilized DSRs and RACB values of various approaches are presented in Tables 4.1 to 4.4. In scenario 1, all methods yield coefficients that are comparable to the ones from the oracle. As anticipated, the SM method performs the best in both sample sizes, since it is consistent with the model specification in the data generation. While the PC GLM in theory also consistently estimates the conditional probability of the event, the choice of the optimal

uniform cutoff simply by grid search may not be precise, and highly variable especially in small sample sizes. Our proposed estimators are more efficient in comparison. In Scenario 2, the OSF method outperforms the other methods. In this scenario, true parameters are unknown except for $\beta_{1,1}$, which should be 0 as the first biomarker has no effect on survival in data generation. We can see that both proposed methods have coefficient estimates close to 0. In scenario 2, the global optimal rules are unknown, and may very likely to be time-dependent. However, when the sample size is 400, our proposed stabilized DSRs outperform the time-varying analog in terms of RACB values. When the sample size is 1500, the time-varying analog only marginally outperforms the stabilized DSRs in terms of RACB values, but the proposed methods yield DSRs that enjoy simpler forms. Our proposed methods outperform PC-GLM with a uniform cutoff in all cases.

4.6 ANALYSIS of the CANARY PASS

The Canary PASS is a multicenter, prospective active surveillance cohort study initiated in 2008 with ongoing accrual. To date over 1,500 patients with prostate cancer managed with AS have been enrolled, with a 4.1-year median follow-up. For our illustration, we include 850 patients with Gleason grade group (GG) 1 prostate cancer at diagnosis, with at least one "confirmatory" biopsy after diagnosis, and enrolled in PASS before 2017. The outcome of interest is the time from the confirmatory biopsy to reclassification, defined as GG 2 or higher on a subsequent biopsy. By study protocol the surveillance biopsies occur first in a 6-month interval, then a 1-year interval in later years. Most patients had their clinical visits following approximately this fixed schedule, but can be earlier or later within a clinically acceptable time window. Thus we fix 6 stages, corresponding to the observations measured at time intervals [0.5, 1), [1, 1.5), [1.5, 2), [2, 2.5), [2.5, 3), [3, 3.5) years after diagnosis, respectively. For patients who have multiple measurements within a single time interval, we select only the earliest measurement within the time interval. Patients who don't have measurements in any of the time frames are removed from the analysis. This results in 832 patients remaining in the final analysis. At the visit time occurs within the stage and based on biomarker and clinical information accumulated up to that time, the decision rule is whether the patient should take a biopsy in the subsequent $\tau_0 = 2$ years. For patient i who was event-free up to stage j, if the event occurred within τ_0 year after stage j, the optimal surveillance rule should recommend biopsy for this patient, and not otherwise. We vary ξ and τ_0 to illustrate how DSRs can

be derived to reflect different clinical applications. In PASS, a biopsy at 6 to 12 months, then at 24 months from diagnosis are expected. To identify patients for whom the surveillance intensity can be relaxed, we derive a DSR to determine for a patient if a biopsy is needed within $\tau_0 = 2$ years. We set a low pre-specified weight of $\xi = 0.5$ to reflect the relative importance of TPF, accounting for the consequence of missing patients who progressed during the time interval if an evaluation with a biopsy is not performed in 2 years. On the other hand, we set $\xi = 1$ to reflect the relative importance of controlling overtreatment. The parameter ξ is actually in one-to-one correspondence to a constraint threshold, where in out case, at $\xi = 0.5$ and $\xi = 1$, no more than 14, and 7 people, respectively, should be evaluated to identify one high-grade cancer under an observed event rate of 0.126. A reasonable range of ξ values can be considered in order to select the rule that achieves the desired clinical utility. [66] provides more guidance on the choice of ξ.

We implemented both the SM and OSF methods to derive the two types of DSRs. Predictors considered in model development included log-transformed years since diagnosis, body mass index (BMI), log-transformed prostate size, log-transformed PSA at diagnosis, prior negative biopsy, maximum percent positive cores, and PSA, ascertained at each measurement time if available. We compared the proposed method with that from the PC-GLM with a uniform cutoff, and also the time-varying counterparts of both methods, where we derived the time-dependent decision rules separately at each visit time.

We carry out a cross-validation procedure to evaluate the performance of both methods. At each run, we partition the whole dataset into two equal parts, with one part serving as training data to estimate the rules with shared parameters using both methods, and the other part as the validation set for implementing the estimated rules with shared parameters. Each part served as the validation subset once, and the cross-validated outcome values of the constructed rules are obtained by averaging the empirical values on both validation subsets. The procedure is repeated 100 times. The average Φ_{RACB} values yielded by each method are presented in Table 5. The stabilized rules tend to have higher or comparable clinical net benefit compared with their time-varying counterparts, while enjoying the additional benefit of ease in implementation. Additionally, the proposed procedures outperform the PC-GLM in terms of higher net benefit and higher efficiency.

To obtain a final set of robust coefficient estimates of the rule, we carry out both methods on the whole dataset. The estimates of coefficients, along with the 95% confidence intervals using a

bootstrap method, are presented in Table 6. We standardize the rules by setting the absolute value of the last covariate "prior negative biopsy (since diagnosis)" to be one.

4.7 DISCUSSION

Clinical decision rules tailored to a patient's past and current biologic and clinical information hold the potential to greatly improve patient outcome and the efficiency in disease management. We have proposed two flexible approaches to estimating DSRs, with the objective of balancing benefit against cost. In particular, the proposed stabilized procedures are easy to implement by modifying standard statistical software, and the resulting stabilized DSRs are convenient for clinicians to implement in practice. We establish the asymptotic properties of the proposed methods. Numerical studies show that the proposed methods have superior performances. Specifically, when the sample size is small, the estimation of time-varying DSRs could have an unstable performance. Conversely, the proposed methods are more robust since they essentially gather information across all stages for estimating the shared parameters.

With the presence of high-dimensional data, L_1 penalties can be added to both the SM and OSF methods. In the SM method, the global time-variant optimal DSRs are estimated by logistic regression, but other non-parametric algorithms can be implemented, such as tree ensemble models or neural network. They could improve the performance by capturing potentially complicated nonlinear relationships between biomarkers and outcomes. Similarly, other classification methods such as SVM can be implemented in the second step. In the direct optimization method, we adopt hinge loss as the surrogate loss, but other types of losses such as logistic loss or ramp loss can also be considered. Last but not least, it is worth investigating the methods for deriving DSRs when there are missing data in addition to censored data present.

Another direction is to identify the optimal time to the next measurement. [69] focus on estimating a continuous quantity: the optimal time to next measurement of longitudinal biomarkers, given the patient is event-free up to time t. They adopt the joint modeling framework to optimize some information theory quantities including cross entropy and Kullback–Leibler divergence. Extending our work to directly estimate the optimal time intervals with the consideration of more clinically relevant criteria is warranted.

Tables

Method	Sample size	$\beta_{1,1}$	$\beta_{1,2}$
Oracle		0.579	-1.736
SM	n=400	0.607(0.1618)	-1.805(0.2524)
	n=1500	0.580(0.0717)	-1.721(0.1076)
OSF	n=400	0.586(0.2272)	-1.637(0.3122)
	n=1500	0.584(0.1130)	-1.643(0.1599)
PC GLM	n=400	0.698(0.3148)	-2.060(0.7693)
	n=1500	0.609(0.1302)	-1.832(0.3456)

Table 4.1. Coefficients (standard error) of the estimated stabilized DSRs in Scenario 1, $\xi = 0.75$.

Method	Sample size	$\Phi_{RACB}(S)$	$\Phi_{RACB}(\mathcal{R})$
Oracle		0.743	0.743
SM	n=400	0.741(0.0024)	0.718(0.0270)
	n=1500	0.742(0.0005)	0.740(0.0028)
OSF	n=400	0.736(0.0082)	0.709(0.0286)
	n=1500	0.741(0.0028)	0.736(0.0048)
PC GLM	n=400	0.733(0.0126)	0.733(0.0126)
	n=1500	0.739(0.0048)	0.739(0.0048)

Table 4.2. RACB values (standard error) of DSRs in Scenario 1, $\xi = 0.75$.

Method	Sample size	$\beta_{1,1}$	$\beta_{1,2}$	$\beta_{1,3}$	$\beta_{1,4}$
SM	n=400	0.095(0.1901)	-0.532(0.1702)	0.846(0.3592)	-1.070(0.2939)
	n=1500	0.109(0.0868)	-0.526(0.0831)	0.876(0.1197)	-1.055(0.0980)
OSF	n=400	0.064(0.0829)	-0.385(0.0950)	0.613(0.0771)	-0.803(0.0815)
	n=1500	0.062(0.0421)	-0.387(0.0462)	0.621(0.0403)	-0.802(0.0432)
PC GLM	n=400	-0.065(0.0586)	-0.408(0.1063)	0.303(0.0902)	-0.702(0.1699)
	n=1500	-0.065(0.0274)	-0.401(0.0625)	0.300(0.0487)	-0.690(0.0980)

Table 4.3. Coefficients (standard error) of the estimated stabilized DSRs in Scenario 2, $\xi = 0.75$.

Method	Sample size	$\Phi_{RACB}(S)$	$\Phi_{RACB}(\mathcal{R})$
SM	n=400	0.489(0.0152)	0.481(0.0224)
	n=1500	0.502(0.0048)	0.513(0.0052)
OSF	n=400	0.501(0.0056)	0.497(0.0123)
	n=1500	0.506(0.0028)	0.516(0.0035)
PC GLM	n=400	0.415(0.0242)	0.415(0.0242)
	n=1500	0.424(0.0115)	0.424(0.0115)

Table 4.4. RACB values (standard error) of DSRs in Scenario 2, $\xi = 0.75$.

Outcome	SM, $\mathcal{R}$	SM, S	OSF, $\mathcal{R}$	OSF, S	PC GLM
$\xi = 0.5$					
Φ_{RACB}	0.525(0.020)	0.560(0.022)	0.539(0.020)	0.564(0.015)	0.554(0.024)
TPF	0.803(0.023)	0.862(0.022)	0.815(0.023)	0.840(0.017)	0.844(0.036)
FPF	0.557(0.022)	0.604(0.027)	0.553(0.013)	0.552(0.014)	0.580(0.055)
$\xi = 1$					
Φ_{RACB}	0.312(0.029)	0.358(0.022)	0.319(0.026)	0.359(0.024)	0.314(0.025)
TPF	0.645(0.030)	0.686(0.020)	0.640(0.027)	0.662(0.024)	0.650(0.054)
FPF	0.333(0.012)	0.328(0.014)	0.321(0.009)	0.302(0.009)	0.337(0.047)

Table 4.5. The RACB values(standard error) of different methods in real data analysis.

$\xi = 0.5$	SM	OSF	PC GLM
Intercept	2.12(-0.16,6.54)	1.09(-1.21,6.88)	2.31(-0.62,7.65)
Max percent positive cores	0.11(0.02,0.27)	0.11(0.01,0.37)	0.10(0.02,0.27)
Ln time since diagnosis (yrs)	-1.56(-2.90,-0.83)	-0.98(-3.21,-0.22)	-1.61(-3.15,-0.73)
BMI	0.09(0.01,0.20)	0.06(-0.01,0.23)	0.09(0.00,0.20)
Ln prostate size (cc)	0.62(-0.03,1.41)	0.55(-0.33,1.74)	0.59(-0.08,1.37)
Ln diagnostic PSA	0.17(-0.38,0.80)	0.14(-0.26,0.44)	0.66(0.21,1.49)
Prostate-specific antigen in blood	0.39(0.02,0.90)	0.23(-0.09,0.79)	0.42(0.04,1.09)
Prior negative biopsy (since diagnosis)	-1.00(-1.00,-1.00)	-1.00(-1.00,-1.00)	-1.00(-1.00,-1.00)
$\xi = 1$			
Intercept	1.59(-0.94,5.34)	1.75(-1.45,5.88)	1.50(-1.30,5.83)
Max percent positive cores	0.10(0.03,0.26)	0.15(0.00,0.36)	0.10(0.02,0.27)
Ln time since diagnosis (yrs)	-1.48(-2.87,-0.69)	-1.74(-3.05,0.00)	-1.61(-3.15,-0.73)
BMI	0.08(0.01,0.20)	0.09(0.00,0.20)	0.09(0.00,0.20)
Ln prostate size (cc)	0.58(0.01,1.27)	0.75(-0.08,1.15)	0.59(-0.08,1.37)
Ln diagnostic PSA	0.01(-0.21,0.34)	-0.06(-0.43,0.20)	0.66(0.21,1.49)
Prostate-specific antigen in blood	0.41(0.00,0.92)	0.49(0.00,1.21)	0.42(0.04,1.09)
Prior negative biopsy (since diagnosis)	-1.00(-1.00,-1.00)	-1.00(-1.00,-1.00)	-1.00(-1.00,-1.00)

Table 4.6. Coefficients (95% CI) of the estimated stabilized DSRs in real data analysis

Appendix

Theoretical properties.

SM method

Let $\mathbb{X}$=

$$\begin{pmatrix} 1 & X_{11} \\ 1 & X_{12} \\ 1 & X_{13} \\ \vdots & \\ 1 & X_{1J} \\ \vdots & \\ 1 & X_{nJ} \end{pmatrix},$$

Let $\tilde{\mathbb{X}}$=

$$\begin{pmatrix} 1 & X_{11} & 0 & 0 & \cdots & 0 & 0 & 0 & \cdots & 0 \\ 1 & 0 & X_{12} & 0 & \cdots & 0 & 1 & 0 & \cdots & 0 \\ 1 & 0 & 0 & X_{13} & \cdots & 0 & 0 & 1 & \cdots & 0 \\ \vdots & \vdots & \vdots & & \ddots & & & & & \\ 1 & 0 & 0 & 0 & \cdots & X_{1J} & 0 & 0 & \cdots & 1 \\ \vdots & & & & & & & & & \\ 1 & 0 & 0 & 0 & \cdots & X_{nJ} & 0 & 0 & \cdots & 1 \end{pmatrix},$$

Let $\beta = (\beta_0, \beta_1)$, and $\tilde{\beta} = (\tilde{\beta}_{10}, \tilde{\beta}_{11}, \tilde{\beta}_{21}, ...\tilde{\beta}_{J1}, \tilde{\beta}_{20} - \tilde{\beta}_{10}, \tilde{\beta}_{30} - \tilde{\beta}_{10}, ..\tilde{\beta}_{J0} - \tilde{\beta}_{10}))$. Let $M_n(\beta^g) = \frac{1}{n}\sum_i^n U_i\{\beta^g, \alpha^*(\beta^g), \hat{\tilde{\beta}}\}$, where $\alpha^*(\beta^g) = \hat{\alpha}\{\beta^g, \hat{\phi}(\beta^g)\}$, $U_i\{\beta^g, \alpha, \tilde{\beta}\} = {D_i}^T W_i(\alpha, \phi)^{-1}(I(\tilde{\mathbb{X}}_i\tilde{\beta} > 0) - \mu_i)$, where $\mu_{ij} = \frac{e^{\mathbb{X}_{ij}^T\beta^g}}{1+e^{\mathbb{X}_{ij}^T\beta^g}}$, $D_{ij} = \frac{\partial\mu_{ij}}{\partial\beta^g}$, $W_i(\alpha, \phi) = Var(Y_i) = A_i^{\frac{1}{2}}R(\alpha)A_i^{\frac{1}{2}}/\phi$. Next we let $M(\beta^g) = EU_i\{\beta^g, \alpha, \tilde{\beta}\}$. We first use z-estimation theory to prove the consistency of $\hat{\beta^g}$ to β^{g*}, where $\hat{\beta^g}$ is a root of $M_n(\beta^g)$, and β^{g*} is the root of $M(\beta^g)$. By z-estimator consistency theorem, $\hat{\beta^g}$ converges in probability to β^{g*} if the following conditions hold:

- Uniform convergence: $\sup_{\beta^g\in\Omega} \|M_n(\beta^g) - M(\beta^g)\| \xrightarrow{p} 0$.

- Identifiability: For all $\epsilon > 0$, $\inf\{\|M(\beta^g)\| : d(\beta^g, \beta^{g*}) \geq \epsilon\} > 0 = \|M(\beta^{g*})\|$.

- Root Approximation: $M_n(\hat{\beta}^g) = op(1)$

We first verify the first condition. Given the consistency of $\hat{\tilde{\beta}}$ to $\tilde{\beta}$ as $n \to \infty$, and the continuity of at least some columns(continuous biomarkers assumption) of $\tilde{\mathbb{X}}_i$, we can establish that $\{I(\tilde{\mathbb{X}}_i\hat{\tilde{\beta}} > 0) - \mu_i\} - \{I(\tilde{\mathbb{X}}_i\tilde{\beta} > 0) - \mu_i\} = op(1)$ by continuous mapping theorem. Therefore, we have $M_n(\beta^g) \xrightarrow{p} M(\beta^g)$ for each fixed β^g. In order to establish uniform covergence, we note that $M(\beta^g)$ is a Glivenko-Cantelli class, with Ω restricted to a compact set. Therefore, the first condition of z-estimation consistency is satisfied. The second condition of identifiability can be satisfied by assuming the uniqueness of β^{g*}. The last condition is satisfied given $\hat{\beta}^g$ is an root of $M_n(\beta^g)$. In conclusion, by z-estimation theory, we establish $\hat{\beta}^g - \beta^{g*} = op(1)$.

We next establish the asymptotic normality of $\hat{\beta}^g$. By taylor expansion, under some regularity conditions, $\sqrt{n}(\hat{\beta}^g - \beta^{g*})$ can be approximated by

$$\left[\frac{1}{n}\sum_i^n \frac{\partial}{\partial \beta^{g*}} U_i\{\beta^{g*}, \alpha^*(\beta^{g*}), \hat{\tilde{\beta}}\}\right]^{-1} \left[\frac{1}{n^{1/2}}\sum_i^n U_i\{\beta^{g*}, \alpha^*(\beta^{g*}), \hat{\tilde{\beta}}\right].$$

Let β^{g*} be fixed. Taylor expansion gives

$$\begin{aligned}
\frac{1}{n^{1/2}}\sum_i^n U_i\{\beta^{g*}, \alpha^*(\beta^{g*}), \hat{\tilde{\beta}}\} &= \frac{1}{n^{1/2}}\sum_i^n U_i\{\beta^{g*}, \alpha, \tilde{\beta}\} + [\frac{1}{n}\sum_i^n \frac{\partial}{\partial \tilde{\beta}} U_i\{\beta^{g*}, \alpha, \tilde{\beta}\}][n^{1/2}(\hat{\tilde{\beta}} - \tilde{\beta})] \\
&+ [\frac{1}{n}\sum_i^n \frac{\partial}{\partial \alpha} U_i\{\beta^{g*}, \alpha, \tilde{\beta}\}][n^{1/2}(\hat{\alpha} - \alpha)] + op(1) \\
&= A^* + B^*C^* + D^*E^* + op(1).
\end{aligned}$$

We prove that it can be written as sums of asymptotic linear estimators, thus establishing its own normality. Note that A^* is asymptotically linear with mean 0 since β^{g*} is the root of $M(\beta^g) = 0$. Next, $B^* = \frac{1}{n}\sum_i^n \frac{\partial}{\partial \tilde{\beta}} U_i\{\beta^{g*}, \alpha, \tilde{\beta}\}$, which converges to $B = EU_i\{\beta^{g*}, \alpha, \tilde{\beta}\} = O_p(1)$ by LLN. Then we have $C^* = [n^{1/2}(\hat{\tilde{\beta}} - \tilde{\beta})]$ is distributed multivariate normally with mean 0 and covariance Σ, as $\hat{\tilde{\beta}}_j$ is an asymptotically linear estimator, $\forall j \in \{1, ...J\}$. Then $D^* = [\frac{1}{n}\sum_i^n \frac{\partial}{\partial \alpha} U_i\{\beta^{g*}, \alpha, \tilde{\beta}\}]$ are

linear functions of op(1)s, so $D^*E^* = op(1)$. Finally, we look at

$$\begin{aligned} & \frac{\partial}{\partial \beta^{g*}} U_i\{\beta^{g*}, \alpha^*(\beta^{g*}), \hat{\tilde{\beta}}\}] \\ = & \frac{\partial}{\partial \beta^{g*}} U_i\{\beta^{g*}, \alpha^*(\beta^{g*}), \hat{\tilde{\beta}}\} + \frac{\partial}{\partial \alpha^*} U_i\{\beta^{g*}, \alpha^*(\beta^{g*}), \hat{\tilde{\beta}}\} * \frac{\partial \alpha^*(\beta^{g*})}{\partial \beta^{g*}} \\ = & A_i + B_i C, \end{aligned}$$

where $\frac{1}{n}\sum_i^n A_i$ converges to as $-\frac{1}{n}\sum_i^n {D_i}^T W_i(\alpha, \phi)^{-1} D_i$ as $n \to \infty, \sum_i^n B_i = op(n), C = Op(1)$.

In scenario 1, we have $\mathbb{X}^T\beta = \tilde{\mathbb{X}}^T\tilde{\beta}, \beta_0 = \tilde{\beta}_{10}, \tilde{\beta}_{j1} = \beta_1, \tilde{\beta}_{j0} - \tilde{\beta}_{10} = 0, \forall j$, and we can prove that $\beta^{g*}/\|\beta^{g*}\| = \beta/\|\beta\|$. We first state the theorem that if the data is linearly separable, the solution of the generalized estimating equations for logistic regression is obtained by finding a vector β such that $\mathbb{X}^T\beta = 0$ separates the class, and then taking the magnitude of β to infinity. We examine the relationship between the parameter β^{g*} and β. In scenario 1, it is clear that $\mathbb{X}^T\beta = \tilde{\mathbb{X}}^T\tilde{\beta}$. Since $\mu_{ij}^* = \frac{e^{\mathbb{X}_{ij}\beta^{g*}}}{1+e^{\mathbb{X}_{ij}\beta^{g*}}}$, and if we find an β^{g*} such that the following holds, then β^{g*} is the obtained solution to $M(\beta^g) = 0$: we observe $I(\tilde{\mathbb{X}}^T\tilde{\beta} > 0) = I(\mathbb{X}^T\beta > 0)$, and if $\beta^{g*} = c\beta$, where $c \to +\infty$, then $I(\mathbb{X}_{ij}^T\beta > 0) \approx (\frac{e^{\mathbb{X}_{ij}\beta^{g*}}}{1+e^{\mathbb{X}_{ij}\beta^{g*}}}) = 1 - \frac{1}{1+e^{\mathbb{X}_{ij}\beta^{g*}}}$. Therefore, we have $\beta^{g*}/\|\beta^{g*}\| = \beta/\|\beta\|$.

OSF Method

Let

$$\begin{aligned} \beta_\phi^* &= \text{argmin} L^\phi(\beta; P_{1j}, w_{ij}) \\ &= \text{argmin} \frac{1}{J}\sum_{j=1}^{J} \Phi_{RACB}(\mathcal{R}_u^j) \\ &= \frac{1}{J}\sum_{j=1}^{J} (\text{TPF}(\mathcal{R}_u^j) - \xi \text{FPF}(\mathcal{R}_u^j)) \\ &= \text{argmin} E \frac{1}{n}\sum_{i=1}^{n}\sum_{j=1}^{n^i} \phi(\mathbb{X}_{ij}^T\beta^\phi) \left(\frac{I(D_{ij}=1)w_{ij}}{P_{ij}} - \epsilon \frac{I(D_{ij}=0)w_{ij}}{(1-P_{ij})} \right), \end{aligned}$$

$$\begin{aligned}\hat{\beta}^{\phi} &= \text{argmin} L_n^{\phi}(\beta^{\phi}; \hat{P_{1j}}, \hat{w}_{ij}) \\ &= \text{argmin} \frac{1}{n} \sum_{i=1}^{n} \sum_{j=1}^{n^i} \phi(\mathbb{X}_{ij}^T \beta^{\phi}) \left(\frac{I(D_{ij}=1)\hat{w}_{ij}}{\hat{P_{1j}}} - \epsilon \frac{I(D_{ij}=0)\hat{w}_{ij}}{(1-\hat{P_{1j}})} \right)\end{aligned}$$

Since $\beta^{\phi*} = \text{argmin} L^{\phi}(\beta^{\phi}; P_{1j}, w_{ij})$, and $\hat{\beta}^{\phi} = \text{argmin} L_n^{\phi}(\beta^{\phi}; \hat{P_{1j}}, \hat{w}_{ij})$, we have that $\beta^{\phi*}$ is the root of $S(\beta^{\phi}; P_{1j}, w_{ij})$, and $\hat{\beta}^{\phi}$ is the root of $S_n(\beta^{\phi}; \hat{P_{1j}}, \hat{w}_{ij})$, where

$$S(\beta^{\phi}; \hat{P_{1j}}, \hat{w}_{ij}) = \frac{\partial L^{\phi}(\beta^{\phi}; P_{1j}, \hat{w}_{ij})}{\partial \beta^{\phi}}, S_n(\beta^{\phi}; \hat{P_{1j}}, \hat{w}_{ij}) = \frac{\partial L_n^{\phi}(\beta^{\phi}; \hat{P_{1j}}, \hat{w}_{ij})}{\partial \beta^{\phi}}.$$

Given $\phi(\mathbb{X}_{ij}^T \beta^{\phi}) = \max(1 - \mathbb{X}_{ij}^T \beta^{\phi}, 0) = I\{1 - \mathbb{X}_{ij}^T \beta^{\phi} > 0\} * (1 - \mathbb{X}_{ij}^T \beta^{\phi})$ is not differentiable at $\mathbb{X}^T \beta^{\phi} = 0$, we use numerical approximation $g((1 - \mathbb{X}_{ij}^T \beta^{\phi})/b)$ to approximate $I\{1 - \mathbb{X}_{ij}^T \beta^{\phi} > 0\}$, where $g(t) = (1 + exp(-t))^{-1}$, and b is a positive constant.

For the consistency proof of $\hat{\beta}^{\phi}$ to $\beta^{\phi*}$, it follows similarly as the consistency proof in the two-step method, where z-estimation theory is applied. Next, we derive the asymptotic normality.

$$\sqrt{n}(\hat{\beta}^{\phi} - \beta^{\phi*}) = \sqrt{n} S_n(\beta^{\phi*}; \hat{P_{1j}}, \hat{w}_{ij}) [\frac{\partial S_n(\beta^{\phi}; \hat{P_{1j}}, \hat{w}_{ij})}{\partial \beta^{\phi}}|_{\beta^{\phi*}}]^{-1}.$$

$$\sqrt{n} S_n(\beta^{\phi*}; \hat{P_{1j}}, \hat{w}_{ij}) = \sqrt{n} S_n(\beta^{\phi*}; P_{1j}, \hat{w}_{ij}) + \frac{\partial S_n(\beta^{\phi*}; P_{1j}, \hat{w}_{ij})}{\partial P_{1j}} \sqrt{n}(\hat{P_{1j}} - P_{1j}) = A + B,$$

where B is asymptotically linear. We can rewrite A as

$$\sqrt{n} S_n(\beta^{\phi*}; P_{1j}, w_{ij}) + (\sqrt{n} S_n(\beta^{\phi*}; P_{1j}, \hat{w}_{ij}) - \sqrt{n} S_n(\beta^{\phi*}; P_{1j}, w_{ij})) = A_1 + A_2,$$

and A_2 as

$$\frac{1}{\sqrt{n}} \sum_{i=1}^{n} \int U_{G_i} dF(u),$$

where $U_{G_i}(t) = \int^t P(Y_i > u)^{-1} [I(Y_i \leq u(1 - \delta_i) + I(Y_i \geq u)] d \log\{G_u\}$, and

$$F(u) = \frac{1}{n} \sum_{i}^{n} \sum_{j=1}^{n_i} I(\max(Y_i, s_{ij} + U) \leq u) w_{ij} \phi(\mathbb{X}_{ij}^T \beta^{\phi*}) \left(\frac{I(D_{ij}=1)}{P_{1j}} - \epsilon \frac{I(D_{ij}=0)}{(1-P_{1j})} \right).$$

Simulation studies scenario 1 data generation

To have the time-invariant intercept, we first let $\theta_{01} = 1$, and given $\theta_1 = 1$, $\theta_2 = -3$, and the distribution of X_{i1}, we can derive P_{11}, and P_{01}, where $P_{11} = \int \text{expit}(\theta_{01}+\theta_{11}X_{i1,1}+\theta_{12}X_{i1,2})f(X_{i1,1})f(X_{i1,2})dX_{i1,1}dX_{i1,2}$, where $f(X_{i1,1})$, and $f(X_{i1,2})$ are the pdfs of a normal distribution of mean 1, and variance 1, and subsequently derive b^*_{01} .

$P_{12} = \int \text{expit}(\theta_{02} + \theta_1 X_{i2,1} + \theta_2 X_{i2,2})f(X_{i2,1}|Q_{i1} = 0)f(X_{i2,2}|Q_{i1} = 0)dX_{i1,1}dX_{i1,2}$

$f(X_{i2}|Q_{i1} = 0) = f(X_{i2}, Q_{i1} = 0)/f(Q_{i1} = 0)$

$f(X_{i2,1}, Q_{i1} = 0) = f(Q_{i1}|X_{i2,1} = 0)f(X_{i2,1})$, where $f(Q_{i1}|X_{i2,1} = 0) = \int f(Q_{i1} = 0, X_{i1}|X_{i2,1})dX_{i1} = \int f(Q_{i1} = 0|X_{i1}, X_{i2,1})f(X_{i1}|X_{i2,1})dX_{i1} = \int f(Q_{i1} = 0|X_{i1})f(X_{i1}|X_{i2,1})dX_{i1}$.

Next, if we set $b^*_{02} = b^*_{01}$, and given we have calculated b^*_{01}, b^*_{02} is thus set. Note that b^*_{02} depends on θ_{02}, P_{12}, and P_{02}, where P_{12} and P_{02} depends on some fixed quantities θ_1, θ_2, the distribution of X_{i2}, and a free parameter θ_{02}, which is not yet set. Therefore, we can vary the value of θ_{02} such that $b^*_{02} = b^*_{01}$. Similar procedures can be done to determine θ_{03}, θ_{04}, and θ_{05} so that the requirement $b^*_{0j} = b^*_{0(j-1)}$ can be met. The idea is that we first freely choose θ_{01} to be arbitrary values and after fixing them, we then solve for $\theta_{0j}, \forall j \in \{2, ..., J\}$, but we have to choose reasonable b_0, and θ_{01} so that there exist solutions for $\theta_{0j}, \forall j \in \{2, ..., J\}$.

Additional Simulation Results

Method	Sample size	$\beta_{1,1}$	$\beta_{1,2}$
Oracle		0.694	-2.083
SM	n=400	0.737(0.2135)	-2.178(0.3472)
	n=1500	0.700(0.0907)	-2.070(0.1464)
OSF	n=400	0.743(0.3498)	-2.058(0.4883)
	n=1500	0.702(0.1356)	-1.984(0.2104)
PC GLM	n=400	0.873(0.7150)	-2.584(2.0674)
	n=1500	0.729(0.1508)	-2.194(0.4046)

Table 4.7. Coefficients (standard error) of the estimated stabilized DSRs in Scenario 1, $\xi = 1$

Method	Sample size	$\Phi_{RACB}(S)$	$\Phi_{RACB}(\mathcal{R})$
Oracle		0.700	0.700
SM	n=400	0.697(0.0028)	0.675(0.0253)
	n=1500	0.699(0.0009)	0.695(0.0029)
OSF	n=400	0.693(0.0077)	0.667(0.0269)
	n=1500	0.697(0.0028)	0.692(0.0047)
PC GLM	n=400	0.689(0.0131)	0.689(0.0131)
	n=1500	0.696(0.0044)	0.696(0.0044)

Table 4.8. RACB values (standard error) of DSRs in Scenario 1, $\xi = 1$

Method	Sample size	$\beta_{1,1}$	$\beta_{1,2}$
Oracle		0.868	-2.603
SM	n=400	0.930(0.2967)	-2.738(0.5176)
	n=1500	0.864(0.1190)	-2.564(0.2063)
OSF	n=400	0.984(0.5420)	-2.729(0.8464)
	n=1500	0.897(0.2006)	-2.567(0.3336)
PC GLM	n=400	1.091(0.8423)	-3.242(2.4593)
	n=1500	0.869(0.2475)	-2.607(0.6568)

Table 4.9. Coefficients (standard error) of the estimated stabilized DSRs in Scenario 1, $\xi = 4/3$

Method	Sample size	$\Phi_{RACB}(S)$	$\Phi_{RACB}(\mathcal{R})$
Oracle		0.651	0.651
SM	n=400	0.649(0.0028)	0.628(0.0239)
	n=1500	0.651(0.0008)	0.647(0.0030)
OSF	n=400	0.646(0.0071)	0.619(0.0263)
	n=1500	0.650(0.0016)	0.644(0.0049)
PC GLM	n=400	0.641(0.0143)	0.641(0.0143)
	n=1500	0.648(0.0053)	0.648(0.0053)

Table 4.10. RACB values (standard error) of DSRs in Scenario 1, $\xi = 4/3$

Method	Sample size	$\beta_{1,1}$	$\beta_{1,2}$	$\beta_{1,3}$	$\beta_{1,4}$
SM	n=400	0.119(0.2604)	-0.737(0.4872)	1.193(1.4807)	-1.493(1.1826)
	n=1500	0.135(0.1076)	-0.706(0.1168)	1.153(0.1862)	-1.407(0.1680)
OSF	n=400	0.090(0.1146)	-0.548(0.1319)	0.895(0.1307)	-1.149(0.1365)
	n=1500	0.096(0.0557)	-0.560(0.0578)	0.909(0.0633)	-1.151(0.0657)
PC GLM	n=400	-0.086(0.0798)	-0.525(0.1487)	0.389(0.1232)	-0.901(0.2285)
	n=1500	-0.085(0.0356)	-0.524(0.0848)	0.393(0.0693)	-0.903(0.1372)

Table 4.11. Coefficients (standard error) of the estimated stabilized DSRs in Scenario 2, $\xi = 1$.

Method	Sample size	$\Phi_{RACB}(S)$	$\Phi_{RACB}(\mathcal{R})$
SM	n=400	0.408(0.0139)	0.399(0.0250)
	n=1500	0.420(0.0037)	0.435(0.0063)
OSF	n=400	0.418(0.0053)	0.416(0.0128)
	n=1500	0.422(0.0016)	0.439(0.0046)
PC GLM	n=400	0.334(0.0246)	0.334(0.0246)
	n=1500	0.344(0.0114)	0.344(0.0114)

Table 4.12. RACB values (standard error) of DSRs in Scenario 2, $\xi = 1$.

Method	Sample size	$\beta_{1,1}$	$\beta_{1,2}$	$\beta_{1,3}$	$\beta_{1,4}$
SM	n=400	0.342(1.2290)	-1.312(1.8779)	2.122(3.7330)	-2.774(5.2394)
	n=1500	0.192(0.1561)	-1.062(0.2154)	1.705(0.3797)	-2.112(0.3799)
OSF	n=400	0.194(0.2173)	-0.959(0.2727)	1.570(0.3772)	-1.991(0.4453)
	n=1500	0.193(0.0986)	-0.957(0.1242)	1.563(0.1701)	-1.970(0.1925)
PC GLM	n=400	-0.114(0.1096)	-0.708(0.2078)	0.523(0.1616)	-1.217(0.3294)
	n=1500	-0.115(0.0512)	-0.712(0.1458)	0.534(0.1149)	-1.228(0.2504)

Table 4.13. Coefficients (standard error) of the estimated stabilized DSRs in Scenario 2, $\xi = 4/3$.

Method	Sample size	$\Phi_{RACB}(S)$	$\Phi_{RACB}(\mathcal{R})$
SM	n=400	0.332(0.0133)	0.318(0.0246)
	n=1500	0.344(0.0036)	0.357(0.0066)
OSF	n=400	0.341(0.0052)	0.337(0.0142)
	n=1500	0.345(0.0023)	0.362(0.0045)
PC GLM	n=400	0.260(0.0239)	0.260(0.0239)
	n=1500	0.267(0.0104)	0.267(0.0104)

Table 4.14. RACB values (standard error) of DSRs in Scenario 2, $\xi = 4/3$.

Bibliography

[1] Raha Akhavan-Tabatabaei, Diana Marcela Sánchez, and Thomas G Yeung. A markov decision process model for cervical cancer screening policies in colombia. *Medical Decision Making*, 37(2):196–211, 2017.

[2] Suresh K Alahari. Nischarin inhibits rac induced migration and invasion of epithelial cells by affecting signaling cascades involving pak. *Experimental cell research*, 288(2):415–424, 2003.

[3] Heejung Bang and Anastasios A Tsiatis. Estimating medical costs with censored data. *Biometrika*, 87(2):329–343, 2000.

[4] Alvaro Barbeira, Kaanan P Shah, Jason M Torres, Heather E Wheeler, Eric S Torstenson, Todd Edwards, Tzintzuni Garcia, Graeme I Bell, Dan Nicolae, Nancy J Cox, et al. Metaxcan: summary statistics based gene-level association method infers accurate predixcan results. *BioRxiv*, page 045260, 2016.

[5] Alvaro N Barbeira, Scott P Dickinson, Rodrigo Bonazzola, Jiamao Zheng, Heather E Wheeler, Jason M Torres, Eric S Torstenson, Kaanan P Shah, Tzintzuni Garcia, Todd L Edwards, et al. Exploring the phenotypic consequences of tissue specific gene expression variation inferred from gwas summary statistics. *Nature communications*, 9(1):1825, 2018.

[6] Richard Barfield, Helian Feng, Alexander Gusev, Lang Wu, Wei Zheng, Bogdan Pasaniuc, and Peter Kraft. Transcriptome-wide association studies accounting for colocalization using egger regression. *Genetic epidemiology*, 42(5):418–433, 2018.

[7] Alexis Battle, Sara Mostafavi, Xiaowei Zhu, James B Potash, Myrna M Weissman, Courtney McCormick, Christian D Haudenschild, Kenneth B Beckman, Jianxin Shi, Rui Mei, et al. Characterizing the genetic basis of transcriptome diversity through rna-sequencing of 922 individuals. *Genome research*, 24(1):14–24, 2014.

[8] Annalisa Buniello, Jacqueline A L MacArthur, Maria Cerezo, Laura W Harris, James Hayhurst, Cinzia Malangone, Aoife McMahon, Joannella Morales, Edward Mountjoy, Elliot Sollis, et al. The nhgri-ebi gwas catalog of published genome-wide association studies, targeted arrays and summary statistics 2019. *Nucleic acids research*, 47(D1):D1005–D1012, 2019.

[9] Stephen Burgess, Frank Dudbridge, and Simon G Thompson. Combining information on multiple instrumental variables in mendelian randomization: comparison of allele score and summarized data methods. *Statistics in medicine*, 35(11):1880–1906, 2016.

[10] Stephen Burgess, Verena Zuber, Elsa Valdes-Marquez, Benjamin B Sun, and Jemma C Hopewell. Mendelian randomization with fine-mapped genetic data: Choosing from large numbers of correlated instrumental variables. *Genetic epidemiology*, 41(8):714–725, 2017.

[11] Raymond J Carroll, David Ruppert, Leonard A Stefanski, and Ciprian M Crainiceanu. *Measurement error in nonlinear models: a modern perspective*. Chapman and Hall/CRC, 2006.

[12] Bibhas Chakraborty, Palash Ghosh, Erica EM Moodie, and A John Rush. Estimating optimal shared-parameter dynamic regimens with application to a multistage depression clinical trial. *Biometrics*, 72(3):865–876, 2016.

[13] Shuai Chen and Hongwei Zhao. Estimating incremental cost-effectiveness ratios and their confidence intervals with different terminating events for survival time and costs. *Biostatistics*, 14(3):422–432, 2013.

[14] Seok-Yong Choi, Ping Huang, Gary M Jenkins, David C Chan, Juergen Schiller, and Michael A Frohman. A common lipid links mfn-mediated mitochondrial fusion and snare-regulated exocytosis. *Nature cell biology*, 8(11):1255, 2006.

[15] ENCODE Project Consortium et al. The encode (encyclopedia of dna elements) project. *Science*, 306(5696):636–640, 2004.

[16] Matthew R Cooperberg, Yingye Zheng, Anna V Faino, Lisa F Newcomb, Kehao Zhu, Janet E Cowan, James D Brooks, Atreya Dash, Martin E Gleave, Frances Martin, et al. Tailoring intensity of active surveillance for low-risk prostate cancer based on individualized prediction of risk stability. *JAMA oncology*, 6(10):e203187–e203187, 2020.

[17] Olivia Corradin, Alina Saiakhova, Batool Akhtar-Zaidi, Lois Myeroff, Joseph Willis, Richard Cowper-Sal, Mathieu Lupien, Sanford Markowitz, Peter C Scacheri, et al. Combinatorial effects of multiple enhancer variants in linkage disequilibrium dictate levels of gene expression to confer susceptibility to common traits. *Genome research*, 24(1):1–13, 2014.

[18] Werner Dinkelbach. On nonlinear fractional programming. *Management science*, 13(7):492–498, 1967.

[19] Editor. Hyphenation exception log. *TUGboat*, 7(3):145, 1986.

[20] Fatih Safa Erenay, Oguzhan Alagoz, and Adnan Said. Optimizing colonoscopy screening for colorectal cancer prevention and surveillance. *Manufacturing & Service Operations Management*, 16(3):381–400, 2014.

[21] Tomas Gal. *Postoptimal Analyses, Parametric Programming, and Related Topics: degeneracy, multicriteria decision making, redundancy*. Walter de Gruyter, 2010.

[22] Eric R Gamazon, Heather E Wheeler, Kaanan P Shah, Sahar V Mozaffari, Keston Aquino-Michaels, Robert J Carroll, Anne E Eyler, Joshua C Denny, Dan L Nicolae, Nancy J Cox, et al. A gene-based association method for mapping traits using reference transcriptome data. *Nature genetics*, 47(9):1091, 2015.

[23] Maya Ghoussaini, Juliet D French, Kyriaki Michailidou, Silje Nord, Jonathan Beesley, Sander Canisus, Kristine M Hillman, Susanne Kaufmann, Haran Sivakumaran, Mahdi Moradi Marjaneh, et al. Evidence that the 5p12 variant rs10941679 confers susceptibility to estrogen-receptor-positive breast cancer through fgf10 and mrps30 regulation. *The American Journal of Human Genetics*, 99(4):903–911, 2016.

[24] Claudia Giambartolomei, Damjan Vukcevic, Eric E Schadt, Lude Franke, Aroon D Hingorani, Chris Wallace, and Vincent Plagnol. Bayesian test for colocalisation between pairs of genetic association studies using summary statistics. *PLoS genetics*, 10(5):e1004383, 2014.

[25] Michel Goossens, Frank Mittelbach, and Alexander Samarin. *The LaTeX Companion*. Addison-Wesley, 1994.

[26] Saisai Guo, Haowen Ran, Dake Xiao, Haohao Huang, Lanjuan Mi, Xinzheng Wang, Lishu Chen, Da Li, Songyang Zhang, Qiuying Han, et al. Nt5dc2 promotes tumorigenicity of glioma stem-like cells by upregulating fyn. *Cancer letters*, 454:98–107, 2019.

[27] Alexander Gusev, Arthur Ko, Huwenbo Shi, Gaurav Bhatia, Wonil Chung, Brenda WJH Penninx, Rick Jansen, Eco JC De Geus, Dorret I Boomsma, Fred A Wright, et al. Integrative approaches for large-scale transcriptome-wide association studies. *Nature genetics*, 48(3):245, 2016.

[28] Fang Han and Wei Pan. A data-adaptive sum test for disease association with multiple common or rare variants. *Human heredity*, 70(1):42–54, 2010.

[29] Farhad Hormozdiari, Martijn Van De Bunt, Ayellet V Segre, Xiao Li, Jong Wha J Joo, Michael Bilow, Jae Hoon Sul, Sriram Sankararaman, Bogdan Pasaniuc, and Eleazar Eskin. Colocalization of gwas and eqtl signals detects target genes. *The American Journal of Human Genetics*, 99(6):1245–1260, 2016.

[30] Nadine Houede, Peter F Thall, Hoang Nguyen, Xavier Paoletti, and Andrew Kramar. Utility-based optimization of combination therapy using ordinal toxicity and efficacy in phase i/ii trials. *Biometrics*, 66(2):532–540, 2010.

[31] Yi-Juan Hu, Sonja I Berndt, Stefan Gustafsson, Andrea Ganna, Reedik Mägi, Eleanor Wheeler, Mary F Feitosa, Anne E Justice, Keri L Monda, Damien C Croteau-Chonka, et al. Meta-analysis of gene-level associations for rare variants based on single-variant statistics. *The American Journal of Human Genetics*, 93(2):236–248, 2013.

[32] Xinyang Huang and Jin Xu. Estimating individualized treatment rules with risk constraint. *Biometrics*, 2020.

[33] Yen-Tsung Huang, Tyler J VanderWeele, and Xihong Lin. Joint analysis of snp and gene expression data in genetic association studies of complex diseases. *The annals of applied statistics*, 8(1):352, 2014.

[34] Jeroen R Huyghe, Stephanie A Bien, Tabitha A Harrison, Hyun Min Kang, Sai Chen, Stephanie L Schmit, David V Conti, Conghui Qu, Jihyoun Jeon, Christopher K Edlund, et al.

Discovery of common and rare genetic risk variants for colorectal cancer. *Nature genetics*, 51(1):76, 2019.

[35] Guoyong Jiang, Jianrong Wu, and G Rhys Williams. Fieller's interval and the bootstrap-fieller interval for the incremental cost-effectiveness ratio. *Health Services & Outcomes Research Methodology*, 1(3-4):291, 2000.

[36] Jumana Karasneh, Ahmet Gül, William E Ollier, Alan J Silman, and Jane Worthington. Whole-genome screening for susceptibility genes in multicase families with behçet's disease. *Arthritis & Rheumatism*, 52(6):1836–1842, 2005.

[37] Dejan Knezevic, Audrey D Goddard, Nisha Natraj, Diana B Cherbavaz, Kim M Clark-Langone, Jay Snable, Drew Watson, Sara M Falzarano, Cristina Magi-Galluzzi, Eric A Klein, et al. Analytical validation of the oncotype dx prostate cancer assay–a clinical rt-pcr assay optimized for prostate needle biopsies. *BMC genomics*, 14(1):690, 2013.

[38] Keith Knight, Wenjiang Fu, et al. Asymptotics for lasso-type estimators. *The Annals of statistics*, 28(5):1356–1378, 2000.

[39] Donald E. Knuth. *The TEX book*. Addison-Wesley, 1984.

[40] Donald E. Knuth. *TEX: The Program*. Addison-Wesley, 1986.

[41] Donald E. Knuth. *Computer Modern Typefaces*. Addison-Wesley, 1986.

[42] Donald E. Knuth. *The Metafont book*. Addison-Wesley, 1986.

[43] Eric B Laber, Daniel J Lizotte, and Bradley Ferguson. Set-valued dynamic treatment regimes for competing outcomes. *Biometrics*, 70(1):53–61, 2014.

[44] John M Lachin, Ionut Bebu, Richard M Bergenstal, Rodica Pop-Busui, Bernard Zinman, David M Nathan, et al. Association of glycemic variability in type 1 diabetes with progression of microvascular outcomes in the diabetes control and complications trial. *Diabetes care*, 40(6):777–783, 2017.

[45] Leslie Lamport. *LATEX: A Document Preparation System*. Addison-Wesley, 2nd edition, 1994.

[46] Jill E Larsen, Sandra J Pavey, Linda H Passmore, Rayleen V Bowman, Nicholas K Hayward, and Kwun M Fong. Gene expression signature predicts recurrence in lung adenocarcinoma. *Clinical Cancer Research*, 13(10):2946–2954, 2007.

[47] Juhee Lee, Peter F Thall, Yuan Ji, and Peter Müller. Bayesian dose-finding in two treatment cycles based on the joint utility of efficacy and toxicity. *Journal of the American Statistical Association*, 110(510):711–722, 2015.

[48] Seunggeun Lee, Michael C Wu, and Xihong Lin. Optimal tests for rare variant effects in sequencing association studies. *Biostatistics*, 13(4):762–775, 2012.

[49] Bingshan Li and Suzanne M Leal. Methods for detecting associations with rare variants for common diseases: application to analysis of sequence data. *The American Journal of Human Genetics*, 83(3):311–321, 2008.

[50] Dan-Yu Lin and Zheng-Zheng Tang. A general framework for detecting disease associations with rare variants in sequencing studies. *The American Journal of Human Genetics*, 89(3):354–367, 2011.

[51] Daniel W Lin, Lisa F Newcomb, Marshall D Brown, Daniel D Sjoberg, Yan Dong, James D Brooks, Peter R Carroll, Matthew Cooperberg, Atreya Dash, William J Ellis, et al. Evaluating the four kallikrein panel of the 4kscore for prediction of high-grade prostate cancer in men in the canary prostate active surveillance study. *European urology*, 72(3):448–454, 2017.

[52] Ying Liu, Yuanjia Wang, Michael R Kosorok, Yingqi Zhao, and Donglin Zeng. Augmented outcome-weighted learning for estimating optimal dynamic treatment regimens. *Statistics in medicine*, 37(26):3776–3788, 2018.

[53] Daniel J Lizotte, Michael Bowling, and Susan A Murphy. Linear fitted-q iteration with multiple reward functions. *The Journal of Machine Learning Research*, 13(1):3253–3295, 2012.

[54] John Lonsdale, Jeffrey Thomas, Mike Salvatore, Rebecca Phillips, Edmund Lo, Saboor Shad, Richard Hasz, Gary Walters, Fernando Garcia, Nancy Young, et al. The genotype-tissue expression (gtex) project. *Nature genetics*, 45(6):580, 2013.

[55] Daniel J Luckett, Eric B Laber, and Michael R Kosorok. Estimation and optimization of composite outcomes. *arXiv preprint arXiv:1711.10581*, 2017.

[56] David P MacKinnon, Jennifer L Krull, and Chondra M Lockwood. Equivalence of the mediation, confounding and suppression effect. *Prevention science*, 1(4):173–181, 2000.

[57] Tracey L Marsh, Holly Janes, and Margaret S Pepe. Statistical inference for net benefit measures in biomarker validation studies. *Biometrics*, 76(3):843–852, 2020.

[58] Marlena Maziarz, Patrick Heagerty, Tianxi Cai, and Yingye Zheng. On longitudinal prediction with time-to-event outcome: comparison of modeling options. *Biometrics*, 73(1):83–93, 2017.

[59] Shane McCarthy, Sayantan Das, Warren Kretzschmar, Olivier Delaneau, Andrew R Wood, Alexander Teumer, Hyun Min Kang, Christian Fuchsberger, Petr Danecek, Kevin Sharp, et al. A reference panel of 64,976 haplotypes for genotype imputation. *Nature genetics*, 48(10):1279, 2016.

[60] Emma McIntosh, Jane Barlow, Hilton Davis, and Sarah Stewart-Brown. Economic evaluation of an intensive home visiting programme for vulnerable families: a cost-effectiveness analysis of a public health intervention. *Journal of Public Health*, 31(3):423–433, 2009.

[61] Alvin I Mushlin, W Jackson Hall, Jack Zwanziger, Elizabeth Gajary, Mark Andrews, Rebecca Marron, Kelly H Zou, and Arthur J Moss. The cost-effectiveness of automatic implantable cardiac defibrillators: results from madit. *Circulation*, 97(21):2129–2135, 1998.

[62] Lisa F Newcomb, Ian M Thompson, Hilary D Boyer, James D Brooks, Peter R Carroll, Matthew R Cooperberg, Atreya Dash, William J Ellis, Ladan Fazli, Ziding Feng, et al. Outcomes of active surveillance for clinically localized prostate cancer in the prospective, multi-institutional canary pass cohort. *The Journal of urology*, 195(2):313–320, 2016.

[63] National Institutes of Health et al. Nih state-of-the-science conference: Role of active surveillance in the management of men with localized prostate cancer, 2011.

[64] Bernie J O'Brien and Andrew H Briggs. Analysis of uncertainty in health care cost-effectiveness

studies: an introduction to statistical issues and methods. *Statistical methods in medical research*, 11(6):455–468, 2002.

[65] Dipen J Parekh, Sanoj Punnen, Daniel D Sjoberg, Scott W Asroff, James L Bailen, James S Cochran, Raoul Concepcion, Richard D David, Kenneth B Deck, Igor Dumbadze, et al. A multi-institutional prospective trial in the usa confirms that the 4kscore accurately identifies men with high-grade prostate cancer. *European urology*, 68(3):464–470, 2015.

[66] Margaret S Pepe, Holly Janes, Christopher I Li, Patrick M Bossuyt, Ziding Feng, and Jørgen Hilden. Early-phase studies of biomarkers: what target sensitivity and specificity values might confer clinical utility? *Clinical chemistry*, 62(5):737–742, 2016.

[67] Min Qian and Susan A Murphy. Performance guarantees for individualized treatment rules. *Annals of statistics*, 39(2):1180, 2011.

[68] Dimitris Rizopoulos. *Joint models for longitudinal and time-to-event data: With applications in R*. CRC press, 2012.

[69] Dimitris Rizopoulos, Jeremy MG Taylor, Joost Van Rosmalen, Ewout W Steyerberg, and Johanna JM Takkenberg. Personalized screening intervals for biomarkers using joint models for longitudinal and survival data. *Biostatistics*, 17(1):149–164, 2016.

[70] Donald B Rubin. Estimating causal effects of treatments in randomized and nonrandomized studies. *Journal of educational Psychology*, 66(5):688, 1974.

[71] Martin G Sanda, Ziding Feng, David H Howard, Scott A Tomlins, Lori J Sokoll, Daniel W Chan, Meredith M Regan, Jack Groskopf, Jonathan Chipman, Dattatraya H Patil, et al. Association between combined tmprss2: Erg and pca3 rna urinary testing and detection of aggressive prostate cancer. *JAMA oncology*, 3(8):1085–1093, 2017.

[72] Phillip J Schulte, Anastasios A Tsiatis, Eric B Laber, and Marie Davidian. Q-and a-learning methods for estimating optimal dynamic treatment regimes. *Statistical science: a review journal of the Institute of Mathematical Statistics*, 29(4):640, 2014.

[73] Thomas Schwarz-Romond, Christian Asbrand, Jeroen Bakkers, Michael Kühl, Hans-Joerg Schaeffer, Jörg Huelsken, Jürgen Behrens, Matthias Hammerschmidt, and Walter Birchmeier. The ankyrin repeat protein diversin recruits casein kinase iε to the β-catenin degradation complex and acts in both canonical wnt and wnt/jnk signaling. *Genes & development*, 16(16):2073–2084, 2002.

[74] William Shakespeare. *Hamlet*. F.S. Crofts & Co., Inc., NY, 1946. Act I, Scene 3, Lines 70-72, are apropos.

[75] Michael E Sobel. Asymptotic confidence intervals for indirect effects in structural equation models. *Sociological methodology*, 13:290–312, 1982.

[76] Spivak, M.D., Ph.D. *PCTEX Manual*. Personal TEX, Inc., CA, 1985.

[77] Spivak, M.D., Ph.D. *The Joy of TEX*. American Mathematical Society, RI, 1986.

[78] Angela A Steinhardt, Mariana F Gayyed, Alison P Klein, Jixin Dong, Anirban Maitra, Duojia Pan, Elizabeth A Montgomery, and Robert A Anders. Expression of yes-associated protein in common solid tumors. *Human pathology*, 39(11):1582–1589, 2008.

[79] Yu-Ru Su, Chongzhi Di, Stephanie Bien, Licai Huang, Xinyuan Dong, Goncalo Abecasis, Sonja Berndt, Stephane Bezieau, Hermann Brenner, Bette Caan, et al. A mixed-effects model for powerful association tests in integrative functional genomics. *The American Journal of Human Genetics*, 102(5):904–919, 2018.

[80] Jianping Sun, Yingye Zheng, and Li Hsu. A unified mixed-effects model for rare-variant association in sequencing studies. *Genetic epidemiology*, 37(4):334–344, 2013.

[81] Richard S Sutton and Andrew G Barto. *Reinforcement learning: An introduction*. MIT press, 2018.

[82] Gulnara R Svishcheva, Nadezhda M Belonogova, Irina V Zorkoltseva, Anatoly V Kirichenko, and Tatiana I Axenovich. Gene-based association tests using gwas summary statistics. *Bioinformatics*, 2019.

[83] Peter F Thall. Bayesian adaptive dose-finding based on efficacy and toxicity. *Journal of Statistical Research*, 46(2):187–202, 2012.

[84] Anirudh Tomer, Daan Nieboer, Monique J Roobol, Ewout W Steyerberg, and Dimitris Rizopoulos. Personalized schedules for surveillance of low-risk prostate cancer patients. *Biometrics*, 75(1):153–162, 2019.

[85] Anastasios A Tsiatis and Marie Davidian. Joint modeling of longitudinal and time-to-event data: an overview. *Statistica Sinica*, pages 809–834, 2004.

[86] Graduate School University of Washington. Format guidelines for theses and dissertations, 2012.

[87] Andrew J Vickers, Ben Van Calster, and Ewout W Steyerberg. Net benefit approaches to the evaluation of prediction models, molecular markers, and diagnostic tests. *bmj*, 352:i6, 2016.

[88] Allan J Wailoo, Nick Bansback, Alan Brennan, Kaleb Michaud, Richard M Nixon, and Fred Wolfe. Biologic drugs for rheumatoid arthritis in the medicare program: a cost-effectiveness analysis. *Arthritis & Rheumatism*, 58(4):939–946, 2008.

[89] Shouao Wang, Erica Em Moodie, David A Stephens, and Jagtar S Nijjar. Adaptive treatment strategies for chronic conditions: shared-parameter g-estimation with an application to rheumatoid arthritis. *Biostatistics*, 2020.

[90] Yanqing Wang, Ying-Qi Zhao, and Yingye Zheng. Learning-based biomarker-assisted rules for optimized clinical benefit under a risk constraint. *Biometrics*, 2019.

[91] Yanqing Wang, Yingqi Zhao, and Yingye Zheng. Learning-based search for individualized clinical decision rules to optimize clinical outcomes. Working paper, 2019.

[92] Yuanjia Wang, Haoda Fu, and Donglin Zeng. Learning optimal personalized treatment rules in consideration of benefit and risk: with an application to treating type 2 diabetes patients with insulin therapies. *Journal of the American Statistical Association*, 113(521):1–13, 2018.

[93] Xiaoquan Wen, Roger Pique-Regi, and Francesca Luca. Integrating molecular qtl data into genome-wide genetic association analysis: Probabilistic assessment of enrichment and colocalization. *PLoS genetics*, 13(3):e1006646, 2017.

[94] Michael C Wu, Seunggeun Lee, Tianxi Cai, Yun Li, Michael Boehnke, and Xihong Lin. Rare-variant association testing for sequencing data with the sequence kernel association test. *The American Journal of Human Genetics*, 89(1):82–93, 2011.

[95] Yizhe Xu, Tom H Greene, Adam P Bress, Brian C Sauer, Brandon K Bellows, Yue Zhang, William S Weintraub, Andrew E Moran, and Jincheng Shen. Estimating the optimal individualized treatment rule from a cost-effectiveness perspective. *Biometrics*, 2020.

[96] Jingyu Zhang, Brian T Denton, Hari Balasubramanian, Nilay D Shah, and Brant A Inman. Optimization of prostate biopsy referral decisions. *Manufacturing & Service Operations Management*, 14(4):529–547, 2012.

[97] Hongwei Zhao, Chen Zuo, Shuai Chen, and Heejung Bang. Nonparametric inference for median costs with censored data. *Biometrics*, 68(3):717–725, 2012.

[98] Ying-Qi Zhao, Ruoqing Zhu, Guanhua Chen, and Yingye Zheng. Constructing dynamic treatment regimes with shared parameters for censored data. *Statistics in Medicine*, 39(9):1250–1263, 2020.

[99] Yingqi Zhao, Donglin Zeng, A John Rush, and Michael R Kosorok. Estimating individualized treatment rules using outcome weighted learning. *Journal of the American Statistical Association*, 107(499):1106–1118, 2012.

[100] Xin Zhou, Nicole Mayer-Hamblett, Umer Khan, and Michael R Kosorok. Residual weighted learning for estimating individualized treatment rules. *Journal of the American Statistical Association*, 112(517):169–187, 2017.

[101] Zhihong Zhu, Futao Zhang, Han Hu, Andrew Bakshi, Matthew R Robinson, Joseph E Powell, Grant W Montgomery, Michael E Goddard, Naomi R Wray, Peter M Visscher, et al. Integration of summary data from gwas and eqtl studies predicts complex trait gene targets. *Nature genetics*, 48(5):481, 2016.